

# 1 Glucosylpolyphenols as Inhibitors of $A\beta$ -Induced Fyn Kinase 2 Activation and Tau Phosphorylation: Synthesis, Membrane 3 Permeability, and Exploratory Target Assessment within the Scope 4 of Type 2 Diabetes and Alzheimer's Disease

5 Ana M. de Matos,<sup>¶</sup> M. Teresa Blázquez-Sánchez,<sup>¶</sup> Andreia Bento-Oliveira, Rodrigo F. M. de Almeida,  
6 Rafael Nunes, Pedro E. M. Lopes, Miguel Machuqueiro, Joana S. Cristóvão, Cláudio M. Gomes,  
7 Cleide S. Souza, Imane G. El Idrissi, Nicola A. Colabufo, Ana Diniz, Filipa Marcelo,  
8 M. Conceição Oliveira, Óscar López, José G. Fernandez-Bolaños, Philipp Dätwyler, Beat Ernst, Ke Ning,  
9 Claire Garwood, Beining Chen,<sup>\*</sup> and Amélia P. Rauter<sup>\*</sup>

Cite This: <https://doi.org/10.1021/acs.jmedchem.0c00841>

Read Online

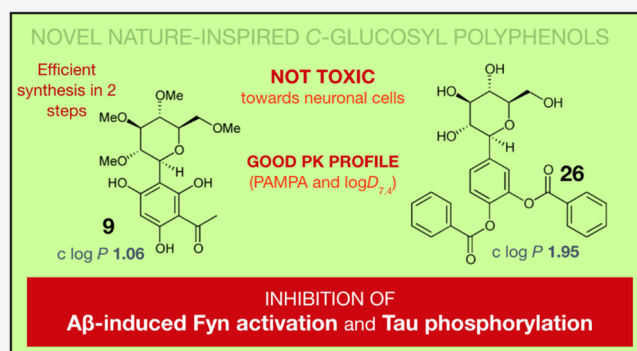
ACCESS |

Metrics & More

Article Recommendations

Supporting Information

10 **ABSTRACT:** Despite the rapidly increasing number of patients  
11 suffering from type 2 diabetes, Alzheimer's disease, and diabetes-  
12 induced dementia, there are no disease-modifying therapies that  
13 are able to prevent or block disease progress. In this work, we  
14 investigate the potential of nature-inspired glucosylpolyphenols  
15 against relevant targets, including islet amyloid polypeptide,  
16 glucosidases, and cholinesterases. Moreover, with the premise of  
17 Fyn kinase as a paradigm-shifting target in Alzheimer's drug  
18 discovery, we explore glucosylpolyphenols as blockers of  $A\beta$ -  
19 induced Fyn kinase activation while looking into downstream  
20 effects leading to Tau hyperphosphorylation. Several compounds  
21 inhibit  $A\beta$ -induced Fyn kinase activation and decrease pTau levels  
22 at 10  $\mu$ M concentration, particularly the per-*O*-methylated  
23 glucosylacetophloroglucinol and the 4-glucosylcatechol dibenzoate, the latter inhibiting also butyrylcholinesterase and  $\beta$ -glucosidase.  
24 Both compounds are nontoxic with ideal pharmacokinetic properties for further development. This work ultimately highlights the  
25 multitarget nature, fine structural tuning capacity, and valuable therapeutic significance of glucosylpolyphenols in the context of these  
26 metabolic and neurodegenerative disorders.



## 27 ■ INTRODUCTION

28 More than 463 million adults are currently suffering from type  
29 2 diabetes (T2D) worldwide,<sup>1</sup> and up to 73% of them are  
30 likely to be diagnosed with dementia, including Alzheimer's  
31 disease (AD). T2D, the non-insulin-dependent type of  
32 diabetes, primarily arises from the ingestion of high-fat diets  
33 and lack of physical exercise, which leads to hyperinsulinemia,  
34 dyslipidemia, insulin resistance, and ultimately, hyperglycemia.  
35 In turn, AD is characterized by the presence of extracellular  
36 deposits of amyloid beta ( $A\beta$ ) in the senile plaques and for  
37 intracellular neurofibrillary tangles induced by deposits of  
38 hyperphosphorylated Tau protein, accompanied by synaptic  
39 dysfunction resulting in neuronal death.<sup>2</sup> A recent report  
40 indicate that the cellular prion protein (PrP<sup>C</sup>) located in the  
41 neuronal cell surface works as a high-affinity binding partner of  
42  $A\beta$  oligomers ( $A\beta$ os), leading to the activation of Fyn kinase,  
43 which triggers a cell signaling pathway culminating in Tau  
44 hyperphosphorylation.<sup>3</sup> Indeed, Fyn activity was found to be

increased in the AD brain by exposure of neurons to  $A\beta$ os via  
45 PrP<sup>C</sup>.<sup>4,5</sup> Moreover, genetic deletion of Fyn prevents  $A\beta$ os-  
46 induced cell death in the hippocampus and Fyn inhibition  
47 restores synapse density and memory function in transgenic  
48 mice.<sup>6,7</sup> Interestingly, Fyn inhibition, deficiency, or genetic  
49 knockout was found to have increased glucose disposal due to  
50 increased insulin sensitivity and improved fatty acid oxidation,  
51 with decreased visceral adipose tissue inflammation.<sup>8–10</sup>  
52 Hence, the inhibition of Fyn activity is also a relevant  
53 approach in the treatment of diabetes-induced dementia  
54 (DID), the so-called “type 3 diabetes”.  
55

Received: May 17, 2020

Published: September 22, 2020

56 Other pathophysiological mechanisms are known to be  
 57 present in both T2D and AD, namely, peripheral and brain  
 58 insulin resistance and insulin-degrading enzyme (IDE) down-  
 59 regulation, leading to increased brain  $A\beta$  levels.<sup>2</sup> Furthermore,  
 60 cross-seeding events between the brain-penetrant islet amyloid  
 61 polypeptide (IAPP) and  $A\beta$  have also been reported, being  
 62 likely to exacerbate the cognitive decline observed in patients  
 63 suffering from both conditions.<sup>11,12</sup> With the lack of  
 64 therapeutic alternatives that are able to block disease  
 65 progression in both cases, we were interested in finding new  
 66 molecular entities able to tackle several molecular targets  
 67 common to AD and DID with disease-modifying effects. For  
 68 this purpose, we turned to nature for inspiration. Polyphenols  
 69 have been widely reported in the literature for their vast  
 70 therapeutic potential, with described antidiabetic, anti-inflam-  
 71 matory, and neuroprotective effects.<sup>2,13–16</sup> Polyphenol gluco-  
 72 sides (*O*-glucosyl polyphenols) and glucosylpolyphenols<sup>17</sup> (*C*-  
 73 glucosyl polyphenols, frequently named as polyphenol *C*-  
 74 glucosides), however, have improved palatability, oral bioavail-  
 75 ability due to increased solubility, and enhanced biological  
 76 activity when compared to the corresponding aglycones,  
 77 including improved amyloid-remodeling effects.<sup>16,18–21</sup> Im-  
 78 portantly, *C*-glucosyl polyphenols are not liable to chemical  
 79 and enzymatic hydrolysis, as sugar is linked to the polyphenol  
 80 by a C–C bond, and have been described to show higher  
 81 antidiabetic effects with improved target selectivity; for  
 82 instance, the glucosyldihydrochalcone analogue of the gluco-  
 83 side phlorizin is selective toward SGLT-2 vs SGLT-1  
 84 transporters, while phlorizin is not.<sup>22–24</sup>

85 For all the above-mentioned reasons, we were interested in  
 86 exploring the potential multitarget bioactivity of glucosylpoly-  
 87 phenols based on the structure of 8- $\beta$ -D-glucosylgenistein (**1**,  
 88 Figure 1), a natural glucosylisoflavone previously reported by  
 89 our group as a new and potent antidiabetic compound with  
 90 potential against  $A\beta(1-42)$ -induced neurotoxicity.<sup>25</sup> This  
 91 compound was found to inhibit IAPP aggregation and to  
 92 interact with  $A\beta(1-42)$  polypeptide through the same binding  
 93 mode, involving the sugar moiety, H-6 of ring A, and the  
 94 aromatic protons of ring B. Yet, we did not have information as  
 95 to whether one or more phenol moieties were beneficial for  
 96 activity or even if the molecular planarity of the aglycone was a  
 97 crucial feature for the binding epitope and antiaggregating  
 98 activity of this compound. Moreover, *C*-glucosyl polyphenols  
 99 derived from acetophloroglucinol or hydroquinone have been  
 100 reported in the literature for having antidiabetic effects.<sup>26,27</sup> On  
 101 the basis of this information, we were interested in synthesizing  
 102 simplified analogues of **1** with a different hydroxylation pattern  
 103 in ring A, maintaining the sugar  $\beta$ -C linkage found in the  
 104 original compound (Figure 1). To keep rings A and B linked  
 105 by a three-bond spacer moiety for mimicking **1**, we planned on  
 106 inserting benzoate moieties in glucosylhydroquinone (a) and  
 107 glucosylcatechol derivatives (b) or ketone moieties in  
 108 glucosylphloroglucinol derivatives (c). Moreover, due to the  
 109 extremely polar nature of the lead compound, we were also  
 110 interested in generating more lipophilic analogues of the  
 111 natural scaffold with higher chances of crossing the blood–  
 112 brain barrier (BBB), namely, by *O*-methyl protection of sugar  
 113 hydroxy groups. The major goal was to explore the therapeutic  
 114 potential and physicochemical properties of compound **1** while  
 115 comparing them to those of the newly synthesized analogues  
 116 and elucidating, whenever possible, structural requirements for  
 117 bioactivity against multiple targets involved in T2D and AD,  
 118 including IAPP, Fyn kinase activation, Tau hyperphosphor-

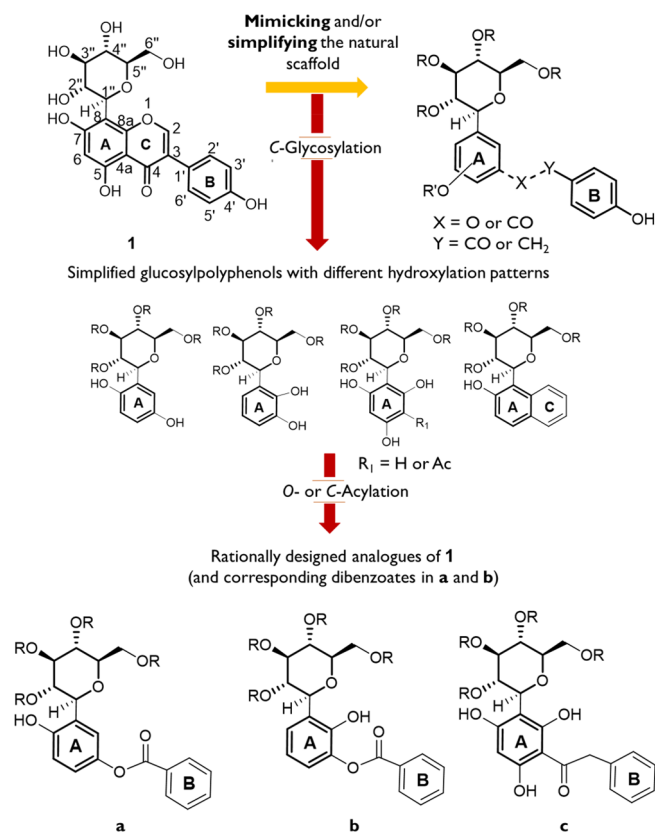


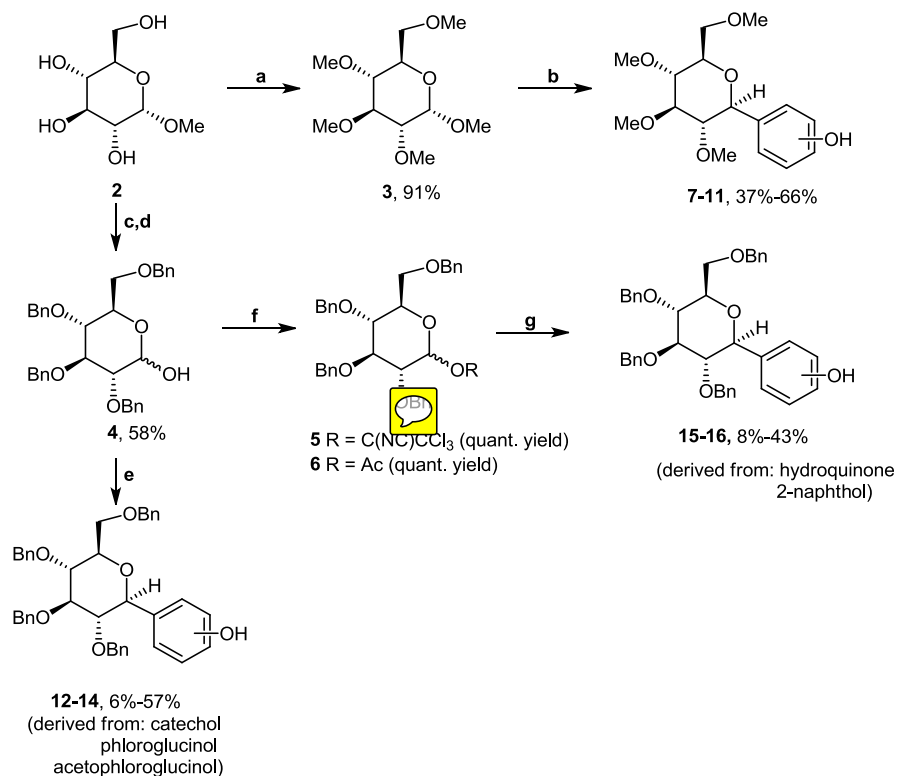
**Figure 1.** Rationale behind the synthesis of simplified analogues of 8- $\beta$ -D-glucosylgenistein (**1**). R = H or Me; R' = H or Bz.

ylation, and glucosidase and cholinesterase enzymes. Ultimately, we were interested in investigating the therapeutic potential of glucosylpolyphenols against T2D and AD while identifying new lead molecules for further pharmaceutical development in the context of these pathologies.

*C*-glycosylation is a key and particularly challenging synthetic step in our strategy. Several methods for *C*-glycosylation are currently known, including nucleophilic attack of aromatic Grignard reagents to glycosyl halides,<sup>28</sup> the use of lactones and lithiated compounds,<sup>29</sup> catalysis by transition metals or samarium diiodide,<sup>30,31</sup> intermolecular free radical reactions,<sup>32</sup> and intramolecular aglycone delivery through the Fries-type rearrangement.<sup>33</sup> The latter approach covers the strategy first developed by Suzuki *et al.*<sup>34</sup> and Kometani *et al.*,<sup>35</sup> and consists of a Lewis acid-catalyzed rearrangement of a phenol glycoside to a *C*-glucosyl derivative, known as the Fries-type rearrangement. It has been exploited by various authors up to the present days and successfully applied to the synthesis of flavonoid *C*-glycosides and of other complex natural products.<sup>25,36–38</sup> In this sense, another goal for this work was to explore the feasibility of *C*-glycosylation by using different glycosyl donors and acceptors while studying their impact in the efficacy of the Fries-type rearrangement.

## RESULTS

**Chemistry. *C*-Glycosylation.** For the generation of glucosylpolyphenols, we employed either a permethylated glucopyranoside<sup>39</sup> (**3**, Scheme 1) or per-benzylated glucosyl donors<sup>25,40</sup> (**4–6**). Polyphenols containing their hydroxy groups in *meta*, *para*, and *ortho* orientations were used as acceptors in a series of *C*-glycosylation reactions, and the

Scheme 1. Preparation of Glucosyl Donors and Protected C-Glucosyl Phenols<sup>a</sup>

<sup>a</sup>Reagents and conditions: (a) DMF, NaH, MeI, 0 °C, 3 h; (b) dry MeCN, polyphenol, drierite, -78 °C → r.t., TMSOTf, 18–48 h; (c) DMF, NaH, BnBr, 0 °C → r.t., 20 h; (d) AcOH, H<sub>2</sub>SO<sub>4</sub>, reflux, 36 h; (e) dichloromethane/MeCN, drierite, -78 °C → r.t. or 40 °C, TMSOTf, 8–64 h; (f) for compound 5: dichloromethane, 3 Å molecular sieves, CCl<sub>3</sub>CN, 0 °C, 1 h; for compound 6: pyridine, DMAP, 0 °C → r.t., Ac<sub>2</sub>O, 2.5 h; (g) for compound 15: dichloromethane/MeCN, drierite, -78 °C → r.t., BF<sub>3</sub>·Et<sub>2</sub>O, 40 h; for compound 16: dichloromethane, 3 Å molecular sieves, 0 °C → r.t., TMSOTf, 20 h.

149 differences in their reactivity were attentively explored. 2-  
150 Naphthol was also used to generate a C-glucosyl analogue with  
151 two fused planar rings to mimic rings A and C in the original  
152 structure.

153 Precursors and conditions leading to the higher yields are  
154 presented in Tables 1 and 2. In the case of catechol and  
155 hydroquinone, when using benzyl-protected sugar donors,  
156 glycosylation yields were drastically lower when compared to  
157 reactions with either phloroglucinol or trihydroxyacetophe-  
158 none as a sugar acceptor. In the first two cases, different  
159 solvent proportions, anomeric protecting groups, and promoter  
160 equivalents were tried, attempting to optimize the reaction  
161 efficacy; yet, after much experimentation, no significant  
162 improvements could be observed. Moreover, no significant  
163 differences were found when trying to improve the efficacy of  
164 hydroquinone and catechol C-glycosylation using either  
165 TMSOTf or BF<sub>3</sub>·Et<sub>2</sub>O. Notwithstanding, for the first time,  
166 per-O-methyl-β-glucosylated polyphenols have been accessed  
167 in good yields by using TMSOTf as the promoter and fully O-  
168 methylated methyl glucoside as the glucosyl donor. This  
169 methodology constitutes an advantage when compared to  
170 other approaches by saving reaction steps in the generation of  
171 donors with good leaving groups.

172 Methyl-protected glucosyl donor gave, by reaction with all  
173 the acceptors tested, C-glucosyl polyphenols as the major  
174 products (7–11, Table 1). Interestingly, with benzyl-protected  
175 glucosyl donors, only glucosylphloroglucinol 13, 3-glucosyl-  
176 2,4,6-trihydroxyacetophenone 14, and 1-glucosylnaphthalen-2-  
177 ol 16 were formed in moderate yields as the electron-donating

178 effects of their aglycones were strong enough to promote C-  
179 glucosylation. On the other hand, catechol and hydroquinone  
180 gave C-glucosyl derivatives in very low yield (Table 1), even  
181 after increasing the reaction time and changing the solvent  
182 and temperature (Table 2).

183  
184 Notably, after careful analysis of the NMR spectra, we  
185 observed that the *para*-isomers are formed in the synthesis of  
186 catechol C-glucosides 7 and 12, thus indicating that the Lewis  
187 acid-promoted Friedel–Crafts-type C-glycosylation is the  
188 favored reaction mechanism, prevalent over the Fries-type  
189 rearrangement described for unprotected phenols. While the  
190 synthesis of D-rhamnosyl<sup>41</sup> and D-glucosyl<sup>42,43</sup> aromatic  
191 derivatives has been previously described with protected  
192 phenols, to the best of our knowledge, this is the first report  
193 of exceptions to the Fries-type rearrangement in the C-  
194 glycosylation of unprotected phenols.

195 *O*-Acylation. A benzoyl group was regioselectively intro-  
196 duced in glucosylhydroquinone derivatives 10 and 15 to afford  
197 analogues of 1 on the basis of a *para* hydroxylation pattern (a,  
198 Figure 1). Using imidazole, DMAP, and benzoyl chloride, the  
199 desired ester derivatives 17 and 19 were obtained as the major  
200 products in good yield, together with their dibenzoate  
201 analogues 18 and 20 (Scheme 2). Further deprotection of  
202 benzyl-protected derivatives through catalytic hydrogenation  
203 gave the corresponding deprotected compounds 21 and 22.  
204 For comparison purposes, compounds 14 and 16 were also  
205 debenzylated to afford compounds 23 and 24, respectively (vd.  
206 Experimental Section).

Table 1. C-Glycosylation of Polyphenols Carried Out with TMSOTf as the Promoter

Phenol	Glycosyl donor	Isolated Yield (%)	Glycosyl donor	Isolated Yield (%)
<b>Catechol</b> <i>ortho</i> -Hydroxylation pattern	<b>7</b> 	63	<b>12</b> 	6 (R = H)
<b>Phloroglucinol</b> <i>meta</i> -Hydroxylation pattern	<b>8</b> 	53	<b>13</b> 	42 (R = H)
<b>Trihydroxyacetophenone</b> <i>meta</i> -Hydroxylation pattern	<b>9</b> 	45	<b>14</b> 	57 (R = H)
<b>Hydroquinone</b> <i>para</i> -Hydroxylation pattern	<b>10</b> 	37	<b>15<sup>a</sup></b> 	8 (R = Ac)
<b>2-Naphthol</b>	<b>11</b> 	66	<b>16</b> 	43 (R = CNHCCl <sub>3</sub> )

<sup>a</sup>Compound 15 was obtained using BF<sub>3</sub>·Et<sub>2</sub>O as the promoter.

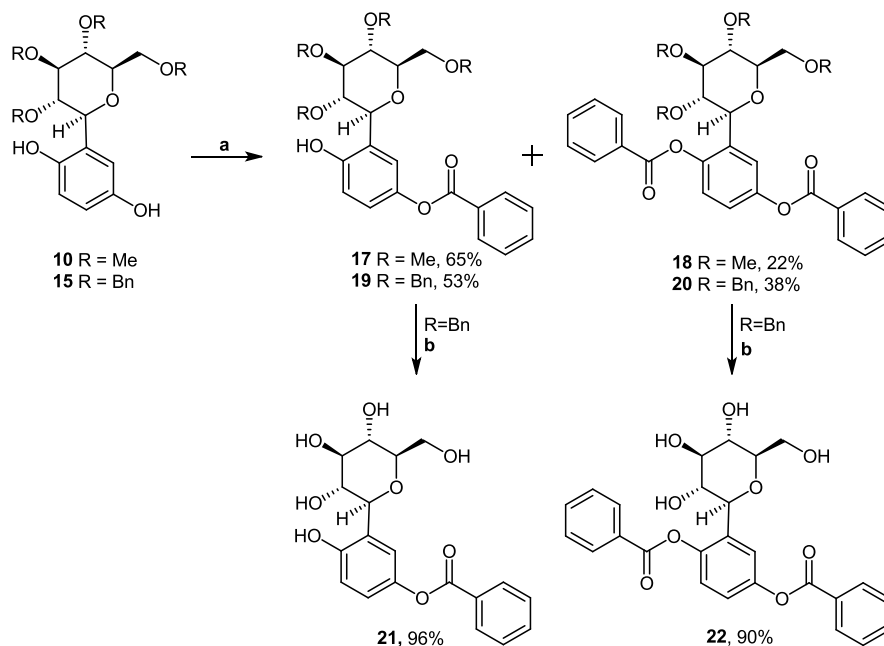
Table 2. Comparison of Experimental Conditions Used in the C-Glycosylation of Hydroquinone and Catechol with Benzyl-Protected Sugar Donors<sup>a</sup>

compound no.	sugar donor no.	polyphenol	solvent	promoter	temperature	time	isolated yield
12	4	catechol (150 mol %)	DCM/MeCN (5:1)	TMSOTf (100 mol %)	-78 °C → 40 °C	64 h	6%
12	6	catechol (150 mmol %)	DCM/MeCN (5:1)	BF <sub>3</sub> ·Et <sub>2</sub> O (100 mol %)	-78 °C → 40 °C	60 h	2%
15	5	hydroquinone (200 mol %)	DCM/MeCN (1:1)	TMSOTf (50 mol %)	-78 °C → 40 °C	21 h	6%
15	5	hydroquinone (150 mol %)	DCM/MeCN (1:1)	TMSOTf (50 mol %)	-78 °C → r.t.	40 h	2%
15	5	hydroquinone (150 mol %)	DCM/MeCN (5:1)	TMSOTf (50 mol %)	-78 °C → 40 °C	40 h	6%
15	5	hydroquinone (150 mol %)	DCM/MeCN (2:1)	TMSOTf (50 mol %)	-78 °C → 40 °C	24 h	6%
15	5	hydroquinone (200 mol %)	MeCN	TMSOTf (100 mol %)	-78 °C → 82 °C	72 h	1%
15	4	hydroquinone (150 mol %)	DCM/MeCN (5:1)	BF <sub>3</sub> ·Et <sub>2</sub> O 100 mol%	-78 °C → 40 °C	96 h	7%
15	6	hydroquinone (150 mol %)	DCM/MeCN (5:1)	BF <sub>3</sub> ·Et <sub>2</sub> O (100 mol %)	-78 °C → 40 °C	40 h	8%

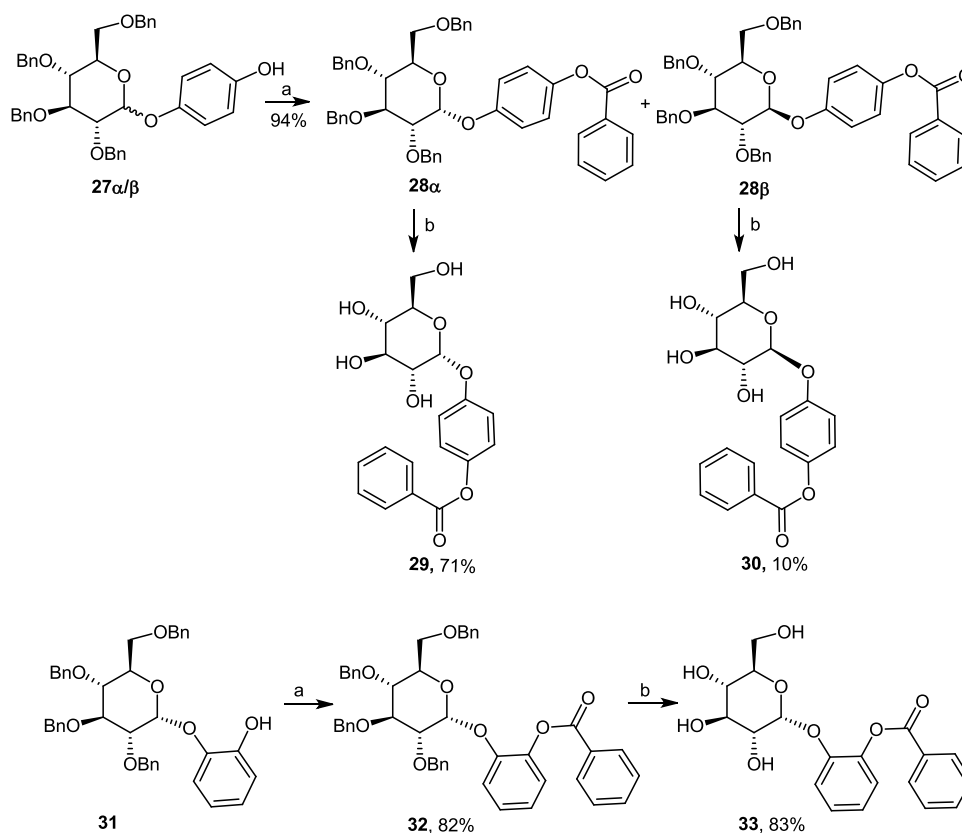
<sup>a</sup>DCM, dichloromethane.

207 The observed regioselectivity of these O-acylation reactions  
 208 may be related with stereochemical hindrance and eventual  
 209 hydrogen bonding between the free hydroxy group and sugar,  
 210 thus enhancing the relative reactivity of the remaining phenol  
 211 hydroxy group toward esterification. Accordingly, regioselective

212 esterification was not observed with glucosylcatechol  
 213 derivatives 7 and 12 (structure type b, Figure 1 and Table 2).  
 214 Instead, by applying the same experimental procedure, an  
 215 inseparable mixture of mono-benzoylated compounds was  
 216 obtained, which supports this hypothesis. For comparison of

Scheme 2. Preparation of Glucosylhydroquinone Benzoates<sup>a</sup>

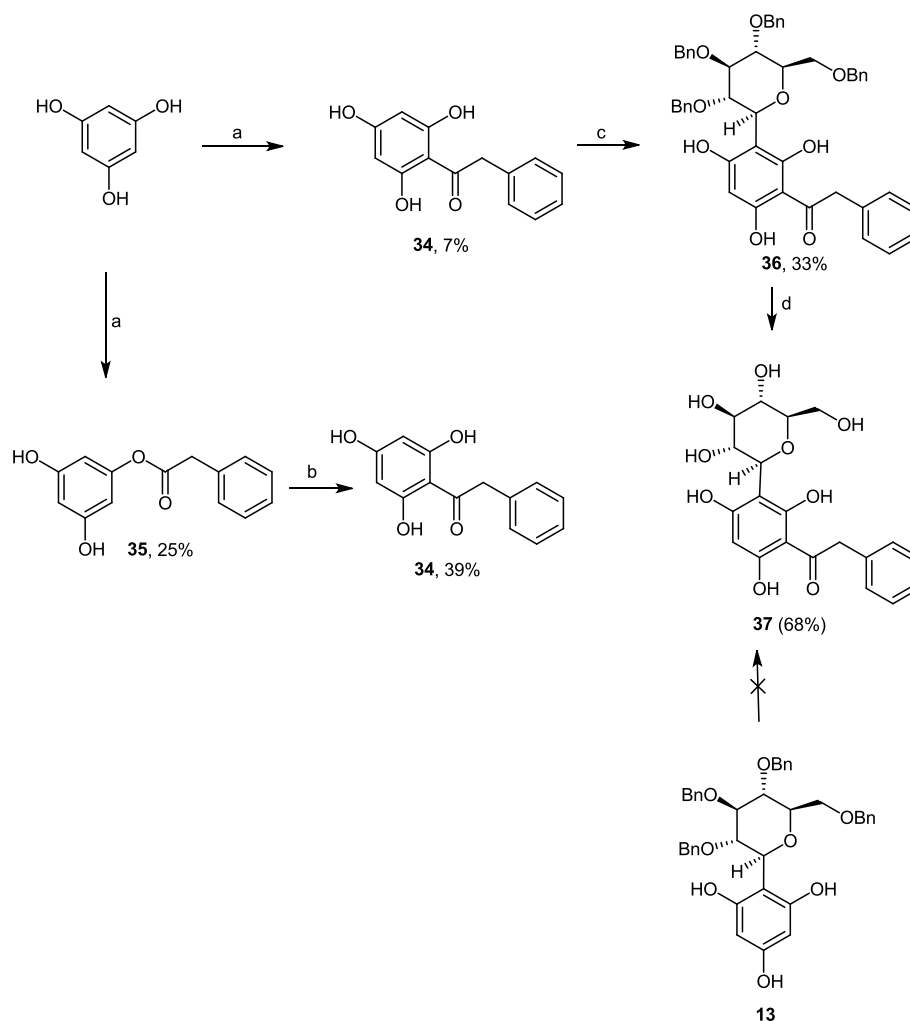
<sup>a</sup>Reagents and conditions: (a) dichloromethane, imidazole, DMAP, BzCl, 0 °C → r.t., 60–120 h; (b) EtOAc, Pd/C, H<sub>2</sub>, r.t., 16–22 h (R = Bn).

Scheme 3. Preparation of *O*-Glucosyl Hydroquinone and *O*-Glucosyl Catechol Benzoates<sup>a</sup>

<sup>a</sup>Reagents and conditions: (a) dichloromethane, imidazole, DMAP, BzCl, 0 °C → r.t., 60–120 h; (b) EtOAc, Pd/C, H<sub>2</sub>, r.t., 16–22 h.

217 bioactivity, the dibenzoate catechol analogues of compounds  
 218 **18** and **22** were also synthesized (*vd.* Experimental Section,  
 219 compounds **25** and **26**, respectively).  
 220 Moreover, the hydroquinone and catechol per-*O*-benzyl  
 221 glycosides **27α,β** and **31** (Scheme 3), obtained as major

products under the *C*-glucosylation reaction conditions (Table  
 222 2), were also benzoated and deprotected to afford the  
 223 corresponding  $\alpha$ -glycosides **29** and **33** as major products in  
 224 excellent overall yield.  
 225

Scheme 4. Preparation of Compound 37<sup>4a</sup>

<sup>a</sup>Reagents and conditions: (a) phenylacetyl chloride, 2% TfOH/MeCN, 0 °C → r.t., overnight; 34, 7%; 35, 25%; (b) TfOH, 100 °C, 2 h, 39%; (c) TMSOTf, dichloromethane/MeCN, compound 4, drierite, -40 °C → r.t., overnight, 33%; (d) MeOH/EtOAc, Pd/C, H<sub>2</sub>, r.t., 3 h, 68%.

226 **C-Acylation.** The glucosylphloroglucinol 13 was originally  
 227 chosen as the precursor of the planned analogue of compound  
 228 1 with the *meta* hydroxylation pattern (c, Figure 1). Provided  
 229 that this trihydroxybenzene is an extremely electron-rich  
 230 aromatic system, we were expecting a very straightforward  
 231 Friedel–Crafts-type acylation to occur with phenylacetyl  
 232 chloride in the presence of a Lewis acid. After much  
 233 experimentation employing a number of Lewis acids (*e.g.*,  
 234 BF<sub>3</sub>·Et<sub>2</sub>O, TMSOTf, FeCl<sub>3</sub>, TfOH) and several different  
 235 conditions without any success, we hypothesized that the  
 236 sugar moiety could be reducing the reactivity of the aromatic  
 237 ring or even being degraded in the course of these reactions.  
 238 The initial C-acylation of the phenol residue followed by C-  
 239 glycosylation turned out to be the best option to address this  
 240 issue. Due to the dual reactivity of unprotected polyphenols  
 241 toward electrophiles, hydroxy groups, and as in this case, highly  
 242 activated nucleophilic carbons, the control of *O*-/*C*-acylation  
 243 was not an easy task. While an equimolecular amount or an  
 244 excess of TfOH in the absence of solvent generated the di-*C*-  
 245 acylated product, the use of 2% TfOH in MeCN rendered a  
 246 mixture of the *O*-/*C*-acylated products in a ratio of ca. 1/0.3  
 247 (Scheme 4). Then, using an excess of TfOH, which acted as  
 248 both the solvent and catalyst, compound 35, obtained in 25%

yield from trihydroxybenzene, was rearranged into the *C*-  
 acylated analogue 34 in 39% yield, which was subsequently *C*-  
 glycosylated to afford compound 36 in 33% yield. After  
 catalytic hydrogenation, the final analogue 37 was isolated in  
 68% isolated yield.

**Computational Studies, Epitope Mapping, and  
 Bioactivity Assays.** *DFT Calculations and Molecular  
 Interactions of Rationally Designed Analogues with hIAPP  
 by STD-NMR.* IAPP is co-secreted with insulin by pancreatic  $\beta$ -  
 cells. In prediabetes, insulin resistance leads to a compensatory  
 hypersecretion of insulin and IAPP, leading to its aggregation  
 and deposition in the pancreas in the form of cytotoxic  
 amyloid oligomers and fibrils. Along with disease progression,  
 this accumulation will lead to the loss and dysfunction of  $\beta$ -  
 cells, which justifies why patients with advanced T2D are no  
 longer able to produce insulin despite being insulin-resistant.<sup>2</sup>  
 Hence, IAPP is an important therapeutic target in T2D,  
 particularly in the prevention of pancreatic dysfunction arising  
 from aberrant insulin secretion. In this context, the interaction  
 of 1 against hIAPP was previously unveiled by saturation-  
 transfer difference (STD) NMR techniques, also being shown,  
 by atomic force microscopy, the ability of this compound to  
 inhibit hIAPP aggregation into amyloid oligomers and fibrils.<sup>23, 271</sup>

272 Based on these findings, we were interested in assessing if the  
 273 rationally designed analogues **21** and **37** (aimed at mimicking  
 274 the original scaffold) would exhibit the same level of  
 275 interaction with hIAPP and if the binding epitope would be  
 276 maintained in the absence of the central fused ring system.  
 277 Being more easily accessed in fewer synthetic steps, both **21**  
 278 and **37** have increased molecular flexibility when compared to  
 279 the lead compound **1**. DFT calculations [PBE0/6-311G\*\*  
 280 (H<sub>2</sub>O)] show that low-energy conformations of compounds **21**  
 281 and **37** are superimposable with compound **1** (Figure 2),

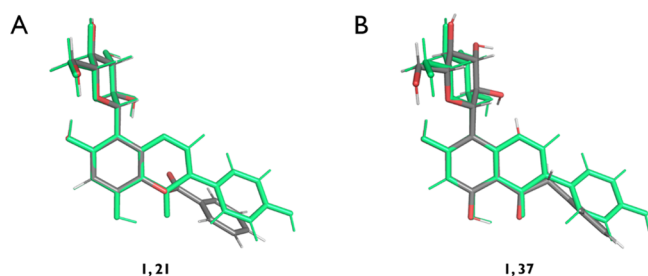


**Figure 2.** DFT-calculated structure of *anti*-**1** (in green), which is the preferentially adopted conformation in the presence of A $\beta$ (1–42) oligomers,<sup>25</sup> superimposed to the lowest energy conformations identified at the PBE0/6-311G\*\* (H<sub>2</sub>O) level of theory for compounds (A) **21** and (B) **37** (in gray, red, and white), obtained by root-mean-square (RMS) fitting using all ring A carbon atoms of each compound.

282 namely, with its *anti*-conformer (defined by an antigeometry  
 283 for the H1''-C1''-C8-C7 torsion angle), which is the  
 284 preferentially adopted conformation of **1** in the presence of  
 285 A $\beta$ (1–42) oligomers,<sup>25</sup> suggesting that these molecules are  
 286 able to mimic the original spatial orientation of the sugar  
 287 moiety relative to rings A and B (see Figures S1 and S2 and  
 288 further details in the Supporting Information).

289 The STD-derived binding epitope obtained for compounds  
 290 **1**, **21**, and **37** against hIAPP by STD-NMR (Figure 3 and

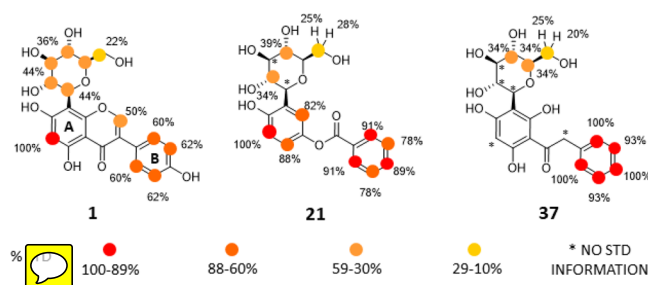


**Figure 3.** STD-derived epitope mapping obtained for compounds **1**,<sup>25</sup> **21**, and **37** with hIAPP oligomers.

291 Figures S3 and S4) suggests that molecular planarity is not a  
 292 structural requirement for binding and the absence of the  
 293 central fused ring system in compounds **21** and **37** does not  
 294 disrupt the interaction of these compounds with hIAPP. As in  
 295 the case of compound **1**, the highest STD intensities  
 296 correspond to the protons of the aromatic core of compounds  
 297 **21** and **37** (% STD > 80%) when compared to those detected  
 298 for the glucosyl group (% STD < 40%).

299 These experiments show that the binding affinity of the  
 300 antidiabetic lead **1** is not related to the molecular planarity of  
 301 the isoflavone core. Being accessed in only five synthetic steps  
 302 (instead of the nine needed for the synthesis of the lead

molecule **1**), compounds **21** and **37** exhibit a clear binding  
 against hIAPP. Given the reported anti-amyloidogenic proper-  
 ties of **1** against hIAPP,<sup>25</sup> these results encourage further  
 studies of these two simpler analogues to evaluate their  
 potential for the prevention of IAPP-induced pancreatic failure.

*Inhibition of PrP<sup>C</sup>-A $\beta$  Oligomer Interaction.* In the past  
 few years, the failure of several clinical trials targeting soluble  
 and fibrillar A $\beta$  by monoclonal antibodies have motivated the  
 scientific community to work in the diversification of  
 therapeutic targets for AD. One possible strategy is to focus  
 on the downstream effects of A $\beta$  rather than on its  
 accumulation and aggregation.<sup>44</sup> Soluble A $\beta$ s were shown  
 to bind to PrP<sup>C</sup> on the neuronal cell surface, initiating a  
 cascade through activation of Fyn kinase. Indeed, it is possible  
 to monitor the activation of Src family kinases (SFKs) such as  
 Fyn kinase by measuring the expression of phosphospecific  
 epitopes, as previously reported.<sup>3</sup>

Furthermore, it is commonly assumed that formation of A $\beta$   
 fibrils and plaque deposits is a crucial event in the pathogenesis  
 of AD.<sup>45</sup> However, there is accumulating evidence that soluble  
 oligomers are the most cytotoxic form of A $\beta$ , although it is still  
 unclear which size and morphology of the aggregates exert  
 neurotoxicity. As with most of the identified A $\beta$  receptors,  
 PrP<sup>C</sup> was found to bind A $\beta$ s with much higher affinity than  
 monomeric A $\beta$  (mA $\beta$ ). In this work, natural A $\beta$ s, a kind gift  
 from Sheffield Institute for Translational Neuroscience  
 (SITraN, U.K.), were used. These were derived from Chinese  
 hamster ovary cells (7PA2 cells) stably transfected with cDNA  
 encoding APP751, an amyloid precursor protein that contains  
 the Val717Phe familial Alzheimer's disease mutation, as  
 previously described.<sup>46</sup> The A $\beta$ s solution contains between  
 12,000 and 14,000 pg/mL total A $\beta$ s as measured by ELISA.  
 This concentration is comparable to that of A $\beta$  peptides  
 detected in human cerebrospinal fluid. The A $\beta$ s prepared  
 represent a heterogeneous population of monomers, dimers,  
 trimers, tetramers, higher state soluble oligomers, and other  
 cellular proteins as previously reported by western blotting<sup>44</sup>  
 without further purification. The A $\beta$ s preparation using the  
 same protocol has been applied in the same way by other  
 groups.<sup>46</sup> The same batch of the recombinant soluble A $\beta$ s was  
 used for all experiments described in the paper to minimize the  
 impact of experimental variations caused by the heterogeneous  
 preparation of the A $\beta$ s. Natural A $\beta$ s (1000 pg/mL) were used  
 to treat HEK 293 cells, immunocytochemistry (ICC) was  
 performed to detect cellular prion protein, and then the slides  
 where imaged with a Confocal Microscope Leica TCS SP5 II  
 objective 63 $\times$  oil form Leica Microsystems (Figure 4A). To  
 validate the observed binding between PrP<sup>C</sup> and A $\beta$ s, we  
 performed a PRNP knockdown by using the commercially  
 available kit ON-TARGETplus Human PRNP (S621) siRNA-  
 SMARTpool. Because only the PrP<sup>C</sup> on the cell surface  
 fraction is involved in the interaction with A $\beta$ s, the  
 knockdown was combined with acute cleavage promoted by  
 phospholipase C (PLC). Live cell staining and imaging were  
 performed, and cells were analyzed by flow cytometry  
 (fluorescence-activated cell sorting, FACS). Untreated cells  
 as controls and cells treated with ON-TARGETplus Non-  
 targeting siRNA Pool (scrambled siRNA) were used. The  
 result was a protein expression reduction by more than 80%  
 (Figure 4B). It is also interesting to note that phospholipase C  
 (PLC) can cleave PrP<sup>C</sup> on the surface and improve the effects  
 of knockdown further, *i.e.*, further reducing the PrP<sup>C</sup> on the cell  
 surface.

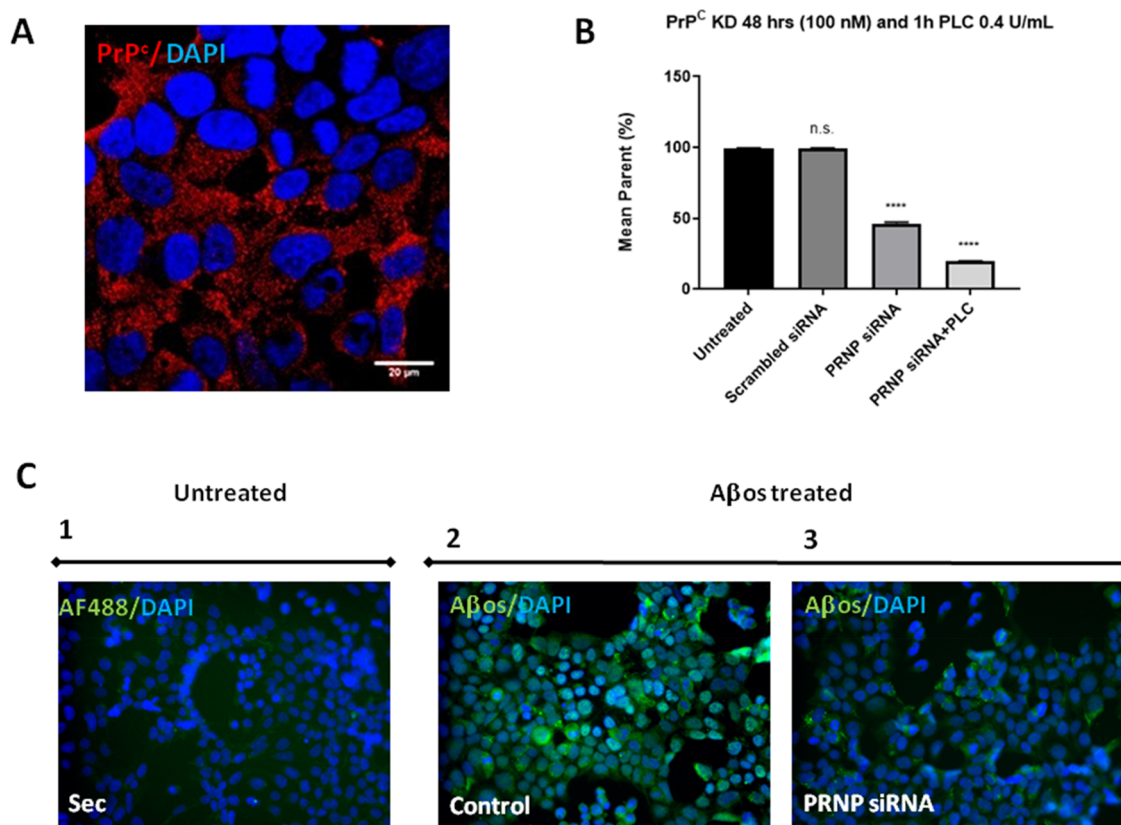


**Figure 4.** (A) Immunocytochemistry (ICC) images of HEK 293 cells treated with natural  $A\beta$ os ( $1 \times 10^3$  pg/mL). Pictures captured with a Leica TCS SP5 II. (B) Flow cytometry analysis (FACS) of transfected HEK 293 cells with PRNP siRNA against cellular prion protein (PrP<sup>C</sup>). Results are expressed as the mean  $\pm$  standard error mean (SEM);  $n = 3$ . Significant differences between control are indicated with \*\*\*\* $p \leq 0.0001$ . (C) Immunocytochemistry (ICC) analysis by the ImageXpress. (1) Negative control represented by HEK cells not transfected, treated with  $A\beta$ os and stained with only the secondary antibody AF488. (2)  $A\beta$ os binding to the prion protein in HEK 293 cell line with “high” PrP<sup>C</sup> expression. (3)  $A\beta$ os binding to the prion protein in HEK 293 cell line with “low” PrP<sup>C</sup> expression following knockdown performed by PRNP siRNA.

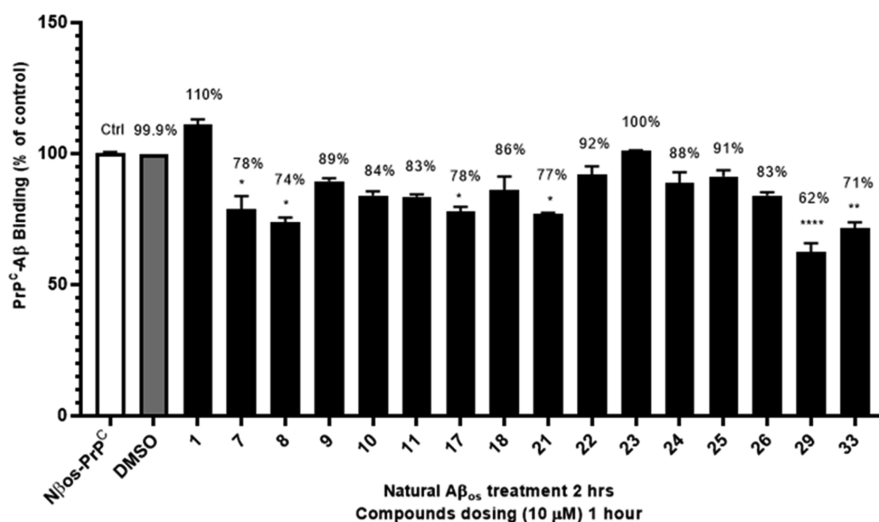


**Figure 5.** Screening for compounds that are able to induce a PrP<sup>C</sup>- $NA\beta$ os binding inhibition. All compounds were tested at  $10 \mu\text{M}$  as the final concentration. Results are expressed as the mean  $\pm$  standard error mean (SEM);  $n = 3$ . Significant differences between control are indicated with \*\*\*\* $p \leq 0.0001$ . The PrP<sup>C</sup>- $NA\beta$ (1-42) binding (%) after treatment with the compounds is also indicated.

366 We were able to test the  $A\beta$ os binding to the prion protein  
 367 in both HEK 293 cell lines with endogenous or “high” PrP<sup>C</sup>  
 368 expression (Figure 4C2) and “low” PrP<sup>C</sup> expression through  
 369 siRNA knockdown (Figure 4C3). The two populations were  
 370 treated with the same concentration ( $1 \times 10^3$  pg/mL) of  $A\beta$ os

for 2 h. Cells were then washed and stained with anti- $A\beta$ os 371  
 antibodies and imaged by the ImageXpress Micro Widefield 372  
 High Content Screening System (Figure 4C). It is clearly seen 373  
 that the binding of  $A\beta$ os to the cell surface is PrP<sup>C</sup>-dependent; 374  
*i.e.*,  $A\beta$ os binds to PrP<sup>C</sup> on the cell surface. 375



376 Compound screening in HEK 293 cell lines, previously  
377 treated with fresh natural A $\beta$ s, showed compounds interfering  
378 with the PrP<sup>C</sup>-A $\beta$ s binding (Figure 5).

379 **Inhibition of A $\beta$ -Induced Fyn Activation.** The Opera High  
380 Content Screening System was used in this section as it is  
381 applied to test drugs capable of reversing the altered phenotype  
382 observed in AD such as Fyn activation.

383 Figure 6 shows that the level of Fyn activation of hiPSC-  
384 derived neural progenitor cells from healthy donors increased  
385 upon treatment with A $\beta$ ; *i.e.*, pFyn production is increased.  
386 However, we observed that the level of A $\beta$ -induced Fyn  
387 activation was reduced back to normal control values in the  
388 presence of the commercial Fyn kinase inhibitor PP1, an  
389 inhibitor of Src family tyrosine kinases Lck, Fyn, Hck, and Src.  
390 Moreover, it shows that compounds 8 and 9 (simple per-*O*-  
391 methylglucosylphenols), 18 (per-*O*-methylglucosylhydroqui-  
392 none dibenzoate), 21 (rationally designed glucosylhydroqui-  
393 none monobenzoate), 25 and 26 (both glucosylcatechol  
394 dibenzoate derivatives), and 23 and 24 (fully unprotected  
395 glucosylacetophloroglucinol and glucosyl-naphthalene-2-ol)  
396 were able to significantly reduce A $\beta$ -induced Fyn activation  
397 at 10  $\mu$ M. Moreover, these C-glucosyl polyphenols are indeed  
398 more active than aglycone genistein.

399 Fyn kinase plays an important role in the physiology of  
400 neuronal cells by regulating cell proliferation and differ-  
401 entiation during the development of the CNS. This enzyme is  
402 also involved in signaling transduction pathways that regulate  
403 survival, metabolism, and neuronal migration.<sup>47</sup> Considering  
404 that Fyn inhibition below the physiological levels (basal levels)  
405 could be deleterious for the homeostasis of the cells, we  
406 decided to investigate the effects of the compounds on the  
407 basal levels of pFyn. Thus, neuronal progenitor cells were  
408 treated with the compounds without the addition of A $\beta$  to  
409 determine whether the effects observed are independent of A $\beta$   
410 treatment, and it was confirmed that tested compounds and  
411 PP1 alone do not reduce the basal levels of pFyn (Figure 6C).

412 A rather diverse selection of compounds was able to produce  
413 the desired effects, ranging from per-*O*-methyl and polyhy-  
414 droxy forms. Curiously, the natural compound that served as  
415 the inspiration for this study (1) was only able to cause a  
416 nonsignificant reduction in A $\beta$ -induced Fyn activation. Yet, the  
417 rationally designed and more flexible hydroquinone mono-  
418 benzoate (21) exhibited significant differences when compared  
419 to A $\beta$  alone. In fact, chemical modifications made in the  
420 original scaffold toward simpler versions of compound 1  
421 without ring B (*e.g.*, in compounds 8, 9, and 23) were generally  
422 more beneficial for the desired activity. On the other hand, no  
423 conclusions could be drawn regarding the advantages or  
424 disadvantages of sugars decorated with per-*O*-methyl groups as  
425 no correlation between structure and activity could be found  
426 regarding this matter. A good example is the presence and  
427 absence of these groups in the two most complex hits found in  
428 this assay, compounds 25 and 26, respectively.

429 We also evaluated the activity of Fyn kinase in the presence  
430 of some compounds by ADP-Glo kinase assay, a luminescent  
431 ADP detection assay (Figure 7). This assay provides a  
432 homogeneous and high-throughput screening method to  
433 measure kinase activity by quantifying the amount of ADP  
434 produced during a kinase reaction.

435 As presented in Figure 7, PP1 was able to reduce the Fyn  
436 kinase activity at different concentrations from 1 to 50  $\mu$ M, as  
437 expected. Furthermore, from the evaluated compounds, only 8  
438 and 10 were able to act as Fyn kinase inhibitors, denoting that

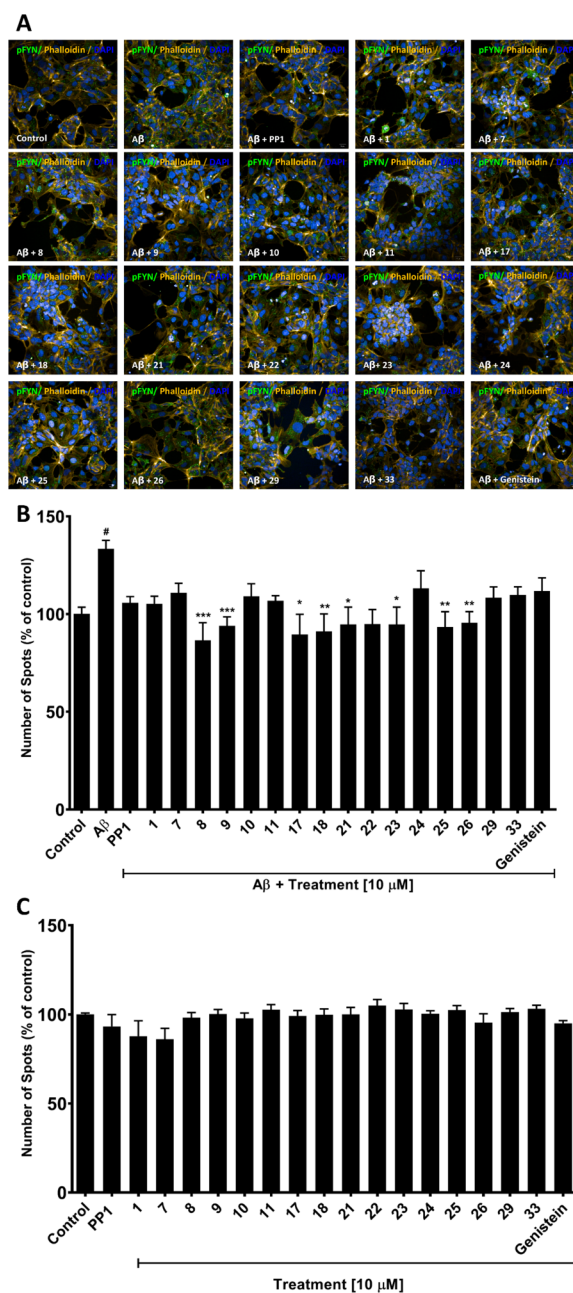


**Figure 6.** (A, B) Effect of glucosylphenols in A $\beta$ -induced Fyn activation and (C) effect of glucosylphenols on the basal levels of pFyn in the absence of A $\beta$ . The indirect activation of Fyn kinase was measured by immunofluorescence using Opera High Content Screening System (A). Cells were exposed to 10  $\mu$ M of compounds in association with A $\beta$ . The results were normalized against the control group, which was considered as 100%. (B, C) Percentage of number of pFyn + spots in each treatment group. Results are expressed as the mean  $\pm$  standard error mean (SEM) = 3. Significant differences between control are indicated with <sup>#</sup> $p \leq 0.05$  and <sup>\*</sup> $p < 0.05$  when compared to A $\beta$  treatment (<sup>\*</sup> $p < 0.05$ ) or <sup>\*\*</sup> $p < 0.01$  or <sup>\*\*\*</sup> $p < 0.001$ .

they may have an added therapeutic value against DID given the recognized role of Fyn kinase activity in insulin sensitivity and lipid utilization.<sup>8–10</sup> The fact that compounds 8 and 10, but not 9, were able to inhibit Fyn activity indicates that in per-*O*-methyl sugar-containing structures, the acetyl moiety is 443

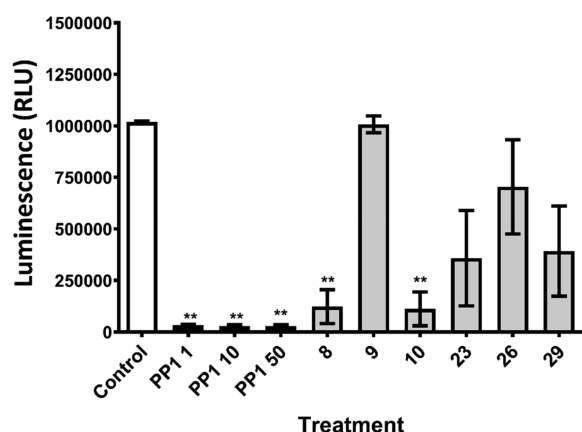


**Figure 7.** Effect of glucosylpolyphenols and the polyphenol glucoside **29** in the inhibition of Fyn kinase activity measured by the  $\gamma$ -P-Glo kinase assay. Results are expressed as the mean  $\pm$  SEM ( $n = 3$ ). Significant differences between control are indicated with \* $p < 0.05$  or \*\* $p < 0.01$  when compared with  $A\beta$  treatment.

detrimental for activity, and the *para*- and *ortho*-hydroxylation pattern of the polyphenol is not relevant.

It is also important to note that, as tested by a thioflavin-T (ThT) fluorescence assay with  $A\beta(1-42)$  (see Figure S5 in the Supporting Information), compounds of this series do not significantly inhibit  $A\beta(1-42)$  aggregation *per se*, which suggests that the inhibition of  $A\beta$ -induced Fyn kinase activation is unlikely to occur exclusively *via* direct interaction with  $A\beta$ . Most importantly, these results indicate that these compounds are not PAINS acting *via* autooxidation of catechol/hydroquinone and subsequent covalent binding to proteins, contrary to quercetin, a well-known PAIN compound<sup>48</sup> used as positive control in this assay.

To estimate eventual behavior of compounds **9**, **23**, and **26** as pan-assay interference compounds (PAINS), in particular as membrane PAINS, we have evaluated their potential using a computational protocol. The potential of mean force (PMF) for translocating a hydrophobic probe across a POPC bilayer loaded with compounds **9**, **23**, and **26** (10% mol/mol) and their calculated membrane permeabilities are shown in Figure 463

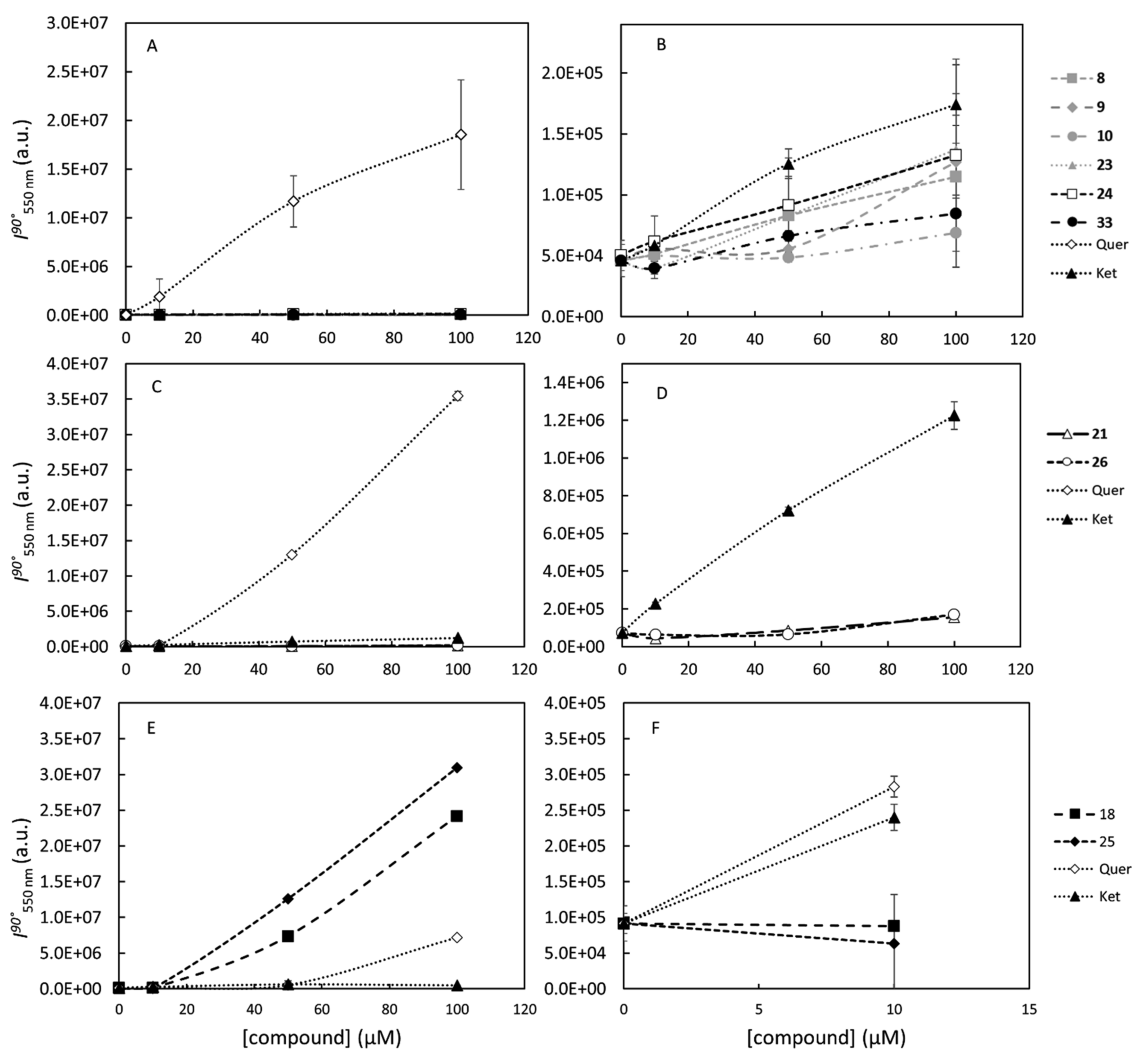


**Figure 8.** Static light scattering intensity at 550 nm and  $90^\circ$  for compounds (A, B) **8**, **9**, **10**, **23**, **24**, and **33**, (C, D) **21** and **26**, and (E, F) **18** and **25** and the respective controls: ketoconazole (Ket) and quercetin (Quer) at 10, 50, and 100  $\mu\text{M}$ . Samples were dissolved in 10 mM PBS (with 100 mM NaCl, pH 7.4) and 1.25% (A, B), 2.5% (C, D), or 5% (E, F) DMSO. The values are the mean  $\pm$  S.D. of at least two independent experiments. The graphics without Quer (B, D) are for a better depiction of the behavior of low scattering compounds. Graphic (F) is a zoom-in of (E) for a better observation of what is happening for the lowest concentration of the compounds. The lines are merely to guide the eye.

464 S6 and Table S1 in the Supporting Information. Membrane  
465 PAINS, even mild ones such as resveratrol,<sup>78</sup> make the  
466 membrane significantly more permeable to hydrophobic  
467 compounds. In contrast, none of our compounds led to a  
468 significant increase in membrane permeability, thus indicating  
469 that they do not act as membrane PAINS. In addition, we  
470 submitted their structure to the Badapple online service,<sup>79</sup> and  
471 the resulting promiscuity indicators also confirm that these  
472 compounds will unlikely act as PAINS.

473 **Aggregation Studies.** With the formation of aggregates, the  
474 concentration of free monomers in solution decreases, while  
475 the number and/or size of particles in suspension increase, and  
476 consequently, so does light scattering.<sup>49</sup> On the other hand,  
477 aggregate formation might also induce changes in vibrational  
478 progression and the appearance of exciton bands, which are  
479 readily detected in the electronic absorption spectra through  
480 changes in the spectral envelope, such as emergence of new  
481 bands, band broadening, and variation of the absorbance at  
482  $\lambda_{\text{max}}$ , which if there is no aggregation and other interferences,  
483 should have a linear relation with the concentration of the  
484 molecule.<sup>54</sup>

485 Aggregating and nonaggregating compounds have been  
486 successfully identified using static light scattering and/or  
487 electronic absorption spectroscopy to detect such alterations  
488 caused by aggregation. For instance, quercetin<sup>52</sup> and  
489 miconazole<sup>50,53</sup> were found to aggregate, while fluconazole  
490 and ketoconazole are nonaggregating molecules.<sup>50</sup>

491 Taking these findings into consideration, static light  
492 scattering and electronic absorption spectroscopy were used  
493 to assess compound aggregation behavior. Only compounds  
494 with interesting bioactivity were selected for these experiments,  
495 namely, compounds 8, 9, 10, 18, 21, 23, 24, 25, 26, and 33.  
496 The compounds under study were compared with ketoconazole, a known nonaggregating molecule acting as the negative  
497 control, and with quercetin, a promiscuous aggregator, used as  
498 the positive control.

500 Light scattering intensity for compounds 8, 9, 10, 23, 24,  
501 and 33 (Figure 8A,B) and 21 and 26 (Figure 8C,D) was  
502 similar or weaker than that for ketoconazole, for concentrations ranging from 10 to 100  $\mu\text{M}$ . Moreover, the values for  
503 those compounds were significantly lower than the light  
504 scattering intensity measured for quercetin. These results  
505 indicate that those eight compounds do not aggregate in this  
506 concentration range. Moreover, by comparing the normalized  
507 absorption spectra for each compound at different concentrations (Figures S7 and S8, Supporting Information), no  
508 alterations were observed in the absorption spectra of those  
509 eight compounds, both in terms of energy, vibrational  
510 progression or number of bands, also pointing to the absence  
511 of aggregation for these compounds. On the other hand, at  
512 high concentrations, the absorption spectra of the positive  
513 control, quercetin, suffers drastic changes (Figure S7,  
514 quercetin). First, the typical band of the monomeric species,  
515 with a maximum at ca. 385 nm,<sup>54</sup> suffers a blue shift to 330 nm  
516 and becomes broader. This is caused by the loss of the double  
517 bond character due to rotation of the 2–1' bond out of plane  
518 and, consequently, the loss of the planar conformation.<sup>54</sup> Also,  
519 new bands are visible at ca. 375 nm that indicate the presence  
520 of extended conjugation through catechol–catechol bonds. A  
521 new band is also visible for the highest concentration of 100  
522  $\mu\text{M}$  between 245 and 270 nm, which when compared with the  
523 absorption spectra of the different ionization states of the  
524 molecule,<sup>55,56</sup> may indicate an increase of the nonprotonated

quercetin species.<sup>57</sup> All these changes are related to the  
525 aggregation of the compound. In fact, the  $\text{p}K_{\text{a}}$  of a compound  
526 in an aggregate (e.g., micellar) environment is different from  
527 the one of the monomeric species in solution, shifting the  
528 ionization equilibrium.<sup>58</sup> If any of the compounds tested were  
529 aggregating, then changes in the absorption spectra would be  
530 readily detected, which was not the case. 533

534 For compounds 18 and 25, solutions with only 1.25 and  
535 2.5% DMSO were visibly turbid, especially for 100  $\mu\text{M}$ , which  
536 is an indication of the low aqueous solubility of these  
537 compounds that might be due to their high lipophilicity.  
538 With a value as high as 5% of DMSO, the solutions with higher  
539 compound concentrations (50 and 100  $\mu\text{M}$ ) were still turbid.  
540 However, this was not the case at 10  $\mu\text{M}$  and, as can be  
541 observed in Figure 8 for this concentration (at which the  
542 cellular studies were conducted), the light scattering intensity  
543 is lower than for the nonaggregating ketoconazole. This  
544 indicates that at this concentration, these two compounds  
545 are not aggregating.

546 Finally, a linear relationship was confirmed between the  
547 concentration and peak absorbance for the lower energy band  
548 of each compound and for the nonaggregating ketoconazole  
549 (Figures S9 and S10), while for the promiscuous quercetin,  
550 such relation does not follow a linear behavior (Figure S9,  
551 quercetin).

552 In summary, compounds 8, 9, 10, 21, 23, 24, 26, and 33 are  
553 not promiscuous aggregators in the concentration range tested,  
554 which encompasses all the concentrations used for the other  
555 assays. Our results for compounds 18 and 25 show that at the  
556 concentration of 10  $\mu\text{M}$ , no aggregation was detected but, at  
557 high concentrations, the herein presented inhibition constants  
558 should be considered only as estimates and interpreted with  
559 caution.

560 The aggregation studies confirm that bioactivities herein  
561 reported are not due to nonspecific effects resulting from the  
562 formation of compound aggregates and are thus the result of  
563 bona fide specific compound activity.

564 **Inhibition of  $A\beta$ -Induced Tau Phosphorylation.** Intra-  
565 neuronal neurofibrillary tangles (NFTs) of paired helical  
566 filaments (PHFs) are a histopathological hallmark of  
567 Alzheimer's disease (AD). This NFTs are formed of hyper-  
568 phosphorylated Tau. Tau is hyperphosphorylated in the AD  
569 brain at multiple sites including at residues Thr181.<sup>59–62</sup> To  
570 assess if the compounds are indeed able to accomplish the  
571 desired downstream effects by reducing  $A\beta$ -induced Tau  
572 pathology, we performed a high-content image screening  
573 (HCS) for phosphorylated Tau (pTau), at Thr181 as  
574 recognized by the antibody AT270, using compounds that  
575 were previously revealed to inhibit  $A\beta$ -induced Fyn activation.  
576 Our data (Figure 9) revealed that cortical neurons exposed to  
577  $A\beta$  have increased pTau levels when compared to DMSO  
578 controls. On the other hand, neurons treated with  $A\beta$  in  
579 addition to 10  $\mu\text{M}$  of compounds 9, 10, 18, 23, 25, 26, and 29  
580 and genistein significantly reduced the levels of pTau when  
581 compared to the  $A\beta$  controls. Even though there was a  
582 reduction of pTau in cells treated with compounds 8 and 33,  
583 this reduction was found not to be statistically significant.  
584 From all tested compounds, 9, 18, 23, 25, and 26 were able to  
585 reduce  $A\beta$ -induced Fyn activation, with concomitant decrease  
586 in  $A\beta$ -induced pTau.

587 **Cytotoxicity in Neuronal Cells Derived from hiPSCs.** To  
588 confirm that the synthesized compounds are not cytotoxic at  
589 relevant concentrations, we have differentiated hiPSC cells

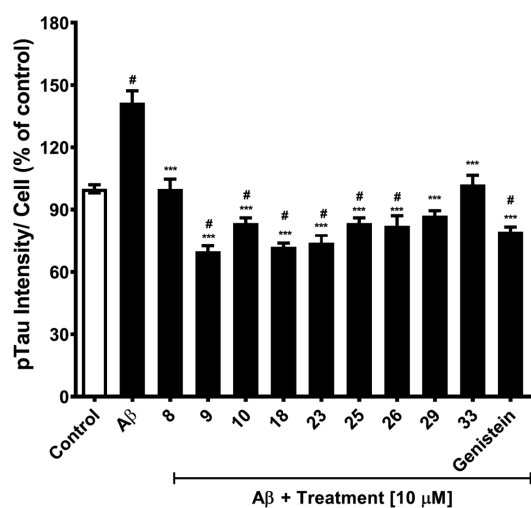


**Figure 9.** Effect of compounds against hyperphosphorylation of Tau induced by A $\beta$ . Neurons treated with A $\beta$  oligomers were evaluated against pTau (AT270). Tau hyperphosphorylation was measured by immunofluorescence using the Opera High Content Screening System. Cells were exposed to 10  $\mu$ M of each compound in association with A $\beta$  for 4 days. Results were normalized against the control group considered as 100%. The values are expressed as the mean  $\pm$  SEM;  $n = 3$ . Significant differences between control are indicated with #  $p \leq 0.05$  and \*  $p < 0.05$ , \*\*  $p < 0.01$ , or \*\*\*  $p < 0.001$  when compared with A $\beta$  treatment.

that are able to be absorbed into the bloodstream and thus contribute to the increase in glycemia levels.<sup>65</sup> Since we had previously elucidated the powerful  $\alpha$ -glucosidase inhibitory activity of the ethyl acetate extract of *Genista tenera* where compound **1** is the major component (97.6% for the extract vs 82.2% for the commercial drug acarbose), we were interested in finding out if it was due to the presence of the lead C-glucosyl isoflavone.<sup>66</sup> However, **1** was found to have only modest activity, with 14% inhibition at 100  $\mu$ M (Table 3). This compound was a slightly better  $\beta$ -glucosidase inhibitor, being able to decrease its activity in 23% at the same concentration. Notably, these activities are cumulative with the antihyperglycemic effects of **1** observed in Wistar rats since treatment was administered intraperitoneally.

Genistein, on the other hand, is a powerful  $\alpha$ -glucosidase uncompetitive inhibitor (84% inhibition at 100  $\mu$ M;  $K_{ib} = 12 \pm 2 \mu$ M) and moderate  $\beta$ -glucosidase competitive inhibitor (44% inhibition at 100  $\mu$ M;  $K_{ia} = 66 \pm 13 \mu$ M), indicating that the presence of the C–C linked sugar moiety at C-8 is, in this case, detrimental to activity. Remarkably, the catechol glucoside **33** was found to be the best glucosidase inhibitor among the synthesized analogues, with an excellent  $\alpha$ -glucosidase competitive inhibitor activity (74% inhibition at 100  $\mu$ M;  $K_{ia} = 39 \pm 4 \mu$ M) and modest  $\beta$ -glucosidase inhibitor activity (13% inhibition at 100  $\mu$ M). Apart from this compound, only three others were able to concomitantly inhibit both glucosidases: the hydroquinone derivatives **17** and **29** and the naphthalen-2-ol derivative **24**.

Acetylcholinesterase (AChE) and butyrylcholinesterase (BuChE) are two well-characterized therapeutic targets in AD owing to their ability to catalyze the hydrolysis of the neurotransmitter acetylcholine, which is responsible for the cognitive functionality and whose level is particularly low in AD patients. Three of the so far four FDA-approved drugs for AD consist of selective or dual cholinesterase inhibitors, including donepezil, galantamine, and rivastigmine.<sup>2</sup> The inhibition of AChE and BuChE correlates with lower A $\beta$  levels, decreased A $\beta$  aggregation, improved learning and memory.<sup>67–70</sup> BuChE is considered to play a minor role in the regulation in acetylcholine levels in healthy brains; however, the levels of this enzyme progressively increase in AD, whereas those of AChE decline or remain unchanged.<sup>71</sup>

Not so well studied and divulged is the role of butyrylcholinesterase in the etiology of T2D. However, elevated AChE, but especially serum BuChE activity, has been correlated with insulin resistance, increased adiposity, and abnormal serum lipid profile, being regarded as a risk factor for T2D.<sup>72–75</sup> Thus, these two enzymes may be regarded as additional therapeutic targets for DID.

Similar to what was described for  $\alpha$ -glucosidase, the ethyl acetate extract of *G. tenera* was capable of inhibiting this enzyme (77.0% at 130  $\mu$ g/mL).<sup>65</sup> Hence, we were interested in assessing whether the anticholinergic activity of the extract was due to the presence of **1** as a major component. This compound was however able to inhibit AChE only by 26% at 100  $\mu$ M (43  $\mu$ g/mL) and, in this assay, genistein presented merely half of the inhibitory capacity of **1** (Table 3). On the contrary, genistein was a much stronger BuChE inhibitor than **1**, displaying 41% inhibition at 100  $\mu$ M. From the synthesized analogues of **1**, only compounds **7**, **17**, **18**, and **33** were active against AChE, while roughly all presented a BuChE inhibition capacity of at least 10%. Compounds **10**, **11**, **22**, and **26** were

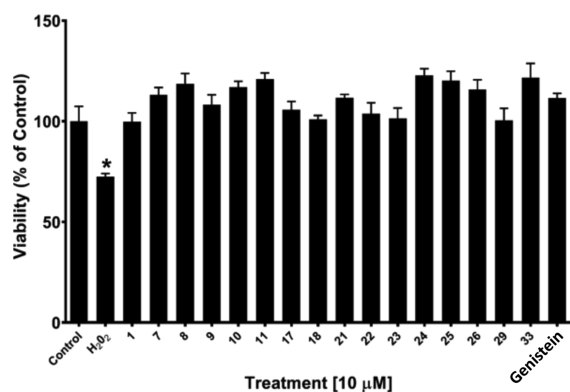


**Figure 10.** Cytotoxicity of C-glucosyl phenols and glucosides **29** and **33** in neuronal cells derived from hiPSCs. Cell viability was measured in an MTT assay. Cells were exposed to 10  $\mu$ M of each compound for 24 h. Results were normalized relative to a control group considered as 100%. The values are expressed as the mean  $\pm$  SEM;  $n = 3$ . Significant differences between control are indicated with \*  $p < 0.05$ .

Table 3. Glycosidase and Cholinesterase (AChE and BuChE) Inhibitory Efficacy of Compound 1 and Analogues at 100  $\mu\text{M}$ <sup>a</sup>

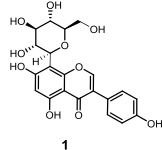
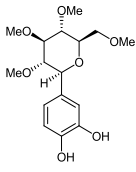
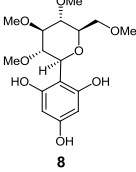
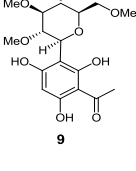
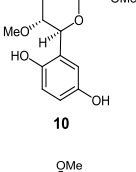
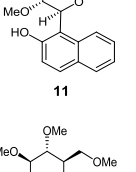
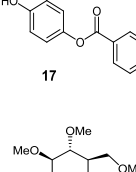
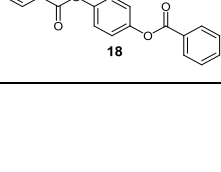
Compound	$\alpha$ -Glucosidase Inhibition	$\beta$ -Glucosidase Inhibition	AChE Inhibition	BuChE Inhibition
 <b>1</b>	14%	23%	26%	n.i.
 <b>7</b>	n.i.	14%	15%	16%
 <b>8</b>	n.i.	15%	n.i.	10%
 <b>9</b>	n.i.	n.i.	n.i.	16%
 <b>10</b>	n.i.	n.i.	n.i.	21%
 <b>11</b>	n.i.	16%	n.i.	23%
 <b>17</b>	11%	24%	14%	12%
 <b>18</b>	n.i.	18%	19%	16%

Table 3. continued

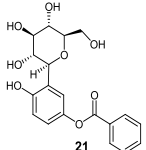
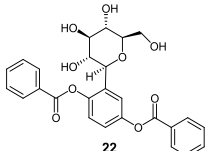
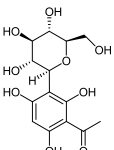
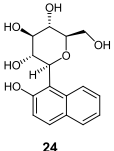
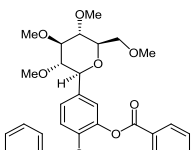
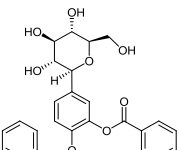
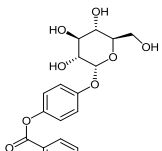
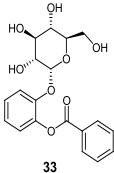
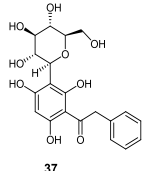
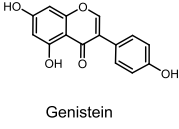
Compound	$\alpha$ -Glucosidase Inhibition	$\beta$ -Glucosidase Inhibition	AChE Inhibition	BuChE Inhibition
 21	n.i.	17%	n.i.	n.i.
 22	n.i.	18%	n.i.	21%
 23	n.i.	24%	n.i.	15%
 24	12%	23%	n.i.	10%
 25	n.i.	27%	n.i.	12%
 26	n.i.	17%	n.i.	39%
 29	18%	19%	n.i.	10%

Table 3. continued

Compound	$\alpha$ -Glucosidase	$\beta$ -Glucosidase	AChE	BuChE
	Inhibition	Inhibition	Inhibition	Inhibition
 33	74% Competitive inhibition $K_{ia} = 39 \pm 4 \mu\text{M}$	13%	10%	17%
 37	n.i.	n.i.	n.i.	17%
 Genistein	84% Uncompetitive inhibition $K_{ib} = 12 \pm 2 \mu\text{M}$	44% Competitive inhibition $K_{ia} = 66 \pm 13 \mu\text{M}$	12%	41%

<sup>a</sup> $K_{ia}$ , inhibition constant of the inhibitor binding the free enzyme;  $K_{ib}$ , inhibition constant of the inhibitor binding the enzyme–substrate complex; n.i., no inhibition; n.d., not determined.

666 able to inhibit BuChE in over 20% at 100  $\mu\text{M}$ , from which  
667 compound **26** stands out with 39% inhibition.

668 **Membrane Permeability Assays.** Compounds were tested  
669 in a parallel artificial membrane permeability assay (PAMPA)  
670 to measure and rationalize their potential to cross membrane  
671 barriers. Testosterone was used as the positive control in this  
672 assay. It is important to note that this assay merely looks into  
673 the ability of compounds to passively diffuse through cell  
674 membranes. Being glycosides, it is possible that the sugar  
675 moiety acts as a shuttle for their passage into the brain through  
676 GLUT-1 transporters highly expressed in the blood–brain  
677 barrier (BBB), as previously reported for similar molecules.<sup>74</sup>  
678 To complete our analysis, the partition coefficient at  
679 physiological pH ( $\log D_{7.4}$ ) was also determined for most  
680 compounds. Ideally,  $\log D$  values should be located between 1  
681 and 4 for a good compromise between solubility and  
682 membrane permeability, allowing oral availability, good cell  
683 permeation, and low metabolic susceptibility.<sup>74</sup> Results are  
684 presented in Table 4.

685 The optimal effective permeability of compound **1** ( $\log P_e >$   
686  $-5.7$ ) indicates that it can cross membrane barriers, which is  
687 consistent with the therapeutic use of the plant *G. tenera* in  
688 traditional medicine in the form of an antidiabetic tea infusion.  
689 Moreover, our results for compounds **7–11** suggest that the  
690 transformation of the sugar hydroxy groups into methyl ether  
691 moieties succeeded at enhancing membrane permeability (see  
692 fully unprotected compounds **23** and **24**). Among these  
693 compounds is **9**, the per-methylglucosyl derivative of  
694 acetophloroglucinol, which was found to decrease  $A\beta$ -induced  
695 Fyn activation with consequent downstream effects in the  
696 reduction of Tau hyperphosphorylation. This compound  
697 presented an effective permeability ( $\log P_e = -4.74 \pm 0.02$ )  
698 and determined  $\log D$  values ( $2.3 \pm 0.3$ ) that are compatible

**Table 4. Calculated Partition Coefficient ( $c \log P$ ), Effective Permeability ( $\log P_e$ ), and Partition Coefficient at pH 7.4 ( $\log D_{7.4}$ ) of the Synthesized Compounds and Genistein<sup>c</sup>**

compound no.	$c \log P^{a,b}$	$\log P_e$	$\log D_{7.4}$
1	-0.17	$-4.63 \pm 0.15$	$-0.1 \pm 0.1$
7	0.74	$-5.33 \pm 0.08$	$1.1 \pm 0.1$
8	0.58	$-5.24 \pm 0.17$	$1.6 \pm 0.2$
9	1.06	$-4.74 \pm 0.02$	$2.3 \pm 0.3$
10	0.75	$-5.52 \pm 0.07$	n.d.
11	1.96	$-4.39 \pm 0.04$	$2.7 \pm 0.2$
17	2.70	membrane retention over 80%	$3.2 \pm 0.1$
18	3.95	equilibrated	$>2.5$
21	0.60	$-6.35 \pm 0.12$	$<0.5$
22	1.93	$-5.18 \pm 0.61$	$2.0 \pm 0.2$
23	-1.23	below detection limit	n.d.
24	-0.44	$-6.41 \pm 0.24$	n.d.
25	3.81	partial membrane retention	$>2.5$
26	1.95	$-5.06 \pm 0.08$	n.d.
29	0.59	below detection limit	$1.0 \pm 0.1$
33	0.58	$-5.85 \pm 0.54$	$0.1 \pm 0.3$
37	0.13	n.d.	n.d.
genistein	2.45	$-4.49 \pm 0.04$	$3.3 \pm 0.2$
testosterone	2.99	$-4.42 \pm 0.09$	

<sup>a</sup>Calculated using ALOGPS 2.1. <sup>b</sup>Based on  $c \log P$  values, **1**, **23**, and **24** are classified as hydrophilic compounds ( $c \log P < 0$ ); **7**, **8**, **10**, **21**, **29**, **33**, and **37** are classified as moderately lipophilic ( $c \log P = 0-1$ ); **9**, **11**, **17**, **18**, **22**, **25**, and **26** and genistein are classified as lipophilic compounds ( $c \log P > 1$ ) (Table 5 and Experimental Section). <sup>c</sup>n.d., not determined.

with the desired pharmacokinetic profile and thus contrasting 699  
with its bioactive polyhydroxy analogue **23**. 700

When applied to compounds with more than one aromatic ring, this sugar per-methylation approach resulted in extremely lipophilic compounds with a tendency to equilibrate or to get retained in biological membranes (compounds **17**, **18**, and **25**). In contrast, with three aromatic rings but without the sugar *O*-methyl groups, compound **26**, another promising hit in our bioactivity experiments, presents an acceptable effective permeability ( $\log P_e = -5.06 \pm 0.08$ ).

## DISCUSSION AND CONCLUSIONS

In the present work, we have developed a library of glucosylpolyphenols inspired in the natural product with therapeutic potential **1** and explored their activity against multiple AD and T2D targets, namely, Fyn kinase, Tau hyperphosphorylation, hIAPP, glucosidase, and cholinesterase enzymes. On the path toward their synthesis, we disclosed the feasibility and effectiveness of *C*-glucosylation of polyphenols with different hydroxylation patterns and rationalized the importance of sugar protecting groups in these reactions. Moreover, we present an exception to the Fries-type rearrangement, leading to the *C*-glucosylation of unprotected polyphenols, which afforded compounds **7** and **12**, two important precursors in the synthesis of novel bioactive molecular entities against our targets of interest.

Being structurally less complex and synthesized in only five steps (*vs* nine steps required for the generation of the natural isoflavone **1**), the rationally designed analogue **21** is here presented as a new alternative for tackling hIAPP detrimental effects in T2D and DID. STD-NMR experiments show that compound **21** clearly binds to hIAPP and, in general, with a similar binding epitope to that of compound **1**, which highlights that the absence of the central fused ring system of isoflavone core does not disrupt the binding toward hIAPP. This result opens the door to further exploit this compound as a molecular probe against IAPP-induced pancreatic failure and IAPP-promoted cross-seeding events with  $A\beta$ . Even though it is not the right option when it comes to glucosidase or cholinesterase inhibition, our investigation revealed that compound **21** is effective in the prevention of  $A\beta$ -induced Fyn activation. Yet, we herein disclose that much simpler *C*-glucosyl polyphenols embody the right scaffold to tackle the chain of processes culminating in Tau hyperphosphorylation. One of these compounds is **9**, embodying a per-*O*-methylglucosyl C–C linked to 2,4,6-trihydroxyacetophenone. It was found to inhibit  $A\beta$ -induced Fyn kinase activation and to consequently reduce the levels of hyperphosphorylated Tau. Moreover, it has the right balance between effective permeability and lipophilicity to be orally available and brain penetrant, as revealed in PAMPA and  $\log D_{7.4}$  determination assays. With the additional advantage of being efficiently synthesized in only two steps, our results indicate that **9** should indeed be regarded as a new promising scaffold for further development against  $A\beta$ -induced Tau pathology in AD.

Another promising compound discovered in this study was **26**, with the free glucosyl group C–C linked to catechol dibenzoate. Indeed, it stood out in the PAMPA assay for being one of the polyhydroxy sugar derivatives with potential to cross biological membranes with the desired activity when it comes to  $A\beta$ -induced Fyn kinase activation and consequent Tau hyperphosphorylation levels. Furthermore, it was found to be a BuChE inhibitor (39% inhibition at 100  $\mu$ M). Curiously, when it comes to therapeutic potential through glucosidase inhibition, its *O*-glucosyl catechol monobenzoate analogue

**33** was the best within this series. It was able to inhibit  $\alpha$ -glucosidase in 74% at 100  $\mu$ M, as well as  $\beta$ -glucosidase, AChE and BuChE, but only to a lower extent (10–17% at 100  $\mu$ M). These results illustrate the impact of *C*-glucosylation *vs* *O*-glucosylation in the fine tuning of bioactivity of analogue structures and present both the *C*-glucosyl catechol **26** and *O*-glucosyl catechol **33** as new lead compounds against DID.

Ultimately, this study strongly evidences the potential of glucosylpolyphenols as therapeutic agents against AD and T2D and offers several lead structures with different hydroxylation patterns and adequate physicochemical profiles for further development against relevant therapeutic targets for both diseases. Very importantly, it shows, for the first time, that *C*-glucosyl polyphenols are promising scaffolds that are able to tackle  $A\beta$ -induced Fyn kinase activation with enough efficacy to reduce Tau phosphorylation, thus having the potential to change the paradigm of drug discovery against AD and DID.

## EXPERIMENTAL SECTION

**Chemistry.** HPLC-grade solvents and reagents were obtained from commercial suppliers and were used without further purification. Genistein was purchased from Sigma-Aldrich, while compound **1** was synthesized according to the previously described methodology.<sup>25</sup> Thin-layer chromatography (TLC) was carried out on aluminum sheets (20 × 20 cm) coated with silica gel 60F-254 (0.2 mm thick, Merck) with detection by charring with 10% H<sub>2</sub>SO<sub>4</sub> in ethanol. Column chromatography (CC) was performed using silica gel 230–400 mesh (Merck). Melting points were obtained with a SMP3 Melting Point Apparatus, Stuart Scientific, Bibby. Optical rotations were measured with a PerkinElmer 343. Nuclear magnetic resonance (NMR) experiments were recorded on a Bruker Avance 400 spectrometer at 298 K, operating at 100.62 MHz for <sup>13</sup>C and at 400.13 MHz for <sup>1</sup>H for solutions in CDCl<sub>3</sub>, CO(CH<sub>3</sub>)<sub>2</sub>, or CD<sub>3</sub>OD (Sigma-Aldrich). Chemical shifts are expressed in  $\delta$  (ppm) and the proton coupling constants *J* in Hertz (Hz), and spectra were assigned using appropriate COSY, DEPT, HMQC, and HMBC spectra (representative examples are provided in the Supporting Information appendix). The high-resolution mass spectra of new compounds were acquired on a Bruker Daltonics HR QqTOF Impact II mass spectrometer (Billerica, MA, USA). The nebulizer gas (N<sub>2</sub>) pressure was set to 1.4 bar, and the drying gas (N<sub>2</sub>) flow rate was set to 4.0 L/min at a temperature of 200 °C. The capillary voltage was set to 4500 V and the charging voltage was set to 2000 V. The purity of the final compounds tested was above 95% as confirmed by HPLC-DAD and/or HPLC-DAD-MS.

**General Methodology for the Synthesis of 2,3,4,6-Tetra-*O*-methyl- $\beta$ -D-glucopyranosyl)polyphenols (7–10) and 2-Hydroxy-1-(2,3,4,6-tetra-*O*-methyl- $\beta$ -D-glucopyranosyl)naphthalene (11).** Methyl 2,3,4,6-tetra-*O*-methyl- $\alpha$ -D-glucopyranoside<sup>39</sup> (1.0 g, 4.0 mmol) and the polyphenol/2-hydroxyaphthalene (8.0 mmol, 2 equiv) were dissolved in dry MeCN (18 mL). The mixture was stirred in the presence of 0.2 g of drierite, under a N<sub>2</sub> atmosphere, for 10 min at room temperature. Then, TMSOTf (0.73 mL, 4.0 mmol, 1 equiv) was added dropwise at –78 °C. The temperature was kept at –78 °C in the first 30 min and then allowed to increase to room temperature. The mixture was stirred for 18–48 h, after which the reaction was quenched by adding a few drops of triethylamine. The mixture was washed with brine and extracted with EtOAc (3 × 20 mL), and the organic layers were combined, dried over MgSO<sub>4</sub>, and concentrated under reduced pressure.

**1,2-Dihydroxy-4-(2,3,4,6-tetra-*O*-methyl- $\beta$ -D-glucopyranosyl)benzene (7).** The reaction crude was purified by column chromatography (dichloromethane/MeOH 1:0 → 50:1) to give **7** as a yellowish solid in 63% yield. *R*<sub>f</sub> (dichloromethane/MeOH, 20:1) = 0.31; m.p. = 117.5–118.4 °C;  $[\alpha]_D^{20} = -2^\circ$  (*c* 0.7, CHCl<sub>3</sub>); <sup>1</sup>H NMR [(CD<sub>3</sub>)<sub>2</sub>CO]  $\delta$  6.96 (s, 1H, H-3), 6.84 (d, 1H, *J*<sub>ortho</sub> = 8.07 Hz, H-6), 6.78 (br d, 1H, *J*<sub>ortho</sub> = 8.07 Hz, H-5), 3.98 (d, 1H, *J*<sub>1'-2'</sub> = 9.47 Hz, H-1'), 3.65 (s, 3H, OCH<sub>3</sub>), 3.61–3.51 (m, 5H, H-6'a and H-6'b,



830 OCH<sub>3</sub>), 3.43–3.39 (m, 1H, H-5'), 3.37 (s, 3H, OCH<sub>3</sub>), 3.29–3.24  
831 (m, 2H, H-3', H-4'), 3.06–3.02 (m, 4H, H-2', OCH<sub>3</sub>). <sup>13</sup>C NMR  
832 [(CD<sub>3</sub>)<sub>2</sub>CO] δ 144.8 (C-1)\*, 144.6 (C-2)\*, 131.5 (C-4), 119.31 (C-  
833 5), 114.7 (C-6), 114.6 (C-3), 88.34 (C-3'), 85.9 (C-2'), 81.0 (C-1'),  
834 79.8 (C-4'), 78.8 (C-5'), 71.7 (C-6'), 60.0, 59.6, 59.4, 58.5 (OCH<sub>3</sub>).  
835 \*Permutable signals. HRMS-ESI (*m/z*): [M + H]<sup>+</sup> calcd for  
836 C<sub>16</sub>H<sub>25</sub>O<sub>7</sub>, 329.1595; found, 329.1597; [M + Na]<sup>+</sup> calcd for  
837 C<sub>16</sub>H<sub>24</sub>NaO<sub>7</sub>, 351.1414; found, 351.1411.  
838 **1,3,5-Trihydroxy-2-(2,3,4,6-tetra-O-methyl-β-D-glucopyranosyl)-**  
839 **benzene (8)**. The reaction crude was purified by column  
840 chromatography (dichloromethane/MeOH, 1:0 → 40:1) followed  
841 by recrystallization in diethyl ether, affording **8** as a white solid in 53%  
842 yield. R<sub>f</sub> (dichloromethane/MeOH, 20:1) = 0.35; m.p. = 181.5–182.1  
843 °C; [α]<sub>D</sub><sup>20</sup> = +25° (c 0.4, CHCl<sub>3</sub>); <sup>1</sup>H NMR [(CD<sub>3</sub>)<sub>2</sub>CO] δ 8.17 (br s,  
844 1H, OH-5), 7.94 (br s, 2H, OH-1, OH-3), 5.93 (s, 2H, H-4, H-6),  
845 4.77 (d, 1H, J<sub>1'-2'</sub> = 9.53 Hz, H-1'), 3.62–3.54 (m, 5H, H-6'a and H-  
846 6'b, OCH<sub>3</sub>), 3.52 (s, 3H, OCH<sub>3</sub>), 3.41 (br d, J<sub>4'-5'</sub> = 9.14 Hz, 1H, H-  
847 5'), 3.34 (s, 3H, OCH<sub>3</sub>), 3.31–3.19 (m, 3H, H-2', H-3', H-4'), 3.10  
848 (s, 3H, OCH<sub>3</sub>). <sup>13</sup>C NMR [(CD<sub>3</sub>)<sub>2</sub>CO] δ 159.6 (C-5), 158.3 (C-1,  
849 C-3), 104.0 (C-2), 96.5 (C-4, C-6), 88.7 (C-3'), 84.7 (C-2'), 80.0 (C-  
850 4'), 79.5 (C-5'), 75.3 (C-1'), 71.7 (C-6'), 60.9, 60.6, 60.2, 59.3  
851 (OCH<sub>3</sub>). [M + H]<sup>+</sup> calcd for C<sub>16</sub>H<sub>25</sub>O<sub>8</sub>, 344.1544; found, 344.1545;  
852 [M + Na]<sup>+</sup> calcd for C<sub>16</sub>H<sub>24</sub>NaO<sub>8</sub>, 367.1363; found, 367.1369.  
853 **1-[2,4,6-Trihydroxy-3-(2,3,4,6-tetra-O-methyl-β-D-**  
854 **glucopyranosyl)phenyl]ethan-1-one (9)**. The reaction crude was  
855 purified by column chromatography (dichloromethane/MeOH, 1:0  
856 → 50:1) to give **9** as a colorless oil in 46% yield. R<sub>f</sub> (dichloro-  
857 methane/MeOH, 20:1) = 0.38 [α]<sub>D</sub><sup>20</sup> = +91° (c 0.4, CHCl<sub>3</sub>); <sup>1</sup>H  
858 NMR (CDCl<sub>3</sub>) δ 8.11 (br s, 1H, OH), 5.91 (br s, 1H, H-5), 4.73 (d,  
859 1H, J<sub>1'-2'</sub> = 9.80 Hz, H-1'), 3.68–3.64 (m, 5H, H-6'a and H-6'b,  
860 OCH<sub>3</sub>), 3.58 (s, 3H, OCH<sub>3</sub>), 3.48–3.44 (m, 4H, H-5', OCH<sub>3</sub>), 3.35–  
861 3.26 (m, 6H, H-2', H-3', H-4', OCH<sub>3</sub>), 2.66 (CH<sub>3</sub>-Ac); <sup>13</sup>C NMR  
862 (CDCl<sub>3</sub>) δ 203.9 (C=O), 164.4 (C-2), 161.8 (C-4)\*, 160.1 (C-6)\*,  
863 106.0 (C-1), 102.3 (C-5), 97.2 (C-3), 87.7 (C-3'), 84.9 (C-2'), 79.0  
864 (C-5'), 78.8 (C-4'), 75.1 (C-1'), 71.0 (C-6'), 61.1, 61.0, 60.7, 59.2  
865 (OCH<sub>3</sub>). \*Permutable signals. HRMS-ESI (*m/z*): [M + H]<sup>+</sup> calcd for  
866 C<sub>18</sub>H<sub>27</sub>O<sub>9</sub>, 387.1660; found, 387.1600; [M + Na]<sup>+</sup> calcd for  
867 C<sub>18</sub>H<sub>26</sub>NaO<sub>9</sub>, 409.1469; found, 409.1473.  
868 **1,4-Dihydroxy-2-(2,3,4,6-tetra-O-methyl-β-D-glucopyranosyl)-**  
869 **benzene (10)**. The reaction crude was purified by column  
870 chromatography (dichloromethane/MeOH, 1:0 → 40:1), followed  
871 by recrystallization in diethyl ether to afford **10** as a white solid in 37%  
872 yield. R<sub>f</sub> (dichloromethane/MeOH 20:1) = 0.34; m.p. = 124.5–125.0  
873 °C; [α]<sub>D</sub><sup>20</sup> = +18° (c 0.5, CHCl<sub>3</sub>); <sup>1</sup>H NMR [(CD<sub>3</sub>)<sub>2</sub>CO] δ 7.77 (s,  
874 1H, OH-1), 7.36 (s, 1H, OH-4), 6.74 (s, 1H, H-3), 6.69–6.64 (m,  
875 2H, H-5, H-6), 4.38 (d, 1H, J<sub>1'-2'</sub> = 9.59 Hz, H-1'), 3.66–3.56 (m,  
876 5H, OCH<sub>3</sub>, H-6'a and H-6'b), 3.52 (s, 3H, OCH<sub>3</sub>), 3.41 (br d, 1H,  
877 J<sub>5'-4'</sub> = 8.11 Hz, H-5'), 3.34 (s, 3H, OCH<sub>3</sub>), 3.29–3.21 (m, 2H, H-3',  
878 H-4'), 3.14 (t, 1H, J<sub>2'-1'-2'-3'</sub> = 9.72 Hz, H-2'), 3.09 (s, 3H, OCH<sub>3</sub>).  
879 <sup>13</sup>C NMR [(CD<sub>3</sub>)<sub>2</sub>CO] δ 150.9 (C-4), 148.7 (C-1), 126.4 (C-2),  
880 117.5 (C-6)\*, 116.0 (C-5)\*, 115.3 (C-3), 88.7 (C-3'), 85.4 (C-2'),  
881 80.0 (C-4'), 79.2 (C-5'), 78.0 (C-1'), 71.0 (C-6'), 60.5, 60.2, 60.1,  
882 58.9 (OCH<sub>3</sub>). \*Permutable signals. HRMS-ESI (*m/z*): [M + H]<sup>+</sup>  
883 calcd for C<sub>16</sub>H<sub>25</sub>O<sub>7</sub>, 329.1595; found, 329.1582; [M + Na]<sup>+</sup> calcd for  
884 C<sub>16</sub>H<sub>24</sub>NaO<sub>7</sub>, 351.1414; found, 351.1395.  
885 **2-Hydroxy-1-(2,3,4,6-tetra-O-methyl-β-D-glucopyranosyl)-**  
886 **naphthalene (11)**. The reaction crude was purified by column  
887 chromatography (Hex/dichloromethane, 1:1 → dichloromethane/  
888 MeOH, 100:1) to give **11** as a yellow oil in 66% yield. R<sub>f</sub> (Hex/  
889 EtOAc) = 0.58; [α]<sub>D</sub><sup>20</sup> = +89° (c 1.0, CHCl<sub>3</sub>); <sup>1</sup>H NMR (CDCl<sub>3</sub>) δ  
890 (ppm) 8.54 (s, 1H, OH-2), 7.97 (d, 1H, J<sub>ortho</sub> = 7.46 Hz, H-8), 7.72–  
891 7.68 (m, 2H, H-4, H-5), 7.43 (t, 1H, J<sub>ortho</sub> = 7.64 Hz, H-7), 7.28 (t,  
892 1H, J<sub>ortho</sub> = 7.39 Hz, H-6), 7.14 (d, 1H, J<sub>ortho</sub> = 8.83 Hz, H-3), 5.24 (d,  
893 1H, J<sub>1'-2'</sub> = 9.65 Hz, H-1'), 3.67–3.58 (m, 8H, 2 × OCH<sub>3</sub>, H-6'a and  
894 H-6'b), 3.51–3.45 (m, 3H, H-2', H-4', H-5'), 3.43–3.27 (m, 4H, H-  
895 3', OCH<sub>3</sub>), 2.70 (s, 3H, OCH<sub>3</sub>). <sup>13</sup>C NMR (CDCl<sub>3</sub>) δ (ppm) 154.5  
896 (C-2), 132.6 (C-8a), 130.3 (C-4), 128.7 (C-4a), 128.3 (C-5), 126.4  
897 (C-7), 123.0 (C-6), 122.6 (C-8), 119.7 (C-3), 114.7 (C-1), 87.8 (C-  
898 3'), 84.2 (C-2'), 78.7 (C-4'), 78.6 (C-5'), 76.7 (C-1'), 70.5 (C-6'),  
899 61.0, 60.7, 60.2, 59.3 (OCH<sub>3</sub>). [M + H]<sup>+</sup> calcd for C<sub>20</sub>H<sub>27</sub>O<sub>6</sub>,

363.1802; found, 363.1796; [M + Na]<sup>+</sup> calcd for C<sub>20</sub>H<sub>26</sub>NaO<sub>6</sub>, 900  
385.1622; found, 385.1624.

**1,2-Dihydroxy-4-(2,3,4,6-tetra-O-benzyl-β-D-**  
**glucopyranosyl)benzene (12)** and **2-Hydroxy-1-(2,3,4,6-tetra-**  
**O-benzyl-α-D-glucopyranosyloxy)benzene (31)**. To a solution of  
2,3,4,6-tetra-O-benzyl-α/β-D-glucopyranose (**4**, 2 g, 3.70 mmol) in  
dry dichloromethane (50 mL), catechol (0.81 g, 7.40 mmol, 2 equiv)  
was added, together with drierite (0.25 g), under a N<sub>2</sub> atmosphere. The mixture was stirred for 5 min at room  
temperature, which was then lowered to –78 °C. TMSOTf (0.68 mL,  
3.70 mmol, 1 equiv) was added in a dropwise manner. After stirring  
for 30 min, the mixture was stirred for 64 h at 40 °C. The reaction was  
stopped by adding a few drops of triethylamine; then, the mixture was  
filtered through a pad of Celite, washed with dichloromethane, and  
concentrated under vacuum. The residue was purified by column  
chromatography (1:0 → 15:1 cyclohexane/AcOEt), affording  
compound **12** in 6% yield as a colorless oil and compound **18** as a  
white solid in 35% yield.

**1,2-Dihydroxy-4-(2,3,4,6-tetra-O-benzyl-β-D-glucopyranosyl)-**  
**benzene (12)**. R<sub>f</sub> (hexane/AcOEt, 4:1) = 0.14; [α]<sub>D</sub><sup>20</sup> = –2° (c 0.1,  
CHCl<sub>3</sub>); <sup>1</sup>H NMR (CDCl<sub>3</sub>) δ (ppm) 7.37–7.16 (m, 18H, benzyl  
aromatics), 6.99–6.97 (m, 2H, benzyl aromatics), 6.85–6.82 (m, 2H,  
H-3, H-6), 6.79–6.76 (m, 1H, H-5), 5.00, 4.96 (part A<sub>1</sub> of A<sub>1</sub>B<sub>1</sub>  
system, 1H, J<sub>A<sub>1</sub>-B<sub>1</sub></sub> = 11.23 Hz, Ph-CH<sub>2</sub>), 4.90 (m, 2H, part B<sub>1</sub> of A<sub>1</sub>B<sub>1</sub>  
system, part A<sub>2</sub> of A<sub>2</sub>B<sub>2</sub> system, Ph-CH<sub>2</sub>), 4.64–4.55 (m, 3H, part B<sub>2</sub>  
of A<sub>2</sub>B<sub>2</sub> system, Ph-CH<sub>2</sub> and Ph-CH<sub>2</sub>), 4.40, 4.36 (part A<sub>3</sub> of A<sub>3</sub>B<sub>3</sub>  
system, 1H, J<sub>A<sub>3</sub>-B<sub>3</sub></sub> = 10.28 Hz, Ph-CH<sub>2</sub>), 4.12 (d, 1H, J<sub>1'-2'</sub> = 9.63 Hz,  
H-1'), 3.92, 3.88 (part B<sub>3</sub> of A<sub>3</sub>B<sub>3</sub> system, 1H, J<sub>A<sub>3</sub>-B<sub>3</sub></sub> = 10.27 Hz, Ph-  
CH<sub>2</sub>), 3.81–3.72 (m, 4H, H-3', H-4', H-6'a and H-6'b), 3.65–3.61  
(m, 1H, H-5'), 3.51 (t, 1H, J<sub>2'-3'-2'-1'</sub> = 9.15 Hz, H-2'). <sup>13</sup>C NMR  
(CDCl<sub>3</sub>) δ (ppm) 144.7 (C-2), 143.2 (C-1), 138.6, 138.1, 137.8,  
137.7 (benzyl C<sub>q</sub>-aromatics), 131.3 (C-4), 128.4–127.6 (benzyl CH-  
aromatics), 120.7 (C-5), 115.2 (C-6), 114.9 (C-3), 86.7 (C-3'), 83.9  
(C-2'), 81.7 (C-1'), 79.0 (C-5'), 78.4 (C-4'), 75.7, 75.1, 74.8, 73.5  
(CH<sub>2</sub>-Ph), 69.2 (C-6'). HRMS-ESI (*m/z*): [M + H]<sup>+</sup> calcd for  
C<sub>40</sub>H<sub>41</sub>O<sub>7</sub>, 633.2847; found, 633.2853; [M + Na]<sup>+</sup> calcd for  
C<sub>40</sub>H<sub>40</sub>NaO<sub>7</sub>, 655.2666; found, 655.2667.

**2-Hydroxy-1-(2,3,4,6-tetra-O-benzyl-α-D-glucopyranosyloxy)-**  
**benzene (31)**. R<sub>f</sub> (Hex/AcOEt, 4:1) = 0.58; m.p. = 104.2–106.0 °C;  
[α]<sub>D</sub><sup>20</sup> = +68° (c 1.0, CHCl<sub>3</sub>); <sup>1</sup>H NMR (CDCl<sub>3</sub>) δ (ppm) 7.37–7.22  
(m, 17H, benzyl aromatics), 7.18–7.15 (m, 3H, benzyl aromatics),  
7.09 (d, 1H, J<sub>ortho</sub> = 8.06 Hz, H-3), 7.02–6.95 (m, 2H, H-4, H-6),  
6.75 (dt, 1H, J<sub>ortho</sub> = 7.68 Hz, J<sub>meta</sub> = 1.58 Hz, H-5), 4.99–4.90 (m,  
3H, H-1', Ph-CH<sub>2</sub>), 4.87–4.81 (m, 2H, part A<sub>1</sub> of A<sub>1</sub>B<sub>1</sub> system, part  
A<sub>2</sub> of A<sub>2</sub>B<sub>2</sub> system, Ph-CH<sub>2</sub>), 4.72, 4.68 (part A<sub>2</sub> of A<sub>2</sub>B<sub>2</sub> system, 1H,  
J<sub>A<sub>2</sub>-B<sub>2</sub></sub> = 11.96 Hz, Ph-CH<sub>2</sub>), 4.64, 4.60 (part A<sub>3</sub> of A<sub>3</sub>B<sub>3</sub> system, 1H,  
J<sub>A<sub>3</sub>-B<sub>3</sub></sub> = 12.08 Hz, Ph-CH<sub>2</sub>), 4.55, 4.51 (part B<sub>1</sub> of A<sub>1</sub>B<sub>1</sub> system, 1H,  
J<sub>A<sub>1</sub>-B<sub>1</sub></sub> = 11.04 Hz, Ph-CH<sub>2</sub>), 4.50, 4.46 (part B<sub>3</sub> of A<sub>3</sub>B<sub>3</sub> system, 1H,  
J<sub>A<sub>3</sub>-B<sub>3</sub></sub> = 11.93 Hz, Ph-CH<sub>2</sub>), 4.21–4.14 (m, 2H, H-3', H-4'), 3.81–  
3.69 (m, 3H, H-6'a and H-6'b, H-5'), 3.67 (dd, 1H, J<sub>1'-2'</sub> = 3.53 Hz,  
J<sub>2'-3'</sub> = 9.65 Hz, H-2'). <sup>13</sup>C NMR (CDCl<sub>3</sub>) δ (ppm) 148.6 (C-2),  
145.2 (C-1), 138.4, 138.1, 137.8, 137.0 (benzyl C<sub>q</sub>-aromatics),  
128.5–127.7 (benzyl CH-aromatics), 125.2 (C-4), 120.3 (C-5)\*,  
119.9 (C-3)\*, 115.8 (C-6), 101.1 (C-1'), 81.9 (C-3'), 79.0 (C-2'),  
77.5 (C-5'), 75.6, 75.0, 74.2, 73.5 (CH<sub>2</sub>-Ph), 71.5 (C-4'), 68.3 (C-6').  
\*Permutable signals. HRMS-ESI (*m/z*): [M + H]<sup>+</sup> calcd for  
C<sub>40</sub>H<sub>41</sub>O<sub>7</sub>, 633.2847; found, 633.2853; [M + Na]<sup>+</sup> calcd for  
C<sub>40</sub>H<sub>40</sub>NaO<sub>7</sub>, 655.2666; found, 655.2667.

**1,3,5-Trihydroxy-2-(2,3,4,6-tetra-O-benzyl-β-D-**  
**glucopyranosyl)benzene (13)**. To a solution of 2,3,4,6-tetra-O-  
benzyl-α/β-D-glucopyranose (2 g, 3.70 mmol) in dry dichloro-  
methane (50 mL), 2,4,6-trihydroxyacetophenone (0.93 g, 7.40 mmol,  
2 equiv) in dry MeCN (50 mL) was added, together with drierite  
(0.25 g), under a N<sub>2</sub> atmosphere. The mixture was stirred for 5 min at  
room temperature, which was then lowered to –78 °C. TMSOTf  
(0.68 mL, 3.70 mmol, 1 equiv) was added in a dropwise manner. After  
stirring for 30 min, the mixture was left at room temperature under  
stirring overnight. The reaction was stopped by adding a few drops of  
triethylamine; then, dichloromethane was evaporated and the mixture  
was washed with brine and extracted with ethyl acetate (3 × 50 mL).

970 The organic layers were combined, dried over  $\text{MgSO}_4$ , filtered, and  
971 concentrated under vacuum. The residue was purified by column  
972 chromatography (10:1  $\rightarrow$  5:1 cyclohexane/acetone), affording  
973 compound **13** in 42% yield as a colorless oil.  $R_f$  (cyclohexane/  
974 acetone, 3:2) = 0.41;  $[\alpha]_D^{20} = +12^\circ$  ( $c$  0.2,  $\text{CHCl}_3$ );  $^1\text{H NMR}$  ( $\text{CDCl}_3$ )  
975  $\delta$  (ppm) 7.35–7.19 (m, 16H, benzyl aromatics), 7.16–7.12 (m, 2H,  
976 benzyl aromatics), 7.08–7.04 (m, 2H, benzyl aromatics), 6.02 (s, 2H,  
977 H-4, H-6), 4.93 ( $A_1B_1$  system, 2H, Ph- $\text{CH}_2$ ), 4.83–4.79 (m, 2H, H-1',  
978 part  $A_2$  of  $A_2B_2$  system, Ph- $\text{CH}_2$ ), 4.65, 4.63 (part  $A_3$  of  $A_3B_3$  system,  
979 1H,  $J_{A_3-B_3} = 10.21$  Hz, Ph- $\text{CH}_2$ ), 4.59, 4.55 (part  $A_4$  of  $A_4B_4$  system,  
980 1H,  $J_{A_4-B_4} = 12.05$  Hz, 1H, Ph- $\text{CH}_2$ ), 4.54, 4.50 (part  $B_3$  of  $A_3B_3$   
981 system, 1H,  $J_{A_3-B_3} = 10.91$  Hz, Ph- $\text{CH}_2$ ), 4.45, 4.41 (part  $B_4$  of  $A_4B_4$   
982 system, 1H,  $J_{A_4-B_4} = 12.05$  Hz, Ph- $\text{CH}_2$ ), 3.88 (t, 1H,  $J_{4'-3'-4'-5'} =$   
983 8.80 Hz, H-4'), 3.79–3.65 (m, 4H, H-2', H-3', H-6'a and H-6'b),  
984 3.56 (br d, 1H,  $J_{5'-4'} = 9.71$  Hz, H-5').  $^{13}\text{C NMR}$  ( $\text{CDCl}_3$ )  $\delta$  (ppm)  
985 157.3 (C-1, C-3), 156.3 (C-5), 138.4, 138.9, 137.6, 136.4 (benzyl  $C_q$ -  
986 aromatics), 128.8–127.5 (benzyl CH-aromatics), 104.1 (C-2), 97.8  
987 (C-4, C-6), 86.2 (C-3'), 82.7 (C-2'), 78.7 (C-5'), 77.2 (C-4'), 76.2  
988 (C-1'), 75.6, 75.5, 75.2, 73.4 ( $\text{CH}_2$ -Ph), 67.6 (C-6'). HRMS-ESI ( $m/z$ )  
989  $z$ :  $[\text{M} + \text{H}]^+$  calcd for  $\text{C}_{40}\text{H}_{41}\text{O}_8$ , 649.2796; found, 649.2806;  $[\text{M} +$   
990  $\text{Na}]^+$  calcd for  $\text{C}_{40}\text{H}_{40}\text{NaO}_8$ , 671.2615; found, 671.2621.

991 **1-[2,4,6-Trihydroxy-3-(2,3,4,6-tetra-O-benzyl- $\beta$ -D-  
992 glucopyranosyl)phenyl]ethan-1-one (14)**. Synthesis and charac-  
993 terization as described in the literature.<sup>25</sup>

994 **1,4-Dihydroxy-2-(2,3,4,6-tetra-O-benzyl- $\beta$ -D-  
995 glucopyranosyl)benzene (15)** and **4-Hydroxy-1-(2,3,4,6-tetra-  
996 O-benzyl- $\alpha/\beta$ -D-glucopyranosyloxy)benzene (27 $\alpha,\beta$ )**. To a  
997 solution of 1-O-acetyl-2,3,4,6-tetra-O-benzyl- $\alpha/\beta$ -D-glucopyranose  
998 (**6**, 2.16 g, 3.70 mmol) in dry dichloromethane (50 mL),  
999 hydroquinone (0.61 g, 5.55 mmol, 1.5 equiv) in dry MeCN (10  
1000 mL) was added, together with drierite (0.25 g), under a  $\text{N}_2$   
1001 atmosphere. The mixture was stirred for 5 min at room temperature,  
1002 which was then lowered to 0  $^\circ\text{C}$ .  $\text{BF}_3\cdot\text{Et}_2\text{O}$  (1.1 mL, 3.70 mmol, 1  
1003 equiv) was added in a dropwise manner. After stirring for 30 min, the  
1004 temperature was raised to 40  $^\circ\text{C}$  and the mixture was stirred for 44 h.  
1005 The reaction was stopped by adding a few drops of triethylamine;  
1006 then, the mixture was filtered through a pad of Celite, washed with  
1007 dichloromethane, and concentrated under vacuum. The residue was  
1008 purified by column chromatography (50:1  $\rightarrow$  30:1 toluene/acetone)  
1009 followed by recrystallization in diethyl ether to afford compound **15** in  
1010 8% yield as a white solid and **27 $\alpha,\beta$**  isolated as a white solid with  $\alpha/\beta$   
1011 ratio = 4:1 in 36% yield.

1012 **1,4-Dihydroxy-2-(2,3,4,6-tetra-O-benzyl- $\beta$ -D-glucopyranosyl)-  
1013 benzene (15)**.  $R_f$  (toluene/acetone, 10:1) = 0.43; m.p. = 107.2–109.1  
1014  $^\circ\text{C}$ ;  $[\alpha]_D^{20} = +16^\circ$  ( $c$  0.3,  $\text{CHCl}_3$ );  $^1\text{H NMR}$  [ $\text{CO}(\text{CD}_3)_2$ ]  $\delta$  (ppm)  
1015 7.40–7.19 (m, 18H, benzyl aromatics), 7.10–7.07 (m, 2H, benzyl  
1016 aromatics), 6.86 (d, 1H,  $J_{\text{meta}} = 2.15$  Hz, H-3), 6.75–6.69 (m, 2H, H-  
1017 5, H-6), 4.97, 4.93 (part  $A_1$  of  $A_1B_1$  system, 1H,  $J_{A_1-B_1} = 11.24$  Hz,  
1018 Ph- $\text{CH}_2$ ), 4.89–4.87 (m, part  $B_1$  of  $A_1B_1$  system, part  $A_2$  of  $A_2B_2$   
1019 system, 2H, Ph- $\text{CH}_2$ ), 4.67–4.53 (m, 4H, part  $B_2$  of  $A_2B_2$  system, Ph-  
1020  $\text{CH}_2$ , H-1'), 4.46, 4.42 ( $A_3$  of  $A_3B_3$  system, 1H,  $J_{A_3-B_3} = 10.41$  Hz, Ph-  
1021  $\text{CH}_2$ ), 4.01, 3.97 ( $B_3$  of  $A_3B_3$  system, 1H,  $J_{A_3-B_3} = 10.45$  Hz, Ph- $\text{CH}_2$ ),  
1022 3.84–3.75 (m, 4H, H-3', H-4', H-6'a and H-6'b), 3.68–3.64 (m, 2H,  
1023 H-2', H-5').  $^{13}\text{C NMR}$  [ $\text{CO}(\text{CD}_3)_2$ ]  $\delta$  (ppm) 151.2 (C-1), 149.2 (C-  
1024 4), 140.0, 139.5, 139.4, 139.0 (benzyl  $C_q$ -aromatics), 129.0–128.0  
1025 (benzyl CH-aromatics), 126.3 (C-2), 117.8 (C-6), 116.4 (C-5), 116.1  
1026 (C-3), 87.0 (C-3'), 83.5 (C-2'), 79.6 (C-5'), 78.8 (C-1'), 78.7 (C-4'),  
1027 75.8, 75.3, 75.2, 73.7 ( $\text{CH}_2$ -Ph), 69.5 (C-6'). HRMS-ESI ( $m/z$ ):  $[\text{M} +$   
1028  $\text{H}]^+$  calcd for  $\text{C}_{40}\text{H}_{41}\text{O}_7$ , 633.2851; found, 633.2853;  $[\text{M} + \text{Na}]^+$  calcd  
1029 for  $\text{C}_{40}\text{H}_{40}\text{NaO}_7$ , 655.2666; found, 655.2671.

1030 **4-Hydroxy-1-(2,3,4,6-tetra-O-benzyl- $\alpha/\beta$ -D-glucopyranosyloxy)-  
1031 benzene (27 $\alpha,\beta$ )**.  $R_f$  (toluene/acetone, 10:1) = 0.50; m.p. = 138.4–  
1032 141.2  $^\circ\text{C}$ ;  $[\alpha]_D^{20} = +53^\circ$  ( $c$  0.4,  $\text{CHCl}_3$ );  $^1\text{H NMR}$  ( $\text{CDCl}_3$ )  $\delta$  7.38–  
1033 7.24 (m, 95H, CH-Ph), 3.18–3.12 (m, 5H, CH-Ph), 6.92–6.88 (m,  
1034 10H, H-3 $_{\omega}$ , H-3 $_{\beta}$ , H-5 $_{\omega}$ , H-5 $_{\beta}$ ), 6.62 (d, 10H,  $J_{\text{ortho}} = 8.73$  Hz, H-2 $_{\omega}$ , H-  
1035 2 $_{\beta}$ , H-6 $_{\omega}$ , H-6 $_{\beta}$ ), 5.32 (d, 4H,  $J_{1'-2'} = 3.33$  Hz, H-1' $_{\alpha}$ ), 5.06, 5.02 (part  
1036  $A_1$  of  $A_1B_1$  system, 5H,  $J_{A_1-B_1} = 10.81$  Hz,  $\text{CH}_2$ -Ph), 4.97, 4.93 (part  
1037  $A_2$  of  $A_2B_2$  system, 1H,  $J_{A_2-B_2} = 10.90$  Hz,  $\text{CH}_2$ -Ph), 4.89–4.76 (m,  
1038 16H, H-1' $_{\beta}$ , part  $B_1$  of  $A_1B_1$  system, part  $B_2$  of  $A_2B_2$  system,  $\text{CH}_2$ -Ph),  
1039 4.69, 4.65 (part  $A_3$  of  $A_3B_3$  system, 4H,  $J_{A_3-B_3} = 11.98$  Hz,  $\text{CH}_2$ -Ph),

4.59–4.47 (m, 11H,  $\text{CH}_2$ -Ph), 4.40, 4.36 (part  $B_3$  of  $A_3B_3$  system, 4H,  
 $J_{A_3-B_3} = 11.99$  Hz,  $\text{CH}_2$ -Ph), 4.20 (t, 4H,  $J_{3'-2'} = J_{3'-4'} = 9.28$  Hz, H-  
3' $_{\alpha}$ ), 3.93 (br d, 4H,  $J_{5'-4'} = 9.59$  Hz, H-5' $_{\alpha}$ ), 3.78–3.63 (m, 17H, H-  
2' $_{\omega}$ , H-4' $_{\omega}$ , H-2' $_{\beta}$ , H-3' $_{\beta}$ , H-4' $_{\beta}$ , H-5' $_{\beta}$ , H-6' $_{\alpha}$ , H-6' $_{\beta}$ ), 3.57 (br d,  
5H,  $J_{6'a-6'b} = 9.94$  Hz, H-6' $_{\alpha}$ , H-6' $_{\beta}$ ).  $^{13}\text{C NMR}$  ( $\text{CDCl}_3$ )  $\delta$  151.6  
(C-4 $_{\beta}$ ), 151.3 (C-1 $_{\beta}$ ), 151.2 (C-4 $_{\alpha}$ ), 150.5 (C-1 $_{\alpha}$ ), 138.7, 138.5, 138.2,  
137.9, 137.9, 137.7 ( $C_q$ -Ph), 128.6–127.8 (CH-Ph), 118.5 (C-3 $_{\beta}$ , C-  
5 $_{\beta}$ ), 118.3 (C-3 $_{\omega}$ , C-5 $_{\alpha}$ ), 116.1 (C-2 $_{\beta}$ , C-6 $_{\beta}$ ), 116.1 (C-2 $_{\omega}$ , C-6 $_{\alpha}$ ), 102.8  
(C-1' $_{\beta}$ ), 96.4 (C-1' $_{\alpha}$ ), 84.6 (C-2' $_{\beta}$ ), 82.1 (C-3' $_{\beta}$ ), 82.0 (C-3' $_{\alpha}$ ), 79.8  
(C-2' $_{\alpha}$ ), 77.8 (C-4' $_{\beta}$ ), 77.5 (C-4' $_{\alpha}$ ), 75.9, 75.2, 75.2 ( $\text{CH}_2$ -Ph), 73.5,  
73.5, 73.4 ( $\text{CH}_2$ -Ph), 70.7 (C-5' $_{\alpha}$ ), 70.2 (C-5' $_{\beta}$ ), 68.9 (C-6' $_{\beta}$ ), 68.3  
(C-6' $_{\alpha}$ ). HRMS-ESI ( $m/z$ ):  $[\text{M} + \text{H}]^+$  calcd for  $\text{C}_{40}\text{H}_{41}\text{O}_7$ , 633.2847;  
found, 633.2847;  $[\text{M} + \text{Na}]^+$  calcd for  $\text{C}_{40}\text{H}_{40}\text{NaO}_7$ , 655.2666; found,  
655.2669.

**2-Hydroxy-1-(2,3,4,6-tetra-O-benzyl- $\beta$ -D-glucopyranosyl)-  
naphthalene (16)**. To a solution of 2,3,4,6-tetra-O-benzyl- $\alpha$ -D-  
glucopyranosyl trichloroacetimidate (**5**, 1.27 g, 1.85 mmol) in dry  
dichloromethane (10 mL), 2-naphthol (0.222 g, 0.83 equiv) was  
added in the presence of activated molecular sieves (3  $\text{\AA}$ ), at 0  $^\circ\text{C}$ ,  
under a  $\text{N}_2$  atmosphere. TMSOTf (0.33 mL, 1.85 mmol, 1 equiv) was  
then added in a dropwise manner and the mixture stirred for 20 h at  
room temperature. The reaction was stopped by adding a few drops of  
triethylamine; then, the mixture was filtered through a pad of Celite,  
washed with dichloromethane, and concentrated under vacuum. The  
residue was purified by column chromatography (p. ether/EtOAc, 1:0  
 $\rightarrow$  15:1), affording compound **16** as a colorless oil in 43% yield.  $R_f$   
(hexane/EtOAc, 5:1) = 0.47;  $[\alpha]_D^{20} = +3^\circ$  ( $c$  0.3,  $\text{CHCl}_3$ );  $^1\text{H NMR}$   
( $\text{CDCl}_3$ )  $\delta$  (ppm) 8.73 (br s, 1H, OH-2), 8.07 (d, 1H,  $J_{\text{ortho}} = 7.75$   
Hz, H-8), 7.87–7.79 (m, 2H, H-4, H-5), 7.48–6.95 (m, 22H, benzyl  
aromatics, H-6, H-7), 6.33 (d, 1H,  $J_{\text{ortho}} = 7.13$  Hz, H-3), 5.47 (d, 1H,  
 $J_{1'-2'} = 9.68$  Hz, H-1'), 5.06–5.46 (m, 6H, Ph- $\text{CH}_2$ ), 4.25–3.41 (m,  
8H, H-2', H-3', H-4', H-5', H-6'a and H-6'b, Ph- $\text{CH}_2$ ).  $^{13}\text{C NMR}$   
( $\text{CDCl}_3$ )  $\delta$  (ppm) 154.8 (C-2), 138.7, 138.1, 137.8, 136.8, (benzyl  
 $C_q$ -aromatics), 132.7 (C-8a), 130.5 (C-4), 128.7–127.5 (benzyl CH-  
aromatics, C-4a, C-5), 126.7 (C-7), 123.2 (C-6), 122.9 (C-8), 119.8  
(C-3), 114.6 (C-1), 86.2 (C-3'), 81.9 (C-2'), 78.7 (C-4'), 77.8 (C-  
5'), 77.1 ( $\text{CH}_2$ -Ph), 76.9 (C-1'), 75.7, 75.4, 73.4 ( $\text{CH}_2$ -Ph), 67.8 (C-  
6'). HRMS-ESI ( $m/z$ ):  $[\text{M} + \text{H}]^+$  calcd for  $\text{C}_{44}\text{H}_{43}\text{O}_6$ , 667.3054;  
found, 667.3047;  $[\text{M} + \text{Na}]^+$  calcd for  $\text{C}_{44}\text{H}_{42}\text{NaO}_6$ , 689.2874; found,  
689.2874.

**4-Hydroxy-3-(2,3,4,6-tetra-O-methyl- $\beta$ -D-glucopyranosyl)-  
benzen-1-yl Benzoate (17)** and **3-(2,3,4,6-Tetra-O-methyl- $\beta$ -D-  
glucopyranosyl)benzen-1,4-diyl Dibenzoate (18)**. Compound  
**10** (0.50 g, 1.55 mmol, 1 equiv) was dissolved in dry dichloromethane  
(21 mL) together with imidazole (0.12 g, 1.71 mmol, 1.1 equiv) and  
DMAP (cat.). After stirring for 10 min at 0  $^\circ\text{C}$ , benzoyl chloride (0.2  
mL, 1.71 mmol, 1.1 equiv) was added dropwise. The reaction mixture  
was stirred at room temperature for 66 h, after which it was washed  
with brine and extracted with dichloromethane (2  $\times$  20 mL). The  
organic layers were combined, dried over  $\text{MgSO}_4$ , and concentrated  
under reduced pressure. The residue was purified by column  
chromatography (p. ether/EtOAc, 1:0  $\rightarrow$  2:1), affording compound  
**17** as a colorless oil in 65% yield and compound **18** as a white solid in  
22% yield.

**4-Hydroxy-3-(2,3,4,6-tetra-O-methyl- $\beta$ -D-glucopyranosyl)-  
benzen-1-yl Benzoate (17)**.  $R_f$  (p. ether/EtOAc, 2:1) = 0.31;  $[\alpha]_D^{20} =$   
 $+16^\circ$  ( $c$  0.7, MeOH);  $^1\text{H NMR}$  ( $\text{CDCl}_3$ )  $\delta$  8.18 (d, 2H,  $J_{\text{ortho}} = 7.38$   
Hz, H-2', H-6'), 7.75 (s, 1H, OH-4), 7.62 (t, 1H,  $J_{\text{ortho}} = 7.38$  Hz, H-  
4'), 7.50 (t, 2H,  $J_{\text{ortho}} = 7.61$  Hz, H-3', H-5'), 7.08–7.04 (m, 2H, H-2,  
H-6), 6.95 (d, 1H,  $J_{\text{ortho}} = 6.95$  Hz, H-5), 4.32 (d, 1H,  $J_{1'-2'} = 9.60$   
Hz, H-1'), 3.67 (s, 3H,  $\text{OCH}_3$ ), 3.64–3.62 (m, 2H, H-6'a and b),  
3.58 (s, 3H,  $\text{OCH}_3$ ), 3.43–3.40 (m, 4H, H-5'',  $\text{OCH}_3$ ), 3.36–3.28  
(m, 2H, H-3'', H-4''), 3.24 (s, 3H,  $\text{OCH}_3$ ), 3.21–3.19 (m, 1H, H-2'').  
 $^{13}\text{C NMR}$  ( $\text{CDCl}_3$ )  $\delta$  165.6 (C=O), 152.7 (C-4), 144.0 (C-1), 133.6  
(C-4'), 130.2 (C-2', C-6'), 129.8 (C-1'), 128.6 (C-3', C-5'), 125.0  
(C-3), 122.4 (C-6), 121.3 (C-2), 118.1 (C-5), 88.2 (C-3''), 84.8 (C-  
2''), 79.2 (C-4''), 79.1 (C-1''), 78.8 (C-5''), 70.9 (C-6''), 61.0, 60.7,  
59.4 ( $\text{OCH}_3$ ). HRMS-ESI ( $m/z$ ):  $[\text{M} + \text{H}]^+$  calcd for  $\text{C}_{23}\text{H}_{29}\text{O}_8$ ,  
433.1857; found, 433.1861;  $[\text{M} + \text{Na}]^+$  calcd for  $\text{C}_{23}\text{H}_{28}\text{NaO}_8$ ,  
455.1676; found, 455.1678.

1110 3-(2,3,4,6-Tetra-O-methyl- $\beta$ -D-glucopyranosyl)benzene-1,4-diyl  
1111 Dibenzoate (18).  $R_f$  (p. ether/EtOAc, 2:1) = 0.47; m.p. = 102.6–  
1112 103.8 °C;  $[\alpha]_D^{20} = +5^\circ$  (c 0.7, CHCl<sub>3</sub>); <sup>1</sup>H NMR (CDCl<sub>3</sub>)  $\delta$  8.24–  
1113 8.20 (m, 4H, H-2', H-6'), 7.65 (t, 2H,  $J_{ortho} = 6.99$  Hz, H-4'), 7.56–  
1114 7.51 (m, 4H, H-3', H-5'), 7.40 (d, 1H,  $J_{meta} = 2.22$  Hz, H-3), 7.32–  
1115 7.24 (m, 2H, H-5, H-6), 4.43 (d, 1H,  $J_{1''-2''} = 8.77$  Hz, H-1''), 3.58 (s,  
1116 3H, OCH<sub>3</sub>), 3.56 (br s, 1H, H-6''a), 3.51 (s, 3H, OCH<sub>3</sub>), 3.48–3.44  
1117 (m, 1H, H-6''b), 3.39–3.33 (m, 4H, OCH<sub>3</sub>, H-5''), 3.23–3.12 (m,  
1118 6H, OCH<sub>3</sub>, H-2'', H-3'', H-4''). <sup>13</sup>C NMR (CDCl<sub>3</sub>)  $\delta$  165.1 (C=O),  
1119 164.7 (C=O), 148.5 (C-1), 146.3 (C-4), 133.8, 133.6 (C-4'), 132.8  
1120 (C-3), 130.4, 130.3 (C-2', C-6'), 129.8, 129.5 (C-1'), 128.7 (C-3', C-  
1121 5'), 124.0 (C-5), 122.1 (C-6), 121.9 (C-2), 88.5 (C-3''), 85.5 (C-2''),  
1122 80.0 (C-4''), 79.4 (C-5''), 76.2 (C-1''), 71.8 (C-6''), 60.9, 60.7, 60.6,  
1123 59.5 (OCH<sub>3</sub>). HRMS-ESI ( $m/z$ ): [M + H]<sup>+</sup> calcd for C<sub>30</sub>H<sub>33</sub>O<sub>9</sub>,  
1124 537.2119; found, 537.2108; [M + Na]<sup>+</sup> calcd for C<sub>30</sub>H<sub>32</sub>NaO<sub>9</sub>,  
1125 559.1939; found, 559.1900.

1126 4-Hydroxy-3-(2,3,4,6-tetra-O-benzyl- $\beta$ -D-glucopyranosyl)-  
1127 benzen-1-yl Benzoate (19) and 3-(2,3,4,6-Tetra-O-benzyl- $\beta$ -D-  
1128 glucopyranosyl)benzen-1,4-diyl Dibenzoate (20). Compound  
1129 19 (0.48 g, 0.77 mmol) was dissolved in dry dichloromethane (50  
1130 mL) together with imidazole (0.081 g, 1.18 mmol, 1.5 equiv) and  
1131 DMAP (cat.). After stirring for 10 min at 0 °C, benzoyl chloride (1.4  
1132 mL, 1.18 mmol, 1.5 equiv) was added dropwise. The reaction mixture  
1133 was stirred at room temperature for 72 h, after which it was washed  
1134 with brine and extracted with dichloromethane (2 × 20 mL). The  
1135 organic layers were combined, dried over MgSO<sub>4</sub>, and concentrated  
1136 under reduced pressure. The residue was purified by column  
1137 chromatography (hexane/acetone, 1:0 → 10:1), affording compound  
1138 19 as a colorless oil in 53% yield and compound 20 as a white solid in  
1139 38% yield.

1140 4-Hydroxy-3-(2,3,4,6-tetra-O-benzyl- $\beta$ -D-glucopyranosyl)-  
1141 benzen-1-yl Benzoate (19).  $R_f$  (hexane/acetone, 3:1) = 0.22;  $[\alpha]_D^{20} =$   
1142 +25° (c 0.1, CHCl<sub>3</sub>); <sup>1</sup>H NMR (CDCl<sub>3</sub>)  $\delta$  (ppm) 8.18 (d, 2H,  $J_{ortho} =$   
1143 7.46 Hz, H-2', H-6'), 7.64 (t, 1H,  $J_{ortho} = 7.20$  Hz, H-4'), 7.51 (t, 2H,  
1144  $J_{ortho} = 7.83$  Hz, H-3', H-5'), 7.35–7.07 (m, 22H, benzyl aromatics,  
1145 H-2, H-6), 6.98 (d, 1H,  $J_{ortho} = 7.73$  Hz, H-5), 4.98–4.89 (m, A<sub>1</sub>B<sub>1</sub>  
1146 system, 2H, Ph-CH<sub>2</sub>), 4.87, 4.83 (part A<sub>2</sub> of A<sub>2</sub>B<sub>2</sub> system, 1H, J<sub>A<sub>2</sub>-B<sub>2</sub></sub> =  
1147 10.85 Hz, Ph-CH<sub>2</sub>), 4.63–4.47 (m, 4H, part B<sub>2</sub> of A<sub>2</sub>B<sub>2</sub> system, part  
1148 A<sub>3</sub> of A<sub>3</sub>B<sub>3</sub> system, Ph-CH<sub>2</sub>), 4.44 (d, 1H,  $J_{1''-2''} = 9.18$  Hz, H-1''),  
1149 4.03, 3.99 (part A<sub>3</sub> of A<sub>3</sub>B<sub>3</sub> system, 1H, J<sub>A<sub>3</sub>-B<sub>3</sub></sub> = 10.15 Hz, Ph-CH<sub>2</sub>),  
1150 3.89 (t, 1H,  $J_{4''-3''-4''-5''} = 9.04$  Hz, H-4''), 3.80–6.69 (m, 4H, H-2'',  
1151 H-3'', H-6''a and H-6''b), 3.59 (br d, 1H,  $J_{5''-4''} = 9.72$  Hz, H-5''). <sup>13</sup>C  
1152 NMR (CDCl<sub>3</sub>)  $\delta$  (ppm) 165.3 (C=O), 153.0 (C-4), 143.7 (C-1),  
1153 138.5, 137.9, 137.8, 137.0 (benzyl C<sub>q</sub>-aromatics), 133.5 (C-4'), 130.1  
1154 (C-2', C-6'), 129.6 (C-1'), 128.8–127.6 (C-3', C-5', benzyl CH-  
1155 aromatics), 124.1 (C-3), 122.6 (C-6), 121.9 (C-2), 118.3 (C-5), 86.1  
1156 (C-3''), 81.7 (C-2''), 80.5 (C-5''), 78.6 (C-1''), 77.3 (C-4''), 75.6,  
1157 75.6, 75.2, 73.4 (Ph-CH<sub>2</sub>), 67.8 (C-6''). HRMS-ESI ( $m/z$ ): [M + H]<sup>+</sup>  
1158 calcd for C<sub>47</sub>H<sub>45</sub>O<sub>8</sub>, 737.3109; found, 737.3116; [M + Na]<sup>+</sup> calcd for  
1159 C<sub>47</sub>H<sub>44</sub>NaO<sub>8</sub>, 759.2928; found, 759.2936.

1160 3-(2,3,4,6-Tetra-O-benzyl- $\beta$ -D-glucopyranosyl)benzen-1,4-diyl  
1161 Dibenzoate (20).  $R_f$  (hexane/acetone, 3:1) = 0.34;  $[\alpha]_D^{20} = +11^\circ$  (c  
1162 0.2, CHCl<sub>3</sub>); <sup>1</sup>H NMR (CDCl<sub>3</sub>)  $\delta$  (ppm) 8.21, 8.16 (d, 4H,  $J_{ortho} =$   
1163 7.48 Hz, H-2', H-6'), 7.64, 7.59 (t, 2H,  $J_{ortho} = 7.31$  Hz, H-4'), 7.52,  
1164 7.45 (t, 4H,  $J_{ortho} = 7.69$  Hz, H-3', H-5'), 7.35–7.05 (m, 23H, benzyl  
1165 aromatics, H-2, H-5, H-6), 4.91–4.82 (A<sub>1</sub>B<sub>1</sub> system, 2H, J<sub>A<sub>1</sub>-B<sub>1</sub></sub> =  
1166 10.82 Hz, Ph-CH<sub>2</sub>), 4.81, 4.87 (part A<sub>2</sub> of A<sub>2</sub>B<sub>2</sub> system, 1H, J<sub>A<sub>2</sub>-B<sub>2</sub></sub> =  
1167 10.73 Hz, Ph-CH<sub>2</sub>), 4.55–4.46 (m, 5H, H-1'', part B<sub>2</sub> of A<sub>2</sub>B<sub>2</sub> system,  
1168 part A<sub>3</sub> of A<sub>3</sub>B<sub>3</sub> system, Ph-CH<sub>2</sub>), 4.22, 4.18 (part B<sub>3</sub> of A<sub>3</sub>B<sub>3</sub> system,  
1169 1H, J<sub>A<sub>3</sub>-B<sub>3</sub></sub> = 10.75 Hz, Ph-CH<sub>2</sub>), 3.77–3.52 (m, 6H, H-2'', H-3'', H-  
1170 4'', H-5'', H-6''a and H-6''b). <sup>13</sup>C NMR (CDCl<sub>3</sub>)  $\delta$  (ppm) 164.9,  
1171 164.7 (C=O), 148.5 (C-1), 146.4 (C-4), 138.6, 138.2, 138.1, 137.8  
1172 (benzyl C<sub>q</sub>-aromatics), 133.7, 133.6 (C-4'), 132.6 (C-3), 130.4 (C-2',  
1173 C-6'), 129.5, 129.4 (C-1'), 128.7–127.6 (C-3', C-5', benzyl CH-  
1174 aromatics), 124.0 (C-5), 122.4 (C-2)\*, 122.3 (C-6)\*, 86.8 (C-3''),  
1175 82.8 (C-2''), 79.5 (C-5''), 78.2 (C-4''), 77.3 (C-1''), 75.6, 75.1, 74.9,  
1176 74.3 (Ph-CH<sub>2</sub>), 69.0 (C-6''). \*Permutable signals. HRMS-ESI ( $m/z$ ):  
1177 [M + H]<sup>+</sup> calcd for C<sub>54</sub>H<sub>49</sub>O<sub>9</sub>, 841.3371; found, 841.3381.

1178 3-( $\beta$ -D-Glucopyranosyl)-4-hydroxybenzen-1-yl Benzoate  
1179 (21). To a solution of compound 19 (0.215 mg, 0.29 mmol) in

ethyl acetate (15 mL), Pd/C (10%, 50 mg) was added. The mixture  
1180 was stirred under a H<sub>2</sub> atmosphere for 26 h at room temperature.  
1181 After reaching completion, the reaction was stopped by filtering Pd/C  
1182 through a pad of Celite and the solvent was evaporated under reduced  
1183 pressure. The residue was purified by column chromatography (30:1  
1184 → 10:1 dichloromethane/MeOH) to afford compound 21 as a  
1185 yellowish oil in 96% yield.  $R_f$  (dichloromethane/MeOH, 7:1) = 0.44;  
1186  $[\alpha]_D^{20} = +50^\circ$  (c 0.2, MeOH); <sup>1</sup>H NMR [CO(CD<sub>3</sub>)<sub>2</sub>]  $\delta$  (ppm) 8.17  
1187 (d, 2H,  $J_{ortho} = 7.38$  Hz, H-2', H-6'), 7.72 (t, 2H,  $J_{ortho} = 7.45$  Hz, H-  
1188 3', H-5'), 7.59 (t, 1H,  $J_{ortho} = 7.67$  Hz, H-4'), 7.26 (d, 1H,  $J_{meta} = 2.35$   
1189 Hz, H-2), 7.06 (dd, 1H,  $J_{ortho} = 8.74$  Hz,  $J_{meta} = 2.58$  Hz, H-6), 6.89  
1190 (d, 1H,  $J_{ortho} = 8.69$  Hz, H-5), 4.60 (d, 1H,  $J_{1''-2''} = 9.34$  Hz, H-1''),  
1191 3.87 (d, 1H,  $J_{6''a-6''b} = 10.59$  Hz, H-6''a), 3.76 (dd, 1H,  $J_{6''b-6''a} = 10.99$   
1192 Hz,  $J_{6''b-5''} = 4.28$  Hz, H-6''b), 3.63–3.47 (m, 4H, H-2'', H-3'', H-4'',  
1193 H-5''). <sup>13</sup>C NMR [CO(CD<sub>3</sub>)<sub>2</sub>]  $\delta$  (ppm) 165.9 (C=O), 153.7 (C-4),  
1194 144.8 (C-1), 134.5 (C-4'), 130.8 (C-1'), 130.7 (C-2', C-6'), 129.6  
1195 (C-3', C-5'), 128.5 (C-3), 122.6 (C-2), 121.7 (C-6), 117.9 (C-5),  
1196 81.9 (C-5''), 79.7 (C-3''), 77.7 (C-1''), 76.6 (C-2''), 71.3 (C-4''), 62.6  
1197 (C-6''). HRMS-ESI ( $m/z$ ): [M + H]<sup>+</sup> calcd for C<sub>19</sub>H<sub>21</sub>O<sub>8</sub>, 377.1231;  
1198 found, 377.1226; [M + Na]<sup>+</sup> calcd for C<sub>19</sub>H<sub>20</sub>NaO<sub>8</sub>, 399.1050; found,  
1199 399.1045.

3-( $\beta$ -D-Glucopyranosyl)benzene-1,4-diyl Dibenzoate (22).  
1201 To a solution of compound 20 (0.273 g, 0.32 mmol) dissolved in  
1202 ethyl acetate (15 mL), Pd/C (10%, 64 mg) was added. The mixture  
1203 was stirred under a H<sub>2</sub> atmosphere for 22 h at room temperature.  
1204 After reaching completion, the reaction was stopped by filtering Pd/C  
1205 through a pad of Celite and the solvent was evaporated under reduced  
1206 pressure. The residue was purified by column chromatography  
1207 (EtOAc) to afford compound 22 as a white solid in 90% yield.  $R_f$   
1208 (EtOAc) = 0.48; m.p. = 99.7–102.5 °C;  $[\alpha]_D^{20} = +11^\circ$  (c 0.8, MeOH);  
1209 <sup>1</sup>H NMR [CO(CD<sub>3</sub>)<sub>2</sub>]  $\delta$  (ppm) 8.25, 8.21 (d, 2H,  $J_{ortho} = 7.46$  Hz, H-  
1210 2', H-6'), 7.77–7.72 (m, 2H, H-4'), 7.64–7.60 (m, 4H, H-3', H-5'),  
1211 7.50 (d, 1H,  $J_{meta} = 2.11$  Hz, H-2), 7.40 (d, 1H,  $J_{ortho} = 8.76$  Hz, H-5),  
1212 7.35 (dd, 1H,  $J_{ortho} = 8.78$  Hz,  $J_{meta} = 2.55$  Hz, H-6), 4.59 (d, 1H,  
1213  $J_{1''-2''} = 9.41$  Hz, H-1''), 3.73 (d, 1H,  $J_{6''a-6''b} =$  Hz, H-6''a), 3.59–3.37  
1214 (m, 5H, H-2'', H-3'', H-4'', H-5'', H-6''b). <sup>13</sup>C NMR [CO(CD<sub>3</sub>)<sub>2</sub>]  $\delta$   
1215 (ppm) 165.5 (C=O), 165.2 (C=O), 149.3 (C-1), 147.6 (C-4),  
1216 134.6 (C-3), 134.4 (C-4'), 130.8, 130.7 (C-2', C-6'), 130.6, 130.3 (C-  
1217 1'), 129.6, 129.6 (C-3', C-5'), 124.6 (C-5), 122.7 (C-6), 122.6 (C-2),  
1218 81.8 (C-3''), 79.6 (C-2''), 77.3 (C-1''), 75.4 (C-4''), 71.6 (C-5''), 63.0  
1219 (C-6''). HRMS-ESI ( $m/z$ ): [M + H]<sup>+</sup> calcd for C<sub>26</sub>H<sub>25</sub>O<sub>9</sub>, 481.1493;  
1220 found, 481.1499; [M + Na]<sup>+</sup> calcd for C<sub>26</sub>H<sub>24</sub>NaO<sub>9</sub>, 503.1313; found,  
1221 503.1308.

4-(2,3,4,6-Tetra-O-methyl- $\beta$ -D-glucopyranosyl)benzene-1,2-  
1223 diyl Dibenzoate (25). Compound 7 (0.650 g, 1.98 mmol) was  
1224 dissolved in dichloromethane (43 mL) and imidazole (0.447 g, 6.57  
1225 mmol, 3.3 equiv) was added at 0 °C. After stirring for 10 min at 0 °C,  
1226 benzoyl chloride (0.78 mL, 6.67 mmol, 3.3 equiv) was added  
1227 dropwise. The reaction mixture was stirred at room temperature for  
1228 24 h, after which it was washed with brine and extracted with  
1229 dichloromethane (2 × 20 mL). The organic layers were combined,  
1230 dried over MgSO<sub>4</sub>, and concentrated under reduced pressure. The  
1231 residue was purified by column chromatography (hexane/acetone,  
1232 10:0 → 5:1), affording compound 25 as a colorless oil in 88% yield.  $R_f$   
1233 (hexane/EtOAc, 2:1) = 0.38;  $[\alpha]_D^{20} = -18^\circ$  (c 0.1, CHCl<sub>3</sub>); <sup>1</sup>H NMR  
1234 (CDCl<sub>3</sub>)  $\delta$  8.05 (br d, 4H,  $J_{ortho} = 7.49$  Hz, H-2', H-6'), 7.53 (t, 2H,  
1235  $J_{ortho} = 6.71$  Hz, H-4'), 7.46 (br s, 1H, H-3), 7.42–7.34 (m, 6H, H-3',  
1236 H-5', H-5, H-6), 4.16 (d, 1H,  $J_{1''-2''} = 9.45$  Hz, H-1''), 3.69 (s, 3H,  
1237 OCH<sub>3</sub>), 3.66–3.65 (m, 2H, H-6''a and H-6''b), 3.59 (s, 3H, OCH<sub>3</sub>),  
1238 3.47–3.42 (m, 4H, H-5'', OCH<sub>3</sub>), 3.37–3.25 (m, 2H, H-3'', H-4''),  
1239 3.16 (s, 3H, OCH<sub>3</sub>), 3.07 (t, 1H,  $J_{2''-1''-3''} = 9.13$  Hz, H-2''). <sup>13</sup>C  
1240 NMR (CDCl<sub>3</sub>)  $\delta$  164.3 (C=O), 142.4 (C-2), 142.3 (C-1), 138.2 (C-  
1241 4), 133.7 (C-4'), 130.2 (C-2', C-6'), 128.9, 128.9 (C-1'), 128.6 (C-3',  
1242 C-5'), 125.6 (C-5), 123.2 (C-6), 122.6 (C-3), 88.5 (C-3''), 86.2 (C-  
1243 2''), 80.5 (C-1''), 79.8 (C-4''), 79.2 (C-5''), 71.8 (C-6''), 61.0, 60.7,  
1244 60.6, 59.6 (OCH<sub>3</sub>). HRMS-ESI ( $m/z$ ): [M + H]<sup>+</sup> calcd for C<sub>30</sub>H<sub>33</sub>O<sub>9</sub>,  
1245 537.2119; found, 537.2102; [M + Na]<sup>+</sup> calcd for C<sub>30</sub>H<sub>32</sub>NaO<sub>9</sub>,  
1246 559.1939; found, 559.1914.

4-( $\beta$ -D-Glucopyranosyl)benzene-1,2-diyl Dibenzoate (26).  
1248 To a solution of compound 25 (0.810 g, 1.51 mmol) in dry  
1249

1250 dichloroethane (90 mL),  $\text{BBr}_3 \cdot \text{SMe}_2$  (11.5 g, 37.12 mmol, 25 equiv)  
1251 was slowly added and the reaction was stirred under reflux for 17 h.  
1252 The mixture was allowed to reach room temperature, washed with  
1253 sodium bicarbonate, and extracted with dichloromethane ( $3 \times 100$   
1254 mL). The organic layers were combined, dried over  $\text{MgSO}_4$ , filtered,  
1255 and concentrated under vacuum. The residue was purified by column  
1256 chromatography (40:1  $\rightarrow$  30:1 EtOAc/MeOH), affording compound  
1257 **26** in 8% yield as a brownish solid.  $R_f$  (dichloromethane/MeOH, 6:1)  
1258 = 0.60; m.p. = 77.3–78.1 °C;  $[\alpha]_{\text{D}}^{20} = -11^\circ$  (c 0.3,  $\text{CHCl}_3$ );  $^1\text{H NMR}$   
1259  $[\text{CO}(\text{CD}_3)_2]$   $\delta$  (ppm) 8.05 (t, 4H,  $J_{\text{ortho}} = 7.23$  Hz, H-2', H-6'),  
1260 7.67–7.62 (m, 2H, H-4'), 7.55 (br s, 1H, H-3), 7.51–7.44 (m, 6H, H-  
1261 3', H-5', H-5, H-6), 4.38 (br s, 1H, OH), 4.31 (d, 1H,  $J_{1'-2'} = 9.41$   
1262 Hz, H-1''), 3.90 (br d, 1H,  $J_{6''a-6''b} = 10.75$  Hz, H-6''a), 3.80 (br s, 1H,  
1263 OH), 3.74 (dd, 1H,  $J_{6''b-6''a} = 10.89$  Hz,  $J_{6''b-5''} = 4.37$  Hz, H-6''b),  
1264 3.61–3.47 (m, 3H, H-3'', H-4'', H-5''), 3.42 (t, 1H,  $J_{2''-1''-2''-3''} = 8.83$   
1265 Hz, H-2'').  $^{13}\text{C NMR}$   $[\text{CO}(\text{CD}_3)_2]$   $\delta$  (ppm) 164.7 (C=O), 143.1  
1266 (C-2), 142.8 (C-1), 140.4 (C-4), 134.7 (C-4'), 130.7 (C-2', C-6'),  
1267 129.8 (C-1'), 129.6 (C-3', C-5'), 126.9 (C-5), 123.6 (C-6), 123.4 (C-  
1268 3), 81.8 (C-1''), 81.7 (C-5''), 79.8 (C-3''), 76.3 (C-2''), 71.7 (C-4''),  
1269 63.1 (C-6''). HRMS-ESI ( $m/z$ ):  $[\text{M} + \text{Na}]^+$  calcd for  $\text{C}_{26}\text{H}_{24}\text{NaO}_9$ ,  
1270 503.1313; found, 503.1326.

1271 **4-(2,3,4,6-Tetra-O-benzyl- $\alpha$ - $\beta$ -D-glucopyranosyloxy)-**  
1272 **benzen-1-yl Benzoate (28 $\alpha,\beta$ )**. Compound **27 $\alpha,\beta$**  ( $\alpha/\beta$  ratio = 4:1,  
1273 0.570 g, 0.90 mmol) was dissolved in dry dichloromethane (20 mL)  
1274 together with imidazole (0.135 g, 1.98 mmol, 2.2 equiv) and DMAP  
1275 (cat). After stirring for 10 min at 0 °C, benzoyl chloride (0.230 mL,  
1276 1.98 mmol, 2.2 equiv) was added dropwise. The reaction mixture was  
1277 stirred at room temperature for 24 h, after which it was washed with  
1278 brine and extracted with dichloromethane ( $2 \times 20$  mL). The organic  
1279 layers were combined, dried over  $\text{MgSO}_4$ , and concentrated under  
1280 reduced pressure. The residue was purified by column chromatog-  
1281 raphy (hexane/EtOAc, 10:1  $\rightarrow$  5:1), affording **28 $\alpha,\beta$**  as a mixture in  
1282  $\alpha/\beta$  ratio = 10:1 as a colorless oil isolated in 94% yield;  $R_f$  (hexane/  
1283 EtOAc, 10:1) = 0.23;  $[\alpha]_{\text{D}}^{20} = -4^\circ$  (c 0.2,  $\text{CHCl}_3$ );  $^1\text{H NMR}$  ( $\text{CDCl}_3$ )  
1284  $\delta$  (ppm) 8.20 (d, 20H,  $J_{\text{ortho}} = 7.65$  Hz, H-2', H-6'), 8.10 (d, 2H,  
1285  $J_{\text{ortho}} = 7.65$  Hz, H-2' $\beta$ , H-6' $\beta$ ), 7.66–7.58 (m, 11H, H-4', H-4' $\beta$ ),  
1286 7.54–7.45 (m, 22H, H-3', H-3' $\beta$ , H-5', H-5' $\beta$ ), 7.40–7.10 (m,  
1287 264H, benzyl aromatics, H-2' $\omega$ , H-3' $\omega$ , H-5' $\omega$ , H-6' $\omega$ , H-2' $\beta\omega$ , H-3' $\beta\omega$ , H-5' $\beta\omega$ , H-  
1288 6' $\beta\omega$ ), 5.44 (d, 10H,  $J_{1'-2'} = 2.84$  Hz, H-1''), 5.08–4.80 (m, 38H, H-  
1289 1' $\beta$ , Ph- $\text{CH}_2$ ), 4.71–4.40 (m, 51H, Ph- $\text{CH}_2$ ), 4.20 (t, 10H,  
1290  $J_{3''\alpha-2''\alpha-3''\alpha-4''\alpha} = 9.17$  Hz, H-3'' $\alpha$ ), 3.90–3.57 (m, 57H, H-2'' $\omega$ , H-  
1291 4'' $\omega$ , H-5'' $\omega$ , H-6'' $\omega$ , H-6'' $\beta\omega$ , H-2'' $\beta\omega$ , H-3'' $\beta\omega$ , H-4'' $\beta\omega$ , H-5'' $\beta\omega$ , H-6'' $\beta\omega$ , H-  
1292 6'' $\beta\omega$ ).  $^{13}\text{C NMR}$  ( $\text{CDCl}_3$ )  $\delta$  (ppm) 165.4 (C=O $\alpha$ ), 165.4 (C=O $\beta$ ),  
1293 155.1 (C-4 $\beta$ ), 154.4 (C-4 $\alpha$ ), 146.0 (C-1 $\beta$ ), 145.6 (C-1 $\alpha$ ), 138.7, 138.5,  
1294 138.1, 138.0, 139.0, 137.7 (benzyl  $\text{C}_q$ -aromatics), 133.6 (C-4' $\alpha/\beta$ ),  
1295 130.2 (C-2' $\omega$ , C-6' $\omega$ ), 129.9 (C-2' $\beta$ , C-6' $\beta$ ), 128.6–127.6 (benzyl CH-  
1296 aromatics, C-3' $\omega$ , C-5' $\omega$ , C-3' $\beta$ , C-5' $\beta$ ), 122.6 (C-2' $\beta$ , C-6' $\beta$ ), 122.5 (C-  
1297 2' $\omega$ , C-6' $\omega$ ), 117.9 (C-3' $\beta$ , C-5' $\beta$ ), 117.5 (C-3' $\omega$ , C-5' $\omega$ ), 102.1 (C-1' $\beta$ ), 95.9  
1298 (C-1' $\alpha$ ), 82.0 (C-3' $\beta$ ), 81.9 (C-3' $\alpha$ ), 79.6 (C-5' $\alpha/\beta$ ), 77.6 (C-4' $\beta$ ),  
1299 77.2 (C-4' $\alpha$ ), 75.8, 75.2, 75.1, 73.5, 73.4 (Ph- $\text{CH}_2$ ), 70.9 (C-2' $\beta$ ),  
1300 70.8 (C-2' $\omega$ ), 68.1 (C-6' $\alpha/\beta$ ). HRMS-ESI ( $m/z$ ):  $[\text{M} + \text{H}]^+$  calcd for  
1301  $\text{C}_{47}\text{H}_{45}\text{O}_8$ , 737.3109; found, 737.3117;  $[\text{M} + \text{Na}]^+$  calcd for  
1302  $\text{C}_{47}\text{H}_{44}\text{NaO}_8$ , 759.2928; found, 759.2938.

1303 **4-( $\alpha$ -D-Glucopyranosyloxy)benzen-1-yl Benzoate (29)**. To a  
1304 solution of the mixture **28 $\alpha,\beta$**  ( $\alpha/\beta$  ratio = 10:1) (0.350 g, 0.47  
1305 mmol) in ethyl acetate (20 mL), Pd/C (10%, 50 mg) was added. The  
1306 mixture stirred under a  $\text{H}_2$  atmosphere for 18 h at room temperature.  
1307 After reaching completion, the reaction was stopped by filtering Pd/C  
1308 through a pad of Celite and the solvent was evaporated under reduced  
1309 pressure. The residue was purified by column chromatography (100:1  
1310  $\rightarrow$  5:1 AcOEt/MeOH) to afford compound **29** as a white powder in  
1311 71% yield.  $R_f$  (dichloromethane/MeOH 9:1) = 0.35; m.p. = 161.7–  
1312 162.6 °C;  $[\alpha]_{\text{D}}^{20} = +74^\circ$  (c 0.1,  $\text{CHCl}_3$ );  $^1\text{H NMR}$  (MeOD)  $\delta$  (ppm)  
1313 8.16 (d, 2H,  $J_{\text{ortho}} = 7.72$  Hz, H-2', H-6'), 7.68 (t, 1H,  $J_{\text{ortho}} = 7.56$  Hz,  
1314 H-4'), 7.55 (t, 2H,  $J_{\text{ortho}} = 7.66$  Hz, H-3', H-5'), 7.26 (d, 2H,  $J_{\text{ortho}} =$   
1315 8.91 Hz, H-2, H-6), 7.15 (d, 2H,  $J_{\text{ortho}} = 8.95$  Hz, H-3, H-5), 5.49 (d,  
1316 1H,  $J_{1'-2'} = 3.36$  Hz, H-1''), 3.99 (t, 1H,  $J_{3''-2''-3''-4''} = 9.11$  Hz, H-3''),  
1317 3.81–3.68 (m, 3H, H-5'', H-6''a and H-6''b), 3.50 (dd, 1H,  $J_{2''-1''} =$   
1318 3.35 Hz,  $J_{2''-3''} = 9.40$  Hz, H-2''), 3.45 (t, 1H,  $J_{4''-3''-4''-5''} = 9.16$  Hz,  
1319 H-4'').  $^{13}\text{C NMR}$  (MeOD)  $\delta$  (ppm) 166.9 (C=O), 156.4 (C-4),

147.2 (C-1), 134.9 (C-4'), 131.0 (C-2', C-6'), 130.8 (C-1'), 129.8  
(C-3', H-5'), 123.6 (C-2, C-6), 119.0 (C-3, C-5), 99.8 (C-1''), 74.9  
(C-3''), 74.5 (C-5''), 73.3 (C-2''), 71.5 (C-4''), 62.4 (C-6''). HRMS-  
ESI ( $m/z$ ):  $[\text{M} + \text{H}]^+$  calcd for  $\text{C}_{19}\text{H}_{21}\text{O}_8$ , 377.1231; found,  
377.1220;  $[\text{M} + \text{Na}]^+$  calcd for  $\text{C}_{19}\text{H}_{20}\text{NaO}_8$ , 399.1050; found,  
399.1040.

1326 **4-( $\beta$ -D-Glucopyranosyloxy)benzen-1-yl Benzoate (30)**. Minor  
1327 product of the reaction that gave compound **29**. Colorless crystals  
1328 obtained in 10% yield;  $R_f$  (dichloromethane/MeOH, 9:1) = 0.35;  
1329 m.p. = 192.0–193.3 °C;  $^1\text{H NMR}$  (MeOD)  $\delta$  (ppm) 8.16 (d, 2H,  
1330  $J_{\text{ortho}} = 8.06$  Hz, H-2', H-6'), 7.69 (t, 1H,  $J_{\text{ortho}} = 7.45$  Hz, H-4'), 7.56  
1331 (t, 1H,  $J_{\text{ortho}} = 7.65$  Hz, H-3', H-5'), 7.20–7.14 (m, 4H, H-2, H-3, H-  
1332 5, H-6), 4.91 (H-1'', superimposed with  $\text{H}_2\text{O}$  solvent peak), 3.91 (d,  
1333 1H,  $J_{6''a-6''b} = 12.06$  Hz, H-6''a), 3.72 (dd, 1H,  $J_{6''b-6''a} = 12.00$  Hz,  
1334  $J_{6''b-5''} = 5.36$  Hz, H-6''b), 3.50–3.38 (m, 4H, H-2'', H-3'', H-4'', H-  
1335 5'').  $^{13}\text{C NMR}$  (MeOD)  $\delta$  (ppm) 166.9 (C=O), 156.9 (C-4), 147.2  
(C-2), 134.9 (C-4'), 131.0 (C-2', C-6'), 130.7 (C-1'), 129.8 (C-3', C-  
1336 5'), 123.6 (C-2, C-6), 118.7 (C-3, C-5), 102.7 (C-1''), 78.2 (C-3''),  
1337 77.9 (C-5''), 74.9 (C-2''), 71.3 (C-4''), 62.5 (C-6''). HRMS-ESI ( $m/z$ ):  
1338  $[\text{M} + \text{Na}]^+$  calcd for  $\text{C}_{19}\text{H}_{20}\text{NaO}_8$ , 399.1050; found, 399.1052.

1340 **2-(2,3,4,6-Tetra-O-benzyl- $\alpha$ -D-glucopyranosyloxy)benzen-**  
1341 **1-yl Benzoate (32)**. Compound **31** (0.360 g, 0.57 mmol) was  
1342 dissolved in dry dichloromethane (15 mL) together with imidazole  
1343 (0.086 g, 1.26 mmol, 2.2 equiv) and DMAP (cat). After stirring for  
1344 10 min at 0 °C, benzoyl chloride (0.143 mL, 1.18 mmol, 2.2 equiv)  
1345 was added dropwise. The reaction mixture was stirred at room  
1346 temperature for 72 h, after which it was washed with brine and  
1347 extracted with dichloromethane ( $2 \times 20$  mL). The organic layers were  
1348 combined, dried over  $\text{MgSO}_4$ , and concentrated under reduced  
1349 pressure. The residue was purified by column chromatography (p.  
1350 ether/EtOAc, 15:1  $\rightarrow$  3:1), affording compound **32** as a colorless oil  
1351 in 82% yield.  $R_f$  (p. ether/EtOAc, 4:1) = 0.52;  $[\alpha]_{\text{D}}^{20} = +50^\circ$  (c 0.1,  
1352  $\text{CHCl}_3$ );  $^1\text{H NMR}$  ( $\text{CDCl}_3$ )  $\delta$  (ppm) 8.17 (d, 2H,  $J_{\text{ortho}} = 7.90$  Hz, H-  
1353 2', H-6'), 7.33 (t, 1H,  $J_{\text{ortho}} = 7.34$  Hz, H-4'), 7.35–7.06 (m, 24H,  
1354 benzyl aromatics, H-3, H-4, H-5, H-6, H-3', H-5'), 5.49 (d, 1H,  $J_{1'-2'} =$   
1355 = 2.81 Hz, H-1''), 4.77, 4.73 (part  $\text{A}_1$  of  $\text{A}_1\text{B}_1$  system, 1H,  $J_{\text{A}_1-\text{B}_1} =$   
1356 10.95 Hz, Ph- $\text{CH}_2$ ), 4.58–4.56 (m, 3H, part  $\text{A}_2$  of  $\text{A}_2\text{B}_2$  system, Ph-  
1357  $\text{CH}_2$ ), 4.43–4.37 (m, 2H, part  $\text{B}_1$  of  $\text{A}_1\text{B}_1$  system, part  $\text{B}_2$  of  $\text{A}_2\text{B}_2$   
1358 system), 4.34, 4.30 (part  $\text{A}_3$  of  $\text{A}_3\text{B}_3$  system, 1H,  $J_{\text{A}_3-\text{B}_3} = 10.77$  Hz,  
1359 Ph- $\text{CH}_2$ ), 4.25, 4.21 (part  $\text{B}_3$  of  $\text{A}_3\text{B}_3$  system, 1H,  $J_{\text{A}_3-\text{B}_3} = 10.95$  Hz,  
1360 Ph- $\text{CH}_2$ ), 3.88 (br d, 1H,  $J_{2''-3''} = 9.46$  Hz, H-2''), 3.79–3.46 (m, 3H,  
1361 H-3'', H-4'', H-6''a), 3.60–3.54 (m, 2H, H-5'', H-6''b).  $^{13}\text{C NMR}$   
1362 ( $\text{CDCl}_3$ )  $\delta$  (ppm) 164.9 (C=O), 148.4 (C-2), 141.1 (C-1), 138.7,  
1363 138.5, 138.3, 137.9 (benzyl  $\text{C}_q$ -aromatics), 133.2 (C-4'), 130.5 (C-2',  
1364 C-6'), 129.6 (C-1'), 128.3–127.5 (benzyl CH-aromatics, C-3', C-5'),  
1365 126.8 (C-4), 123.0 (C-5)\*, 122.5 (C-6)\*, 116.0 (C-3), 96.2 (C-1''),  
1366 81.7 (C-3''), 77.2 (C-5''), 76.9 (C-4''), 75.3, 74.7, 73.4, 72.6 (Ph-  
1367  $\text{CH}_2$ ), 71.2 (C-2''), 68.2 (C-6''). HRMS-ESI ( $m/z$ ):  $[\text{M} + \text{H}]^+$  calcd  
1368 for  $\text{C}_{47}\text{H}_{45}\text{O}_8$ , 737.3109; found, 737.3109;  $[\text{M} + \text{Na}]^+$  calcd for  
1369  $\text{C}_{47}\text{H}_{44}\text{NaO}_8$ , 759.2928; found, 759.2934.

1370 **2-( $\alpha$ -D-Glucopyranosyloxy)benzen-1-yl Benzoate (33)**. To a  
1371 solution of compound **32** (0.275 mg, 0.37 mmol) in ethyl acetate (6  
1372 mL), Pd/C (10%, 32 mg) was added. The mixture stirred under a  $\text{H}_2$   
1373 atmosphere for 20 h at room temperature. After reaching completion,  
1374 the reaction was stopped by filtering Pd/C through a pad of Celite  
1375 and the solvent was evaporated under reduced pressure. The residue  
1376 was purified by column chromatography (1:0  $\rightarrow$  30:1 AcOEt/  
1377 MeOH) to afford compound **33** as colorless crystals in 83% yield.  $R_f$   
1378 (dichloromethane/MeOH, 7:1) = 0.35; m.p. = 54.5–55.0 °C;  $[\alpha]_{\text{D}}^{20} =$   
1379 +123° (c 0.1, MeOH);  $^1\text{H NMR}$   $[\text{CO}(\text{CD}_3)_2]$   $\delta$  (ppm) 8.20 (d, 2H,  
1380  $J_{\text{ortho}} = 7.88$  Hz, H-2', H-6'), 7.70 (t, 1H,  $J_{\text{ortho}} = 7.56$  Hz, H-4'), 7.58  
1381 (t, 2H,  $J_{\text{ortho}} = 7.59$  Hz, H-3', H-5'), 7.42 (d, 1H,  $J_{\text{ortho}} = 8.56$  Hz, H-  
1382 3), 7.28–7.24 (m, 2H, H-4, H-6), 7.10 (t, 1H,  $J_{\text{ortho}} = 7.73$  Hz, H-5),  
1383 5.56 (d, 1H,  $J_{1'-2'} = 3.19$  Hz, H-1''), 3.74–3.59 (m, 4H, H-3'', H-4'',  
1384 H-6''a and H-6''b), 3.53–3.43 (m, 2H, H-2'', H-5'').  $^{13}\text{C NMR}$   
1385  $[\text{CO}(\text{CD}_3)_2]$   $\delta$  (ppm) 165.0 (C=O), 149.6 (C-2), 141.3 (C-1), 1385  
1386 134.1 (C-4'), 130.6 (C-2', C-6'), 130.1 (C-1'), 129.3 (C-3', C-5'),  
1387 127.4 (C-4), 123.7 (C-6), 122.9 (C-5), 117.9 (C-3), 99.1 (C-1''),  
1388 74.4 (C-4'), 74.0 (C-3''), 72.7 (C-2''), 70.8 (C-5''), 62.0 (C-6'').

1389 HRMS-ESI ( $m/z$ ):  $[M + Na]^+$  calcd for  $C_{19}H_{21}O_8$ , 399.1050; found, 1390 399.1064.

1391 **General Procedure for Debenzylation Leading to C-**  
1392 **Glucosyl Polyphenols 23 and 24.** To a solution of 0.016 mmol  
1393 of benzylated C-glucosyl polyphenol (**14** or **16**) in ethyl acetate (6  
1394 mL), Pd/C (10%, 32 mg) was added. The mixture stirred under a  $H_2$   
1395 atmosphere for 15–26 h at room temperature. After reaching  
1396 completion, the reaction was stopped by filtering Pd/C through a pad  
1397 of Celite and the solvent was evaporated under reduced pressure. The  
1398 residue was purified by column chromatography.

1399 **1-[5-( $\beta$ -D-Glucopyranosyl)-2,4,6-trihydroxyphenyl]ethan-1-one**  
1400 (**23**). Compound synthesized by debenzoylation of compound **14**. The  
1401 reaction crude was purified by column chromatography (10:1  $\rightarrow$  5:1  
1402 dichloromethane/MeOH) to give **23** as a yellowish powder in 93%  
1403 yield.  $R_f$  (dichloromethane/MeOH, 5:1) = 0.23; m.p. = 150.8–153.0  
1404  $^{\circ}C$ ;  $[\alpha]_D^{20} = +57^{\circ}$  ( $c$  0.6, MeOH);  $^1H$  NMR (MeOD)  $\delta$  (ppm) 5.88  
1405 (s, 1H, H-5), 4.79 (s, 1H,  $J_{1'-2'}$  = 9.94 Hz, H-1'), 3.93 (t, 1H,  
1406  $J_{2'-1'-2'-3'}$  = 9.26 Hz, H-2'), 3.82 (d, 1H,  $J_{6'a-6'b}$  = 11.91 Hz, H-6'a),  
1407 3.71 (dd, 1H,  $J_{6'b-6'a}$  = 12.11 Hz,  $J_{6'b-5'}$  = 4.87 Hz, H-6'b), 3.46–3.31  
1408 (m, 3H, H-3', H-4', H-5').  $^{13}C$  NMR (MeOD)  $\delta$  (ppm) 204.9 (C=  
1409 O), 165.7 (C-2), 165.1 (C-4), 164.2 (C-6), 105.6 (C-1), 104.1 (C-3),  
1410 96.7 (C-5), 82.5 (C-5'), 79.9 (C-3'), 75.6 (C-1'), 73.1 (C-2'), 71.5  
1411 (C-4'), 62.5 (C-6'), 33.0 ( $CH_3$ -Ac). HRMS-ESI ( $m/z$ ):  $[M + H]^+$   
1412 calcd for  $C_{14}H_{19}O_9$ , 331.1024; found, 331.1020;  $[M + Na]^+$  calcd for  
1413  $C_{14}H_{18}NaO_9$ , 353.0843; found, 353.0843.

1414 **1-( $\beta$ -D-Glucopyranosyl)-2-hydroxynaphthalene (24).** Compound  
1415 synthesized by debenzoylation of compound **16**. The reaction crude  
1416 was purified by column chromatography (20:1  $\rightarrow$  10:1 dichloro-  
1417 methane/MeOH) to give **24** as a yellowish oil in 91% yield.  $R_f$   
1418 (dichloromethane/MeOH, 10:1) = 0.26;  $[\alpha]_D^{20} = +45^{\circ}$  ( $c$  0.5,  
1419 MeOH);  $^1H$  NMR [ $CO(CD_3)_2$ ]  $\delta$  (ppm) 8.16 (br s, 1H, H-8), 7.75  
1420 (m, 2H, H-4, H-5), 7.39 (t, 1H,  $J_{ortho}$  = 7.58 Hz, H-6), 7.27 (t, 1H,  
1421  $J_{ortho}$  = 7.36 Hz, H-7), 7.07 (t, 1H,  $J_{ortho}$  = 8.31 Hz, H-3), 5.43 (d, 1H,  
1422  $J_{1'-2'}$  = 9.64 Hz, H-1'), 3.93–3.83 (m, 3H, H-2', H-6'a and H-6'b),  
1423 3.78–3.68 (m, 2H, H-3', H-4'), 3.64–3.60 (m, 1H, H-5').  $^{13}C$  NMR  
1424 [ $CO(CD_3)_2$ ]  $\delta$  (ppm) 155.2 (C-2), 134.3 (C-8a), 130.5 (C-4), 129.7  
1425 (C-5), 129.0 (C-4a), 126.6 (C-7), 124.8 (C-8), 123.4 (C-6), 120.2  
1426 (C-3), 116.7 (C-1), 82.0 (C-5'), 79.4 (C-3'), 78.2 (C-1'), 74.4 (C-  
1427 2'), 70.7 (C-4'), 61.8 (C-6'). HRMS-ESI ( $m/z$ ):  $[M + Na]^+$  calcd for  
1428  $C_{16}H_{19}NaO_6$ , 329.0996; found, 329.1001.

1429 **2-Phenyl-1-(2,4,6-trihydroxyphenyl)ethan-1-one (34) and**  
1430 **3,5-Dihydroxyphenyl 2-Phenylacetate (35).** 1,3,5-Trihydroxy-  
1431 benzene (1.0 g, 7.93 mmol) was dissolved in 2% TfOH/ $CH_3CN$  (10  
1432 mL) and cooled down to 0  $^{\circ}C$ . Phenylacetyl chloride (1.0 mL, 7.93  
1433 mmol) was added at 0  $^{\circ}C$  and the reaction was stirred overnight at  
1434 room temperature. Then, the crude was poured into ice and extracted  
1435 with EtOAc. The organic phase was washed with 2 M HCl,  $NaHCO_3$ ,  
1436 and brine and dried over  $MgSO_4$  and the solvent was eliminated  
1437 under reduced pressure. After column chromatography (5:1  $\rightarrow$  3:1  
1438 hexane/acetone), compounds **34** and **35** were obtained in 7 and 25%  
1439 yields, respectively.

1440 **3,5-Dihydroxyphenyl 2-Phenylacetate (35).**  $R_f$  = 0.36 (hexane/  
1441 acetone, 3:1); m.p. = 77.9–79.6  $^{\circ}C$ ;  $^1H$  NMR ( $CDCl_3$ )  $\delta$  (ppm)  
1442 11.70 (s, 2H, OH), 9.30 (s, 1H, OH), 7.30–7.20 (m, 5H, ArCH),  
1443 5.94 (s, 2H, ArH), 4.41 (s, 2H,  $CH_2$ ).  $^{13}C$  NMR ( $CDCl_3$ )  $\delta$  (ppm)  
1444 200.5 (C=O), 165.6 (ArC, C-4), 165.4 (ArCx2, C-2, C-6), 137.1  
1445 (ArC, C-1'), 130.6 (ArCHx2, C-2', C-6'), 128.5 (ArCHx2, C-3', C-  
1446 5'), 127.0 (ArCH, C-4'), 104.8 (ArC, C-1), 96.2 (ArCHx2, C-3, C-5),  
1447 50.0 ( $CH_2$ ). HRMS-ESI ( $m/z$ ):  $[M + H]^+$  calcd for  $C_{14}H_{13}O_4$ ,  
1448 245.0808; found, 245.0806;  $[M + Na]^+$  calcd for  $C_{14}H_{12}NaO_4$ ,  
1449 267.0628; found, 267.0627.

1450 **2-Phenyl-1-(2,4,6-trihydroxyphenyl)ethan-1-one (34).** Com-  
1451 pound **35** (0.56, 2.49 mmol) was treated with trifluoromethanesul-  
1452 fonic acid (2.2 mL, 25 mmol) at 0  $^{\circ}C$ . The reaction mixture was  
1453 warmed up at room temperature for 1 h and then heated for 1 h at 40  
1454  $^{\circ}C$  and then at 100  $^{\circ}C$ . After an additional 1 h, the crude was poured  
1455 into ice and extracted with EtOAc. The organic phase was washed  
1456 with 2 M HCl,  $NaHCO_3$ , and brine and dried over  $MgSO_4$  and the  
1457 solvent was eliminated under reduced pressure. After column  
1458 chromatography (5:1  $\rightarrow$  3:1 hexane/acetone), compound **34** was

isolated in 39% yield.  $R_f$  = 0.4 (hexane/acetone, 3:1);  $^1H$  NMR  
( $CDCl_3$ )  $\delta$  (ppm) 7.30–7.27 (m, 5H, ArCH), 6.03–6.00 (m, 3H,  
ArH, C-2, C-4, C-6), 3.82 (s, 2H,  $CH_2$ ).  $^{13}C$  NMR ( $CDCl_3$ )  $\delta$  (ppm)  
171.9 (C=O), 157.2 (C-2, C-3, C-5), 157.1 (C-1), 129.3 (C-2', C-  
6'), 128.8 (C-3', C-5'), 127.5 (C-4'), 101.7 (C-2, C-6), 101.2 (C-4),  
41.3 ( $CH_2$ ). HRMS-ESI ( $m/z$ ):  $[M + H]^+$  calcd for  $C_{14}H_{13}O_4$ ,  
245.0808; found, 245.0805;  $[M + Na]^+$  calcd for  $C_{14}H_{12}NaO_4$ ,  
267.0628; found, 267.0729.

**2,4,6-Trihydroxy-3-(2,3,4,6-tetra-O-benzyl- $\beta$ -D-**  
**glucopyranosyl)phenyl]-2-phenylethan-1-one (36).** A solution  
of compound **34** (0.22 g, 0.89 mmol), 2,3,4,6-tetra-O-benzyl-D-  
glucopyranose (0.34, 0.64 mmol), and drierite (0.3 g) in a mixture of  
dichloromethane/ $CH_3CN$  (1:1) was stirred for 10 min at room  
temperature. To this solution lowered at  $-40^{\circ}C$ , TMSOTf (0.16 mL,  
0.89 mmol) was added dropwise. The mixture was left at room  
temperature under stirring overnight. Then, the reaction was stopped  
by adding trimethylamine and the reaction mixture was filtered  
through a Celite pad. The solvent was evaporated under reduced  
pressure and the residue was purified by column chromatography  
(hexane/acetone, 7:1) to render compound **36** in 33% yield.  $R_f$  = 0.24  
(hexane/acetone, 3:1); m.p. = 113.0–114.9  $^{\circ}C$ ;  $[\alpha]_D^{20} = +25^{\circ}$  ( $c$  1,  
 $CHCl_3$ );  $^1H$  NMR ( $CDCl_3$ )  $\delta$  (ppm) 7.38–7.19 (m, 23H, benzyl  
aromatics), 7.03–7.01 (m, benzyl aromatics), 6.02 (br s, 1H, Ph-HS),  
4.98 (br s, 2H, Ph- $CH_2$ ), 4.89–4.85 (m, 2H, H-1'''), part  $A_1$  of  $A_1B_1$   
system, Ph- $CH_2$ ), 4.74 (d,  $J$  = 10.5 Hz, 1H, part  $A_2$  of  $A_2B_2$  system,  
4.60–4.56 (m, 2H, part  $A_3$  of  $A_3B_3$  system; part  $B_1$  of  
system  $A_1B_1$ , Ph- $CH_2$ ), 4.48 (d,  $J$  = 11.9 Hz, 1H, part  $B_3$  of  $A_3B_3$   
system, Ph- $CH_2$ ), 4.35–4.31 (m, 2H, part  $A_4$  of  $A_4B_4$  system, part  $B_2$   
of  $A_2B_2$  system, Ph- $CH_2$ ), 4.22 (d,  $J$  = 16.8 Hz, part  $B_4$  of  $A_4B_4$  system,  
Ph- $CH_2$ ), 3.94 (t,  $J$  = 9.2 Hz, 1H, H-3'''), 3.85–3.70 (m, H-5''', H-2''',  
H-6''', H-6'''), 3.63–3.60 (m, 1H, H-4''').  $^{13}C$  NMR ( $CDCl_3$ )  $\delta$   
(ppm) 203.4 (C-1), 164.4 (C-6), 161.3 (C-4), 160.5 (C-2), 138.3,  
137.6, 137.4, 135.9, 135.4 (benzyl  $C_q$ -aromatics), 129.8–126.6  
(benzyl CH-aromatics), 105.9 (C-1), 102.8 (C-3), 98.2 (C-5), 86.2  
(C-5'), 82.1 (C-2'), 78.6 (C-4'), 76.8 (C-3'), 76.3, 75.7, 75.3 ( $CH_2$ -  
Ph), 74.8 (C-1'), 73.3 ( $CH_2$ -Ph), 67.4 (C-6'), 50.3 ( $CH_2$ -Ph).  
HRMS-ESI ( $m/z$ ):  $[M + H]^+$  calcd for  $C_{48}H_{47}O_9$ , 767.3215; found,  
767.3223;  $[M + Na]^+$  calcd for  $C_{48}H_{46}NaO_9$ , 789.3034; found,  
789.3049.

**3-[( $\beta$ -D-Glucopyranosyl)-2,4,6-trihydroxyphenyl]-2-phenyle-**  
**than-1-one (37).** Compound **36** (0.13 g, 0.17 mmol) was dissolved  
in ethyl acetate (4.0 mL) and methanol (4.0 mL). Then, a suspension  
of Pd/C (10%) (130 mg) in ethyl acetate–methanol was added and  
the mixture was stirred under a  $H_2$  atmosphere for 3 h at room  
temperature. Pd/C was filtered through a pad of Celite and the  
solvent was evaporated under reduced pressure. The residue was  
purified by column chromatography (dichloromethane/MeOH, 7:1)  
to afford compound **37** in 68% yield. m.p. = 128.5–129.3  $^{\circ}C$ ;  $[\alpha]_D^{20} =$   
 $+47^{\circ}$  ( $c$  0.4, MeOH);  $^1H$  NMR [ $CO(CD_3)_2$ ]  $\delta$  (ppm) 7.28–7.15 (m,  
5H, ArCH), 5.93 (s, 1H, H-5), 4.86 (d,  $J$  = 9.8 Hz, 1H, H-1''), 4.38  
(s, 2H,  $CH_2$ ), 3.80–3.70 (m, 3H, H6''a, H6''b, H-2), 3.59–3.47 (m,  
2H, H-4', H-3'), 3.42 (dt,  $J$  = 9.5, 3.2 Hz, 1H, H-5'').  $^{13}C$  NMR  
[ $CO(CD_3)_2$ ]  $\delta$  (ppm) 203.0 (C-1), 163.5 (C-4), 163.4 (C-2), 162.6  
(C-6), 135.9 (C-1'), 129.7 (C-4'), 127.9 (C-3', C-5'), 126.1 (C-2', C-  
6'), 104.1 (C-1), 103.3 (C-3), 95.1 (C-5), 80.9 (C-5''), 78.3 (C-3''),  
74.9 (C-1''), 72.6 (C-2''), 69.6 (C-4''), 60.7 (C-6''), 49.4 ( $CH_2$ ).  
HRMS-ESI ( $m/z$ ):  $[M + H]^+$  calcd for  $C_{20}H_{23}O_9$ , 407.1337; found,  
407.1341.

**Biological Activity Assays. STD-NMR Binding Studies with**  
**IAPP.** NMR experiments were recorded on a Bruker Avance 600 MHz  
spectrometer equipped with a triple channel cryoprobe head.  
Immediately before use, lyophilized IAPP was dissolved in 10 mM  
NaOD in  $D_2O$  at a concentration of 160  $\mu M$  and then diluted 1:1  
with 10 mM phosphate-buffered saline (pH 7.4) containing 100 mM  
NaCl. To these samples were added the compounds in study, **21** and  
**37**, to a final concentration of 2 mM. The pH of each sample was  
verified with a Microelectrode (Mettler Toledo) for 5 mm NMR  
tubes and adjusted with NaOD and/or DCl. Selective saturation of  
the protein resonances (on resonance spectrum) was performed by  
irradiating at  $-0.5$  ppm using a series of Eburp2.1000-shaped pulses

1529 (50 ms) for a total saturation time of 2.0 s. For the reference spectrum  
1530 (off-resonance), the samples were irradiated at 100 ppm. STD  
1531 experiments were recorded at two temperatures, 298 and 310 K, with  
1532 a ligand/amyloid oligomer molar ratio of 12:1. Control STD  
1533 experiments with IAPP without any ligand and only with ligands 21  
1534 and 37 without IAPP were also recorded and taken into account in  
1535 the STD epitope determination. To determine the epitope mapping  
1536 of each ligand shown in Figure 3, the STD intensities of each proton  
1537 were normalized with respect to that with the highest response.  
1538 Proton resonances from which it was not possible to have an accurate  
1539 STD information are identified with an asterisk symbol in Figure 3.

1540 **Glucosidase and Cholinesterase Inhibition Assays.** Measurement  
1541 of the glucosidase inhibition was carried out using the methodology  
1542 previously reported by Bols and co-workers.<sup>80</sup> Inhibition assays were  
1543 conducted in a double-beam Hitachi U-2900 spectrophotometer, with  
1544 PS cuvettes at the wavelength indicated in each case.  $\alpha$ -Glucosidase (  
1545 *Saccharomyces cerevisiae*) and  $\beta$ -glucosidase (almonds) were used as  
1546 model enzymes and the corresponding *p*-nitrophenyl glycosides as  
1547 substrates. Initial screening for determining the percentage of  
1548 inhibition was conducted at a 100  $\mu$ M inhibitor concentration.  
1549 Inhibitor mother solutions were prepared in DMSO and the ratio of  
1550 DMSO in the cuvette was maintained at 5%. Two 1.2 mL samples in  
1551 PS cuvettes containing 0.1 M phosphate buffer (pH 6.8) were  
1552 prepared using the corresponding nitrophenyl glucopyranoside as a  
1553 substrate at a concentration equal to the expected value of  $K_M$ . Water  
1554 (control) or inhibitor solution plus water (100  $\mu$ M final  
1555 concentration) was added to a constant value of 1.14 mL. Finally,  
1556 reaction was initiated by the addition of a solution of properly diluted  
1557 enzyme (60  $\mu$ L) at 25 °C and monitored by registering the increase in  
1558 absorbance at 400 nm for 125 s.

1559 Initial rates were obtained from the slopes of the plots (Abs. vs *t*)  
1560 and used for calculating the percentage of inhibition using the  
1561 following equation

$$\% \text{Inhibition} = \frac{v_0 - v}{v_0} \times 100$$

1562 where  $v_0$  refers to the rate in the control experiment (enzyme), and  $v$   
1563 refers to the rate in the experiment containing the inhibitor solution.  
1564 For determining the percentage of inhibition, the substrate  
1565 concentration was fixed at the  $K_M$  value for each enzyme ( $[S] =$   
1566 0.25 mM for  $\alpha$ -glucosidase, and  $[S] = 4.0$  mM for  $\beta$ -glucosidase). For  
1567 compounds showing a significant percentage of inhibition, the mode  
1568 of inhibition was obtained using the Lineweaver–Burk plot and  
1569 Cornish–Bowden ( $1/v$  vs  $[I]$ ,  $[S]/v$  vs  $[I]$ ) plots.<sup>81</sup> The procedure  
1570 followed was the same as above, but using five different substrate  
1571 concentrations, ranging from 0.25 to 4.0 of the expected  $K_M$ , while  
1572 keeping the inhibitor concentration constant (three different inhibitor  
1573 concentrations). The reaction rate for the cuvette containing the  
1574 highest substrate concentration was allowed to be within 0.12–0.15  
1575 Abs/min. Kinetic parameters ( $K_M$ ,  $V_{max}$ ) were obtained using  
1576 nonlinear regression analysis (least squares fit) using the Michaelis–  
1577 Menten equation tool implemented in GraphPad Prism 8.01 software,  
1578 which in turn were used to calculate the inhibition constants,  
1579 according to the equations indicated below.

1580 For cholinesterase inhibition tests (acetylcholinesterase, AChE;  
1581 *Electrophorus electricus*) and butyrylcholinesterase (BuChE, equine  
1582 serum), Ellman's colorimetric assay<sup>82</sup> was followed, with minor  
1583 modifications. DMSO was kept within 1.25% cuvette concentration.  
1584 The chromogenic agent DTNB [5,5'-dithiobis(2-nitrobenzoic acid)]  
1585 was fixed at 0.975 mM concentration; 0.1 M phosphate buffer (pH  
1586 8.0) was employed,  $T = 25$  °C, and the reaction was monitored for  
1587 125 s at 405 nm. For determining the percentage of inhibition, the  
1588 substrate concentration (acetylthiocholine iodide for AChE; S-  
1589 butyrylthiocholine iodide for BuChE) was fixed at 29  $\mu$ M for AChE  
1590 and at 18.2  $\mu$ M for BuChE.

1591 The mode of inhibition and inhibition constants were obtained as  
1592 described above for glucosidases.

1593 Competitive inhibition (inhibitor only binds the free enzyme)

$$K_{ia} = \frac{[I]}{\frac{K_{M \text{ app}}}{K_M} - 1}$$

Mixed inhibition (inhibitor binds both the free and complexed  
enzymes) 1594 1595

$$K_{M \text{ app}} = K_M \frac{1 + \frac{[I]}{K_{ia}}}{1 + \frac{[I]}{K_{ib}}}$$

$$V_{\text{max app}} = \frac{V_{\text{max}}}{1 + \frac{[I]}{K_{ib}}}$$

Uncompetitive (the inhibitors only bind the complexed enzyme) 1596

$$K_{M \text{ app}} = \frac{K_M}{1 + \frac{[I]}{K_{ib}}}$$

$$V_{\text{max app}} = \frac{V_{\text{max}}}{1 + \frac{[I]}{K_{ib}}}$$

Noncompetitive (inhibitor binds both the free enzyme and  
complexed enzyme with equal affinity) 1597 1598

$$K_{M \text{ app}} = K_M$$

$$V_{\text{max app}} = \frac{V_{\text{max}}}{1 + \frac{[I]}{K_{ib}}}$$

The following inhibitor concentrations were used for the  
calculation of the inhibition constants: 1599 1600

Genistein 1601

•  $\alpha$ -Glucosidase: 0, 10, 20, 30  $\mu$ M. 1602

•  $\beta$ -Glucosidase: 0, 50, 83.3  $\mu$ M. 1603

Compound 33 1604

•  $\alpha$ -Glucosidase: 0, 33.3, 50  $\mu$ M. 1605

Experiments were carried out in duplicate, and the data are  
expressed as the mean  $\pm$  SD. 1606 1607

**Cell Culture.** The human induced pluripotent stem cell (hiPSC)  
line derived from a health control individual was used in this study.  
The hiPS (control MIF1)<sup>70</sup> was kindly provided by Professor Peter  
Andrews and Dr. Ivana Barbaric (Centre for Stem Cell Biology, The  
University of Sheffield). hiPSCs were maintained in Vitronectin-  
coated plates (0.5  $\mu$ g/cm<sup>2</sup>; Thermo Fisher Scientific) according to the  
manufacturer's recommendations in complete TeSR-E8 Medium  
(StemCell Technologies). The culture medium was changed every  
day. Cells were passaged every 5–7 days as clumps using ReLeSR, an  
enzyme-free reagent for cell dissociation (StemCell Technologies),  
according to the manufacturer's recommendations. For all the  
experiments in this study, hiPSCs were used between passages 18  
and 26, and all hiPSCs were cultured in 5% O<sub>2</sub> and 5% CO<sub>2</sub> at 37 °C.

**Natural A $\beta$  Oligomer and Control Solutions.** A solution  
containing natural amyloid-beta (A $\beta$ ) oligomers (a kind gift of Dr.  
Claire Garwood) was derived from the conditioned medium of 7PA2  
cells,<sup>46</sup> Chinese Hamster Ovary cells stably transfected with cDNA  
encoding APP751, and an amyloid precursor protein that contains the  
Val717Phe familial Alzheimer's disease mutation.<sup>83,84</sup> To obtain  
natural A $\beta$  oligomers,  $5 \times 10^6$  cells were seeded in a T175 flask and  
cultured in Dulbecco's modified Eagle's medium (DMEM, Sigma)  
supplemented with 10% fetal bovine serum (Thermo Fisher), 2 mM  
L-glutamine (Sigma-Aldrich), and 50 mg/mL penicillin/streptomycin.  
Cells were incubated for 24 h in 5% CO<sub>2</sub> at 37 °C. After 24 h of  
incubation, the cells were washed with serum-free medium and  
conditioned in 5 mL of plain DMEM without phenol red (Thermo  
Fisher) and lacking any additives overnight. The oligomer-containing  
conditioned medium (CM) was collected and cleared of cells and  
debris by centrifugation at 200g for 10 min at 4 °C. The CM was used  
as the natural A $\beta$  oligomer solution in the fear conditioning

1638 experiments for HCS. The concentrated CM contained between 1000  
1639 and 2000 pg/mL  $A\beta(1-42)$  as measured by ELISA (Thermo Fisher).  
1640 **Knockdown Experiment.** The knockdown is an experimental  
1641 technique by which the expression of a gene is transiently reduced; for  
1642 this reason, it is necessary to find out the optimal condition in which  
1643 we have the maximum effect preserving the cell viability. In HEK cells,  
1644 we observed that the detection should not be carried out prior to 24 h  
1645 post-transfection and, in terms of gene silencing, 24 h siRNA  
1646 transfection at a nontoxic concentration of 200 nM and 0.2  $\mu$ L of  
1647 DharmaFECT reagent was found to yield good knockdown results. It  
1648 was interesting to observe also how the gene expression started to  
1649 recover after 24 h, even if still under treatment, and also when the  
1650 transfection medium was replaced with complete medium and  
1651 incubated for further 24 h.

1652 Like other GPI-anchored proteins, PrP<sup>C</sup> can be released from the  
1653 cell surface *in vitro* by the action of exogenous bacterial  
1654 phosphatidylinositol-specific phospholipase C (PI-PLC). PLC acute  
1655 cleavage was therefore used to enhance the effect of the transient  
1656 knockdown.

1657 All reagents for the knockdown experiment, such as ON-  
1658 TARGETplus Human PRNP (5621) siRNA-SMARTpool, ON-  
1659 TARGETplus Non-targeting Pool, ON-TARGETplus GAPD Control  
1660 Pool, 5 $\times$  siRNA Buffer, DharmaFECT 1 Transfection Reagent, and  
1661 Molecular Grade RNase-free water, were purchased from GE  
1662 Healthcare Dharmacon. TrypLE Express Enzyme (1 $\times$ ) phenol red  
1663 was from Gibco via Thermo Fisher. Opti-MEM Reduced Serum  
1664 Medium and phospholipase C were obtained from Thermo Fisher.

1665 **HEK Cell Dosing.** Cells from the routine cell culture were seeded in  
1666 the 96-well plates (15,000 cells/well), previously coated with  
1667 polyornithin hydrobromide. After 24 h, the cells were checked to  
1668 ensure that they had attached and were ready for dosing. The  
1669 complete medium was replaced with conditioning medium containing  
1670  $1 \times 10^3$  pg/mL natural  $A\beta(1-42)$  for 2 h and washed with PBS  
1671  $Mg^{2+}/Ca^{2+}$  before being dosed with the compounds, dissolved in  
1672 phenol red medium, for 1 h. After that, cells were dosed for 2 h with  
1673 compounds at 10  $\mu$ M final concentration. The screen of each  
1674 compound was carried out in triplicate and repeated at least two  
1675 times. Negative control cells were treated with 0.5% DMSO, vehicle  
1676 of dilution of the drug, and positive control cells with only  $A\beta$ os.  
1677 Once dosing was completed, cells were rinsed with PBS (Sigma) and  
1678 fixed with 100  $\mu$ L/well of 4% PFA and incubated for 15 min at room  
1679 temperature. PFA was removed and cells were washed once or twice  
1680 with 100  $\mu$ L PBS if the plates have to be stored in the fridge in PBS.  
1681 The cells were blocked in 100  $\mu$ L of PBS-T 5% Donkey serum for 1 h  
1682 at r.t. and incubated with anti- $\beta$  amyloid 1-16 clone 6E10 anti-mouse  
1683 (BioLegend) overnight at 4  $^{\circ}$ C. The antibody was made up in 50  $\mu$ L  
1684 of PBS-T 5% Donkey serum with a dilution factor of 1:250. The  
1685 primary antibody was removed, and the cells washed three times with  
1686 50  $\mu$ L of PBS-T for 5 min each at r.t. before adding the secondary  
1687 antibody Alexa Fluor 594 to each well and incubating for 1 h at r.t.  
1688 The antibody was made up in PBS-T with a dilution factor of 1:500.  
1689 Cells were washed two times with PBS-T and one time with PBS (50  
1690  $\mu$ L) and nuclei were stained with 100 ng/mL DAPI in PBS prepared  
1691 from 5 mg/mL stock. After the last two washes, cells were left in 100  
1692  $\mu$ L of PBS to be analyzed. Image acquisition was performed by the  
1693 ImageXpress Micro Widefield High Content Screening System and  
1694 analysis of data with MetaXpress Software Multi-Wavelength  
1695 Translocation Application Module.

1696 **Neural Differentiation.** Neural induction of hiPSCs (Figure 11)  
1697 was performed using the modified version of dual SMAD inhibition  
1698 protocol.<sup>85</sup> hiPSCs were detached by 3 min of incubation with  
1699 Versene solution (Gibco); after incubation, the solution was removed,  
1700 1 mL of complete TeSR-E8 Medium (StemCell Technologies) was  
1701 added per well of a six-well plate and detached with a cell lifter  
1702 (Corning), and then, the cell suspension was transferred to a  
1703 Matrigel-coated plate (Corning Matrigel Growth Factor Reduced).  
1704 On the day after plating (day 1), after the cells have reached  $\sim$ 100%  
1705 confluence, the cells were washed once with PBS and then the  
1706 medium was replaced with neural medium (50% DMEM/F-12, 50%  
1707 neurobasal, 0.5 $\times$  N<sub>2</sub> supplement, 1 $\times$  Gibco GlutaMAX Supplement,

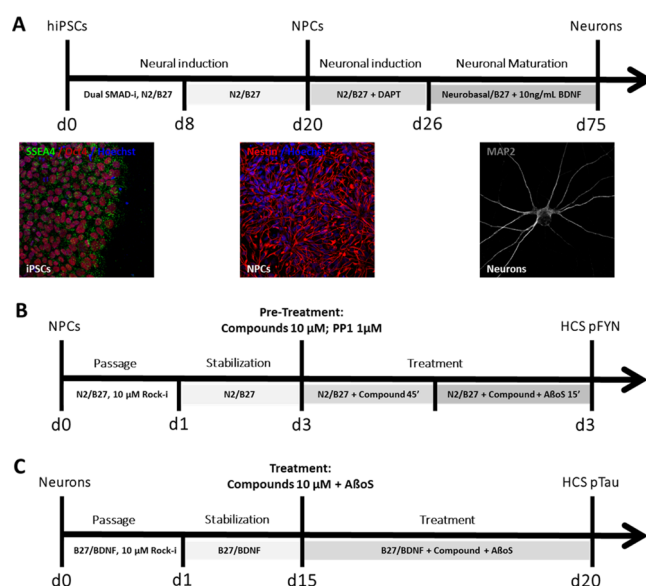


**Figure 11.** Differentiation of cortical neurons from iPSCs. (A) Outline of cortical differentiation protocol. (B) Outline of the treatment and high-content screening for pFyn kinase. (C) Outline of the treatment and high-content screening for pTau.

0.5 $\times$  B-27, 50 U mL<sup>-1</sup> penicillin and 50 mg mL<sup>-1</sup> streptomycin) 1708  
supplemented with SMAD inhibitors (SMAD-i, 2  $\mu$ M DMH-1, 2–10 1709  
 $\mu$ M SB43154, Tocris). The medium was changed every day for 7 1710  
days; on day 8, when it is possible to see a uniform neuroepithelial 1711  
sheet, the cells were split into 1:1 with Accutase (StemPro Accutase 1712  
Cell Dissociation Reagent, Gibco A1110501) onto a Matrigel 1713  
substrate in the presence of 10  $\mu$ M Rock inhibitor (Rock-i, Y- 1714  
27632 dihydrochloride, Tocris), giving rise to a sheet of neural 1715  
progenitor cells (NPCs). After 24 h of incubation, the medium was 1716  
removed and replaced with neural medium without Rock-i. The 1717  
culture medium was changed every second day and, once confluent, it 1718  
was split. 1719

Neuronal induction from neural progenitor cells was obtained from 1720  
previously described methods with modifications.<sup>84</sup> NPCs were 1721  
transferred to poly-L-ornithine/laminin-coated plates (10  $\mu$ g/mL) 1722  
and the medium was replaced with neuronal medium (neurobasal 1723  
medium, 1 $\times$  Gibco GlutaMAX Supplement, 1 $\times$  B-27) supplemented 1724  
with 10  $\mu$ M DAPT. The medium was changed every day for 6 days, 1725  
and immature neurons emerged around day 26. On day 40, the young 1726  
neurons were split with Accutase onto to poly-L-ornithine/laminin- 1727  
coated plates (10  $\mu$ g/mL) and the medium was replaced with 1728  
neuronal medium without DAPT and supplemented with 10 nM 1729  
BDNF. The cells were then fed at alternate days with neuronal 1730  
medium until day 75. 1731

**Fluorescence-Activated Cell Sorting (FACS) Analysis.** After 1732  
treatment with 100 nM siRNA (48 h), samples were washed with 1733  
 $Ca^{++}/Mg^{++}$  PBS and treated for 1 h with 0.4 U/mL PLC before being 1734  
harvested by TrypLE Express Enzyme (1 $\times$ ) phenol red. Cells were 1735  
resuspended in fresh medium, counted with a hemocytometer, 1736  
transferred into an Eppendorf tube ( $11.5 \times 10^6$  to  $1.5 \times 10^6$  cells) and 1737  
spun down at 1000 rpm for 5 min. The supernatant was decanted, and 1738  
the pellets were resuspended with cold  $Ca^{++}/Mg^{++}$  PBS to wash the 1739  
cells one time at 2000 rpm for 5 min at 4  $^{\circ}$ C. During the experiment, 1740  
it was always useful to check the viability of the cells as in which 1741  
should be around 95% and not less than 90%. The cells were then 1742  
resuspended in 1 mL of ice-cold FACS buffer ( $Ca^{++}/Mg^{++}$  PBS, 10% 1743  
FBS, 1% sodium azide) for 5–10 min. Sodium azide prevents the 1744  
modulation and internalization of surface antigens, which can produce 1745  
a loss of fluorescence intensity. The primary anti- $A\beta$ os 8H4 1746  
(concentration, 0.01 M) was diluted 1:200 in 100  $\mu$ L of PBS and 1747  
5% BSA and then the cells were resuspended in this solution, 1748  
incubated for 1 h on ice, and protected from light. The same was done 1749

for the 0.8:200 isotype (concentration, 2.5 mg/mL). The cells were washed two times with cold  $\text{Ca}^{++}/\text{Mg}^{++}$  PBS by centrifugation at 2000 rpm for 5 min and incubated with the secondary antibody in the dark for 1 h under gentle agitation. The fluorochrome-labeled secondary antibody Alexa Fluor 488 was diluted 1:500 in 100  $\mu\text{L}$  of PBS and 5% BSA. Before the analysis, the cells were washed and resuspended in 300  $\mu\text{L}$  of cold  $\text{Ca}^{++}/\text{Mg}^{++}$  PBS and 2  $\mu\text{L}$  of propidium iodide (PI) was added to each sample to exclude dead cells. For best results, all reagents/solutions used were cold and cells were kept on ice and analyzed immediately on the flow cytometer.

**Immunocytochemistry (ICC) Analysis.** After the transfection with 100 nM siRNA (48 h), the same samples were treated for 1 h with 0.4 U/mL PLC. The cells were rinsed with PBS and conditioning medium containing natural  $\text{A}\beta(1-42)$  ( $1 \times 10^3$  pg/mL) was added. After 2 h, cells were washed with  $\text{Mg}^{2+}/\text{Ca}^{2+}$  PBS, fixed with 100  $\mu\text{L}$  well 4% PFA, and incubated for 15 min at room temperature. PFA was removed and cells were washed once or twice with 100  $\mu\text{L}$  of PBS if the plates had to be stored in the fridge in PBS. The cells were blocked in 100  $\mu\text{L}$  of PBS-T 5% Donkey serum for 1 h at r.t. and incubated with anti- $\beta$  amyloid 1-16 clone 6E10 anti-mouse overnight at 4  $^{\circ}\text{C}$ . The antibody was made up in 50  $\mu\text{L}$  of PBS-T 5% Donkey serum with a dilution factor of 1:250. The primary antibody was removed, and the cells were washed three times with 50  $\mu\text{L}$  of PBS-T for 5 min each at r.t. before adding the secondary antibody Alexa Fluor 488 to each well and incubating for 1 h at r.t. The antibody was made up in PBS-T with a dilution factor of 1:500. Cells were washed two times with PBS-T and one time with PBS (50  $\mu\text{L}$ ) and nuclei were stained with 100 ng/mL 4,6-diamidino-2-phenylindole (DAPI) in PBS prepared from 5 mg/mL stock. After the last two washes, cells were left in 100  $\mu\text{L}$  of PBS to be analyzed. Image acquisition was performed by the ImageXpress Micro Widefield High Content Screening System and analysis of data with MetaXpress Software Multi-Wavelength Translocation Application Module.

**Treatments.** The cells were exposed to the solution containing natural  $\text{A}\beta$  oligomers obtained from 7PA2 cells [1000 pg/mL  $\text{A}\beta(1-42)$ ]. The compounds were diluted at 10 mM in DMSO (Sigma Chemical Co) and kept out of light at  $-20$   $^{\circ}\text{C}$  until use. PP1 (potent, selective Src family kinase inhibitor) was obtained from Tocris (1397), stored at 1 mM in DMSO (Sigma Chemical Co), and kept out of light at  $-20$   $^{\circ}\text{C}$  until use. To determine the effects of the compounds on inhibiting the activation of Fyn Kinase, NPC cultures were pretreated for 45 min with 10  $\mu\text{M}$  of the compounds or 1  $\mu\text{M}$  PP1 diluted in neurobasal medium without phenol red. After pretreatment, the cells were exposed to 1000 pg/mL of  $\text{A}\beta$  oligomers in association with the compounds for 15 min; control cultures were treated with DMSO, the vehicle of dilution of the drugs. PP1 was used as a control of inhibition of Fyn activation. To evaluate the potential of the compounds to inhibit the hyperphosphorylation of Tau, cortical neurons were exposed to 1000 pg/mL of  $\text{A}\beta$  oligomers in association with 10  $\mu\text{M}$  of the compounds for 5 days.

**Immunofluorescence.** For immunostaining, hiPSCs, NPCs, and neurons were washed with phosphate-buffered saline (PBS) and fixed by immersion in 4% *p*-formaldehyde for 15 min at room temperature. Following fixation, samples were washed three times with PBS and permeabilized with 0.3% Triton X-100 in PBS (Sigma) for 5 min to detect intracellular antigens. After permeabilization, cells were blocked by incubation with PBS containing 5% Donkey serum (DS) (Millipore) for 1 h. After blocking, cell cultures were incubated overnight at 4  $^{\circ}\text{C}$  with primary antibodies diluted in PBS containing 1% DS. After three washes with PBS, cells were incubated with secondary antibodies diluted in PBS containing 1% DS for 1 h at room temperature in the dark. The samples were washed three more times with PBS and incubated with 1.0 mg/mL DAPI for nuclear staining. The following primary antibodies were used at the indicated dilutions: anti-SSEA4 (MC813-70) (mouse, 1:200; Thermo Fisher, 41-4000), anti-Oct4 [EPRI7929] (rabbit, 1:250; Abcam, ab181557), anti-Nestin [EPRI7929] (rabbit, 1:500; BioLegend, 841901), anti-Tubulin  $\beta$ 3 (TUJ1) (mouse, 1:1000; BioLegend, 801201), anti-MAP2 (guinea pig, 1:1000; Synaptic Systems, 188004), anti-phospho-Tau PHF-Tau (Thr181) (mouse, 1:500; Thermo Fisher, MN1050),

and Phospho-Fyn (Tyr530) (rabbit, 1:500; Thermo Fisher, PA-36644). The following secondary antibodies were used at the indicated dilutions: Alexa Fluor 488-conjugated Donkey anti-mouse IgG (1:400; Thermo Fisher, A-21202), Alexa Fluor 594-conjugated Donkey anti-rabbit IgG (1:400; Thermo Fisher, A-31572), Alexa Fluor 594-conjugated Donkey anti-mouse IgG (1:400; Thermo Fisher, A-21203), Alexa Fluor 647-conjugated Goat anti-guinea pig IgG (1:400; Thermo Fisher, A-21450). All experiments included cultures where the primary antibodies were not added, and unspecific stain was not observed in such negative controls. Images were taken from the 63 $\times$  objective on a Leica TCS SP5 confocal laser scanning microscope coupled with LAS AF lite software (Wetzlar, Germany). We used 386, 488, and 594 nm lasers, along with the appropriate excitation and emission filters. These settings were kept consistent while taking images from all cultures.

**High-Content Image Screening (HCS).** NPCs were plated at  $1 \times 10^4$  cells per well on poly-L-ornithine/laminin-coated 96-well plates; after 3 days, the cells were treated. After the treatment, the cells were fixed and stained for pFyn kinase and Alexa Fluor 594 Phalloidin was used as a marker that defines the boundary of cells and DAPI for nuclear staining. A quantitative imaging analysis of the NPCs was conducted through the Opera Phenix High Content Screening System at 40 $\times$  magnification using the Columbus Image analysis system. The morphological features such as the number of cells and number of spots per cell were assessed for both treated and control cells. At least 15 fields were randomly selected and scanned per well of a 96-well plate in triplicate. To identify and remove any false readings generated by the system, three random  $\text{A}\beta$  and control wells were selected and counted manually (blind to the group). For the pTau experiment, the treatment with compounds was done concomitantly, with  $\text{A}\beta$  medium being changed after 3 days of treatment, and cells were allowed to differentiate for 2 more days. On day 5, cells were fixed for immunocytochemistry. The morphological features assessed for both treated and control cells were the number of cells and intensity of Alexa 568 per cell.

**MTT Assay.** Cortical neural cells were plated on a 96-well plate at a density of  $1 \times 10^4$  cells/well and kept in a controlled environment (37  $^{\circ}\text{C}$  and 5%  $\text{CO}_2$ ). After 3 days, cells were exposed for 24 h to the medium containing the compounds at a concentration of 1–50  $\mu\text{M}$ . The effect of treatment on cell viability was assessed by measuring mitochondrial enzymatic activity by the 3-(4,5-dimethylthiazol-2-yl)-2,5-diphenyltetrazolium bromide assay (MTT formazan; Sigma-Aldrich). Two hours before the end of the treatment, the MTT solution was added to each well (10  $\mu\text{L}$ /well) at a final concentration of 1  $\mu\text{g}$ /mL and diluted in neural medium. After 2 h, the cells were lysed with a volume of 60  $\mu\text{L}$ /well acidified isopropanol solution at room temperature under agitation for 10 min to complete the dissolution of the formazan crystals. The optical absorbance of each sample was measured using the spectrophotometer at a wavelength of 490 nm (PHERAstar FS microplate reader). The cell cytotoxicity was quantified by measuring the conversion of MTT into MTT formazan by mitochondrial dehydrogenases of viable cells. Each experimental condition was performed in eight replicate wells in at least three independent experiments. The results show the percentage of viability of the cells, and control cells treated with DMSO were considered to be 100%.

**Aggregation Assays.** For light scattering and spectrophotometric measurements, each compound was dissolved in 10 mM phosphate-buffered saline (PBS) containing 100 mM NaCl (pH 7.4, filtered through paper with 5  $\mu\text{m}$  pores) and 1.25% DMSO for compounds 8, 9, 10, 23, 24, and 33, 2.5% for compounds 21 and 26, and 5% for compounds 18 and 25 to a final concentration of 10, 50, or 100  $\mu\text{M}$ . After mixing with a vortex, samples were incubated for 2 h at room temperature and protected from light. The positive and negative controls were prepared under the same conditions, *i.e.*, in PBS and the same DMSO concentrations used for the compounds: 1.25, 2.5, or 5%.

Absorbance measurements were performed at room temperature ( $24 \pm 1$   $^{\circ}\text{C}$ ) with a Jasco V-560 UV/Vis double beam spectrophotometer using quartz cuvettes with a 1 cm optical path.



1890 Light scattering (Rayleigh) was determined by measuring the  
1891 intensity of light scattered at 90° and 550 nm with a Fluorolog model  
1892 3.22 spectrofluorimeter in right-angle geometry (Horiba Jobin Yvon)  
1893 at room temperature using 1 cm × 1 cm quartz Suprasil cuvettes and  
1894 setting both excitation and emission wavelengths to 550 nm with a  
1895 bandwidth of 1 nm. Three independent replicates were performed for  
1896 each compound at each concentration, with at least 10 measurements  
1897 per replicate.

1898 **Log  $D_{7.4}$  Determination.** The *in silico* prediction tool ALOGPS<sup>86</sup>  
1899 was used to estimate the octanol–water partition coefficients (log  $P$ )  
1900 of the compounds. Depending on these values, the compounds were  
1901 classified either as hydrophilic (log  $P$  below zero), moderately  
1902 lipophilic (log  $P$  between zero and one), or lipophilic (log  $P$  above  
1903 one) compounds. For each category, two different ratios (volume of  
1904 octan-1-ol to volume of buffer) were defined as experimental  
1905 parameters (Table 5).

**Table 5. Compound Classification Based on Estimated Log  $P$  Values**

compound category	log $P$	ratios (octan-1-ol:buffer)
hydrophilic	<0	30:140, 40:130
moderately lipophilic	0–1	70:110, 110:70
lipophilic	>1	3:180, 4:180

1906 Equal amounts of phosphate buffer (0.1 M, pH 7.4) and octan-1-ol  
1907 were mixed and shaken vigorously for 5 min to saturate the phases.  
1908 The mixture was left until separation of the two phases, and the buffer  
1909 was retrieved. Stock solutions of the test compounds were diluted  
1910 with buffer to a concentration of 1 μM. For each compound, three  
1911 determinations per octan-1-ol:buffer ratio were performed in different  
1912 wells of a 96-well plate. The respective volumes of buffer containing  
1913 an analyte (1 μM) were pipetted to the wells and covered by saturated  
1914 octan-1-ol according to the chosen volume ratio. The plate was sealed  
1915 with aluminum foil, shaken (1350 rpm, 25 °C, 2 h) on a Heidolph  
1916 Titramax 1000 plate shaker (Heidolph Instruments GmbH & Co.  
1917 KG, Schwabach, Germany), and centrifuged (2000 rpm, 25 °C, 5 min,  
1918 5804 R Eppendorf centrifuge, Hamburg, Germany). The aqueous  
1919 phase was transferred to a 96-well plate for analysis by liquid  
1920 chromatography–mass spectrometry (LC–MS, see below). Log  $P$   
1921 coefficients were calculated from the octan-1-ol:buffer ratio (o:b), the  
1922 initial concentration of the analyte in buffer (1 μM), and the  
1923 concentration of the analyte in buffer ( $c_B$ ) according to the following  
1924 equation

$$\log P = \log \left( \frac{1 \mu\text{M} - c_B}{c_B} \times \frac{1}{o:b} \right)$$

1925 Results are presented as the mean ± SD of three independent  
1926 experiments. If the mean of two independent experiments obtained  
1927 for a given compound did not differ by more than 0.1 units, then the  
1928 results were accepted.

1929 **Parallel Artificial Membrane Permeability Assay (PAMPA).**  
1930 Effective permeability (log  $P_e$ ) was determined in a 96-well format  
1931 with PAMPA.<sup>87</sup> For each compound, measurements were performed  
1932 at pH 7.4 in quadruplicates. Four wells of a deep-well plate were filled  
1933 with 650 μL of PRISMA HT universal buffer, adjusted to pH 7.4 by  
1934 adding the requested amount of NaOH (0.5 M). Samples (150 μL)  
1935 were withdrawn from each well to determine the blank spectra by  
1936 UV/Vis spectroscopy (190 to 500 nm, SpectraMax 190, Molecular  
1937 Devices, Silicon Valley, CA, USA). Then, an analyte dissolved in  
1938 DMSO (10 mM) was added to the remaining buffer to yield 50 μM  
1939 solutions. To exclude precipitation, the optical density (OD) was  
1940 measured at 650 nm, and solutions exceeding OD 0.01 were filtrated.  
1941 Afterward, samples (150 μL) were withdrawn to determine the  
1942 reference spectra. Further, 200 μL of samples was transferred to each  
1943 well of the donor plate of the PAMPA sandwich (pIon, P/N 110163).  
1944 The filter membranes at the bottom of the acceptor plate were infused  
1945 with 5 μL of GIT-0 Lipid Solution and 200 μL of Acceptor Sink

1946 Buffer was filled into each acceptor well. The sandwich was  
1947 assembled, placed in the GutBox, and left undisturbed for 16 h.  
1948 Then, it was disassembled and samples (150 μL) were transferred  
1949 from each donor and acceptor well to UV plates for determination of  
1950 the UV/Vis spectra. Effective permeability (log  $P_e$ ) was calculated  
1951 from the compound flux deduced from the spectra, the filter area, and  
1952 the initial sample concentration in the donor well with the aid of the  
1953 PAMPA Explorer Software (pIon, version 3.5).

1954 **LC–MS Measurements.** Analyses were performed using a 1100/  
1955 1200 Series HPLC System coupled to a 6410 Triple Quadrupole mass  
1956 detector (Agilent Technologies, Inc., Santa Clara, CA, USA)  
1957 equipped with electrospray ionization. The system was controlled  
1958 with the Agilent MassHunter Workstation Data Acquisition software  
1959 (version B.01.04). The column used was an Atlantis T3 C18 column  
1960 (2.1 × 50 mm) with a 3 μm particle size (Waters Corp., Milford, MA,  
1961 USA). The mobile phase consisted of eluent A (10 mM ammonium  
1962 acetate, pH 5.0, in 95:5 H<sub>2</sub>O:MeCN) and eluent B (MeCN  
1963 containing 0.1% formic acid). The flow rate was maintained at 0.6  
1964 mL/min. The gradient was ramped from 95% A/5% B to 5% A/95%  
1965 B over 1 min and then held at 5% A/95% B for 0.1 min. The system  
1966 was then brought back to 95% A/5% B, resulting in a total duration of  
1967 4 min. MS parameters such as fragmentor voltage, collision energy,  
1968 and polarity were optimized individually for each drug, and the  
1969 molecular ion was followed for each compound in the multiple  
1970 reaction monitoring mode. The concentrations of the analytes were  
1971 quantified by Agilent Mass Hunter Quantitative Analysis software  
1972 (version B.01.04).

## ■ ASSOCIATED CONTENT

### Supporting Information

The Supporting Information is available free of charge at  
<https://pubs.acs.org/doi/10.1021/acs.jmedchem.0c00841>.

DFT calculations, STD-NMR experiments, ThT fluo-  
rescence assays, membrane PAINS calculations, aggre-  
gation studies, <sup>1</sup>H NMR and <sup>13</sup>C NMR spectra of novel  
final compounds and key intermediates, analysis of the  
purity of tested compounds by HPLC-DAD-ESI(–)MS,  
and analysis of the purity of tested compounds by  
HPLC-DAD (PDF)

Molecular formula strings (CSV)

## ■ AUTHOR INFORMATION

### Corresponding Authors

**Beining Chen** – Department of Chemistry, The University of  
Sheffield, Sheffield S3 7HF, United Kingdom;

Phone: +447710075082; Email: [b.chen@sheffield.ac.uk](mailto:b.chen@sheffield.ac.uk)

**Amélia P. Rauter** – Centro de Química Estrutural, Faculdade de  
Ciências, Universidade de Lisboa, Lisboa 1749-016, Portugal;

[orcid.org/0000-0003-3790-7952](https://orcid.org/0000-0003-3790-7952);

Phone: +351968810971; Email: [aprauter@fc.ul.pt](mailto:aprauter@fc.ul.pt)

### Authors

**Ana M. de Matos** – Centro de Química Estrutural, Faculdade de  
Ciências, Universidade de Lisboa, Lisboa 1749-016, Portugal

**M. Teresa Blázquez-Sánchez** – Centro de Química Estrutural,  
Faculdade de Ciências, Universidade de Lisboa, Lisboa 1749-  
016, Portugal

**Andreia Bento-Oliveira** – Centro de Química Estrutural,  
Faculdade de Ciências, Universidade de Lisboa, Lisboa 1749-  
016, Portugal

**Rodrigo F. M. de Almeida** – Centro de Química Estrutural,  
Faculdade de Ciências, Universidade de Lisboa, Lisboa 1749-  
016, Portugal

**Rafael Nunes** – Centro de Química Estrutural, Faculdade de  
Ciências and Biosystems & Integrative Sciences Institute,

2008 Faculdade de Ciências, Universidade de Lisboa, Lisboa 1749-  
2009 016, Portugal; [orcid.org/0000-0002-9014-0570](https://orcid.org/0000-0002-9014-0570)  
2010 **Pedro E. M. Lopes** – Centro de Química Estrutural, Faculdade  
2011 de Ciências and Biosystems & Integrative Sciences Institute,  
2012 Faculdade de Ciências, Universidade de Lisboa, Lisboa 1749-  
2013 016, Portugal  
2014 **Miguel Machuqueiro** – Centro de Química Estrutural,  
2015 Faculdade de Ciências and Biosystems & Integrative Sciences  
2016 Institute, Faculdade de Ciências, Universidade de Lisboa, Lisboa  
2017 1749-016, Portugal  
2018 **Joana S. Cristóvão** – Biosystems & Integrative Sciences Institute,  
2019 Faculdade de Ciências, Universidade de Lisboa, Lisboa 1749-  
2020 016, Portugal  
2021 **Cláudio M. Gomes** – Biosystems & Integrative Sciences  
2022 Institute, Faculdade de Ciências, Universidade de Lisboa, Lisboa  
2023 1749-016, Portugal; [orcid.org/0000-0003-4662-6933](https://orcid.org/0000-0003-4662-6933)  
2024 **Cleide S. Souza** – Department of Chemistry, The University of  
2025 Sheffield, Sheffield S3 7HF, United Kingdom  
2026 **Imane G. El Idrissi** – Dipartimento di Farmacia-Scienze del  
2027 Farmaco, Università degli Studi di Bari “A. Moro”, 70125 Bari,  
2028 Italy  
2029 **Nicola A. Colabufo** – Dipartimento di Farmacia-Scienze del  
2030 Farmaco, Università degli Studi di Bari “A. Moro”, 70125 Bari,  
2031 Italy; [orcid.org/0000-0001-5639-7746](https://orcid.org/0000-0001-5639-7746)  
2032 **Ana Diniz** – UCIBIO, REQUIMTE, Faculdade de Ciências e  
2033 Tecnologia, Universidade Nova de Lisboa, Caparica 2829-516,  
2034 Portugal  
2035 **Filipa Marcelo** – UCIBIO, REQUIMTE, Faculdade de Ciências  
2036 e Tecnologia, Universidade Nova de Lisboa, Caparica 2829-  
2037 516, Portugal  
2038 **M. Conceição Oliveira** – Mass Spectrometry Facility at CQE,  
2039 Instituto Superior Técnico, Lisboa 1049-001, Portugal  
2040 **Óscar López** – Departamento de Química Orgánica, Facultad  
2041 de Química, Universidad de Sevilla, Sevilla E-41071, Spain  
2042 **José G. Fernandez-Bolaños** – Departamento de Química  
2043 Orgánica, Facultad de Química, Universidad de Sevilla, Sevilla  
2044 E-41071, Spain; [orcid.org/0000-0003-1499-0650](https://orcid.org/0000-0003-1499-0650)  
2045 **Philipp Dätwyler** – Department of Pharmaceutical Sciences,  
2046 University of Basel, Basel CH-4056, Switzerland  
2047 **Beat Ernst** – Department of Pharmaceutical Sciences, University  
2048 of Basel, Basel CH-4056, Switzerland; [orcid.org/0000-0001-5787-2297](https://orcid.org/0000-0001-5787-2297)  
2049  
2050 **Ke Ning** – Department of Neuroscience, Sheffield Institute for  
2051 Translational Neuroscience, The University of Sheffield, Sheffield  
2052 S10 2HQ, United Kingdom  
2053 **Claire Garwood** – Department of Neuroscience, Sheffield  
2054 Institute for Translational Neuroscience, The University of  
2055 Sheffield, Sheffield S10 2HQ, United Kingdom

2056 Complete contact information is available at:  
2057 <https://pubs.acs.org/10.1021/acs.jmedchem.0c00841>

#### 2058 Author Contributions

2059 <sup>¶</sup>A.M.d.M. and M.T.B.-S. contributed equally to this work.

#### 2060 Notes

2061 The authors declare no competing financial interest.

#### 2062 ■ ACKNOWLEDGMENTS

2063 The European Union is gratefully acknowledged for the  
2064 support of the project entitled “Diagnostic and Drug Discovery  
2065 Initiative for Alzheimer’s Disease” (D3i4AD), FP7-PEOPLE-  
2066 2013-IAPP, GA 612347. The authors also thank the  
2067 Portuguese Foundation for Science and Technology (FCT)

for the Ph.D. scholarships attributed to A.M.d.M. (SFRH/BD/ 2068  
93170/2013), R.N. (SFRH/BD/116614/2016), A.D. (PD/ 2069  
BD/142847/2018), and A.B.-O. (SFRH/BD/145600/2019), 2070  
for the research grant CEECIND/03414/2018 given to 2071  
R.F.M.d.A., and for the support of ~~both the~~ Centro de 2072  
Química Estrutural (project UIDB/00100/2020), and the 2073  
Applied Molecular Biosciences Unit (UCIBIO project UID/ 2074  
Multi/04378/2019), and F.M. also thanks FCT for the IF 2075  
investigator project (IF/00780/2015). The NMR spectrom- 2076  
eters are part of the National NMR Network (PTNMR) and 2077  
are partially supported by Infrastructure Project No. 22161 2078  
(cofinanced by FEDER through COMPETE 2020, POCI and 2079  
PORK and FCT through PIDDAC). ~~M.M. also acknowledges~~ 2080  
~~FCT for the individual grant CEECIND/02300/2017 and the~~ 2081  
~~Research Unit grant UID/MULTI/04046/2019.~~ Diogo Vila- 2082  
Viçosa is also acknowledged for fruitful discussion on 2083  
performed DFT calculations. The Dirección General de 2084  
Investigación of Spain (CTQ2016-78703-P), the Junta de 2085  
Andalucía (FQM134), and FEDER (S01100008530) are also 2086  
acknowledged for the financial support. 2087

#### 2088 ■ ABBREVIATIONS USED

AChE, acetylcholinesterase; AD, Alzheimer’s disease;  $A\beta$ , 2089  
amyloid beta;  $A\beta$ os,  $A\beta$  oligomers; AFM, atomic force 2090  
microscopy; BBB, blood–brain barrier; BuChE, butyrylcholi- 2091  
nesterase; cDNA, complementary DNA; CHO, Chinese 2092  
hamster ovary cells;  $c \log P$ , calculated partition coefficient; 2093  
CM, conditioned medium; DAPI, 4,6-diamidino-2-phenyl- 2094  
indole; DFT, density functional theory; DID, diabetes-induced 2095  
dementia; DMAP, 4-dimethylaminopyridine; DMEM, Dulbec- 2096  
co’s modified Eagle’s medium; DMSO, dimethyl sulfoxide; 2097  
DTNB, 5,5’-dithiobis(2-nitrobenzoic acid); ELISA, enzyme 2098  
-linked immunosorbent assay; FACS, fluorescence-activated 2099  
cell sorting; GLUT, glucose transporter; GPI, glycosylphos- 2100  
phatidylinositol; HCS, high-content image screening; HEK, 2101  
human embryonic kidney; HPLC, high-performance liquid 2102  
chromatography; IAPP, islet amyloid polypeptide; ICC, 2103  
immunocytochemistry; IDE, insulin-degrading enzyme; 2104  
hipSC, human induced pluripotent stem cell line; Ket, 2105  
ketoconazole; LC–MS, liquid chromatography coupled to 2106  
mass spectrometry;  $\log D$ , distribution coefficient;  $\log P$ , 2107  
partition coefficient;  $\log P_e$ , effective permeability;  $mA\beta$ , 2108  
monomeric  $A\beta$ ; MeCN, acetonitrile; MTT, 3-(4,5-dimethylth- 2109  
iazol-2-yl)-2,5-diphenyl-2H-tetrazolium bromide; NFT, neuro- 2110  
fibrillary tangles; NPC, neural progenitor cell; PAINS, pan- 2111  
assay interference compounds; PAMPA, parallel artificial 2112  
membrane permeability assay; PBS, phosphate-buffered saline; 2113  
PFA, paraformaldehyde; pFyn, Src family kinase; PHF, paired 2114  
helical filaments; PMF, potential of mean force; PLC, 2115  
phospholipase C; POPC, 1-palmitoyl-2-oleoyl-*sn*-glycero-3- 2116  
phosphocholine; PPI, protein phosphatase 1; PrP<sup>C</sup>, cellular 2117  
prion protein; pTau, phosphorylated Tau; Quer, quercetin; 2118  
SGLT, sodium glucose-linked transporter; siRNA, small 2119  
interfering RNA; SFK, Src family kinases; STD, saturation- 2120  
transfer difference; T2D, type 2 diabetes; TfOH, trifluor- 2121  
omethanesulfonic acid; ThT, thioflavin-T; TMSOTf, trime- 2122  
thylsilyl trifluoromethanesulfonate; UV, ultraviolet; Vis, visible 2123

#### 2124 ■ REFERENCES

(1) Williams, R.; Colagiuri, S.; Chan, J.; Gregg, E. W.; Ke, C.; Lim, 2125  
L. L.; Yang, X. *IDF Diabetes Atlas*; 9<sup>th</sup> ed., eds. Karuranga, S.; Malanda, 2126  
B.; Saedi, P.; Salpea, P., International Diabetes Federation: United 2127  
kingdom, 2019, p.35. 2128

- (2) de Matos, A. M.; de Macedo, M. P.; Rauter, A. P. Bridging type 2 diabetes and Alzheimer's disease: assembling the puzzle pieces in the quest for the molecules with therapeutic and preventive potential. *Med. Res. Rev.* **2018**, *38*, 261–324.
- (3) Nygaard, H. B. Targeting Fyn kinase in Alzheimer's disease. *Biol. Psychiatry.* **2018**, *83*, 369–376.
- (4) Um, J. W.; Strittmatter, S. M. Amyloid- $\beta$  induced signaling by cellular prion protein and Fyn kinase in Alzheimer disease. *Prion* **2013**, *7*, 37–41.
- (5) Smith, L. M.; Zhu, R.; Strittmatter, S. M. Disease-modifying benefit of Fyn blockade persists after washout in mouse Alzheimer's model. *Neuropharmacology* **2018**, *130*, 54–61.
- (6) Kaufman, A. C.; Salazar, S. V.; Haas, L. T.; Yang, J.; Kostylev, M. A.; Jeng, A. T.; Robinson, S. A.; Gunther, E. C.; van Dyck, C. H.; Nygaard, H. B.; Strittmatter, S. M. Fyn inhibition rescues established memory and synapse loss in Alzheimer mice. *Ann. Neurol.* **2015**, *77*, 953–971.
- (7) Lambert, M. P.; Barlow, A. K.; Chromy, B. A.; Edwards, C.; Freed, R.; Liosatos, M.; Morgan, T. E.; Rozovsky, I.; Trommer, B.; Viola, K. L.; Wals, P.; Zhang, C.; Finch, C. E.; Krafft, G. A.; Klein, W. L. Diffusible, nonfibrillar ligands derived from A $\beta$ (1–42) are potent central nervous system neurotoxins. *Proc. Natl. Acad. Sci. U. S. A.* **1998**, *95*, 6448–6453.
- (8) Yamada, E.; Pessin, J. E.; Kurland, I. J.; Schwartz, G. J.; Bastie, C. C. Fyn-dependent regulation of energy expenditure and body weight is mediated by tyrosine phosphorylation of LKB1. *Cell Metab.* **2010**, *11*, 113–124.
- (9) Lee, T.-W. A.; Kwon, H.; Zong, H.; Yamada, E.; Vatish, M.; Pessin, J. E.; Bastie, C. C. Fyn deficiency promotes a preferential increase in subcutaneous adipose tissue mass and decreased visceral adipose tissue inflammation. *Diabetes* **2013**, *62*, 1537–1546.
- (10) Yang, Y.; Tarabra, E.; Yang, G. S.; Vaitheesvaran, B.; Palacios, M. G.; Kurland, I. J.; Pessin, J. E.; Bastie, C. C. Alteration of de novo glucose production contributes to fasting hypoglycaemia in Fyn deficient mice. *PLoS One* **2013**, *8*, No. e81866.
- (11) Oskarsson, M. E.; Paulsson, J. F.; Schultz, S. W.; Ingelsson, M.; Westermark, P.; Westermark, G. T. In vivo seeding and cross-seeding of localized amyloidosis: a molecular link between type 2 diabetes and Alzheimer's disease. *Am. J. Pathol.* **2015**, *185*, 834–846.
- (12) Baram, M.; Atsmon-Raz, Y.; Ma, B.; Nussinov, R.; Miller, Y. Amylin- $\beta$  oligomers at atomic resolution using molecular dynamics simulations: a link between Type 2 diabetes and Alzheimer's disease. *Phys. Chem. Chem. Phys.* **2016**, *18*, 2330–2338.
- (13) Nabavi, S. F.; Sureda, A.; Dehpour, A. R.; Shirooie, S.; Silva, A. S.; Devi, K. P.; Ahmed, T.; Ishaq, N.; Hashim, R.; Sobarzo-Sánchez, E.; Daglia, M.; Braidy, N.; Volpicella, M.; Vacca, R. A.; Nabavi, S. M. Regulation of autophagy by polyphenols: Paving the road for treatment of neurodegeneration. *Biotechnol. Adv.* **2017**, *36*, 1768–1778.
- (14) Jia, J. J.; Zeng, X. S.; Song, X. Q.; Zhang, P. P.; Chen, L. Diabetes mellitus and Alzheimer's disease: The protection of epigallocatechin-3-gallate in streptozotocin injection-induced models. *Front. Pharmacol.* **2017**, *8*, 834.
- (15) Guo, Y.; Zhao, Y.; Nan, Y.; Wang, X.; Chen, Y.; Wang, S. (–)-Epigallocatechin-3-gallate ameliorates memory impairment and rescues the abnormal synaptic protein levels in the frontal cortex and hippocampus in a mouse model of Alzheimer's disease. *Neuroreport.* **2017**, *28*, 590–597.
- (16) Chen, S.; Nimick, M.; Cridge, A. G.; Hawkins, B. C.; Rosengren, R. J. Anticancer potential of novel curcumin analogs towards castrate-resistant prostate cancer. *Int. J. Oncol.* **2018**, *52*, 2190–2197.
- (17) Rauter, A. P.; Ennis, M.; Hellwich, K. H.; Herold, B. J.; Horton, D.; Moss, G. P.; Schomburg, I. Nomenclature of flavonoids (IUPAC recommendations 2017). *Pure Appl. Chem.* **2018**, 1429–1486.
- (18) Biasutto, L.; Marotta, E.; Bradaschia, A.; Fallica, M.; Mattarei, A.; Garbisa, S.; Zoratti, M.; Paradisi, C. Soluble polyphenols: synthesis and bioavailability of 3,4',5-tri-( $\alpha$ -D-glucose-3-O-succinyl) resveratrol. *Bioorg. Med. Chem. Lett.* **2009**, *19*, 6721–6724.
- (19) Hollman, P. C. H. Absorption, bioavailability, and metabolism of flavonoids. *Pharm. Biol.* **2004**, *42*, 74–83.
- (20) Xiao, J. Dietary flavonoid aglycones and their glycosides: Which show better biological significance? *Crit. Rev. Food Sci. Nutr.* **2017**, *57*, 1874–1905.
- (21) Ladiwala, A. R. A.; Mora-Pale, M.; Lin, J. C.; Bale, S. S.; Fishman, Z. S.; Dordick, J. S.; Tessier, P. M. Polyphenolic glycosides and aglycones utilize opposing pathways to selectively remodel and inactivate toxic oligomers of amyloid  $\beta$ . *ChemBioChem* **2011**, *12*, 1749–1758.
- (22) Xiao, J.; Capanoglu, E.; Jassbi, A. R.; Miron, A. Advance on the flavonoid C-glycosides and health benefits. *Crit. Ver. Food Sci. Nutr.* **2016**, *56*, S29–S45.
- (23) Jesus, A. R.; Vila-Viçosa, D.; Machuqueiro, M.; Marques, A. P.; Dore, T. M.; Rauter, A. P. Targeting type 2 diabetes with C-glucosyl dihydrochalcones as selective sodium glucose co-transporter 2 (SGLT2) inhibitors: Synthesis and biological evaluation. *J. Med. Chem.* **2017**, *60*, 568–579.
- (24) de Matos, A. M.; Calado, P.; Rauter, A. P. Recent Advances on SGLT2 Inhibitors: Synthetic Approaches, Therapeutic Benefits and Adverse Events. In *Successful Drug Discovery*; Volume 5, Eds Fischer, J.; Klein, C.; Childers, W. E., Wiley-VCH: Weinheim, in press, 2020. DOI: DOI: 10.1002/9783527826872.ch4
- (25) Jesus, A. R.; Dias, C.; Matos, A. M.; de Almeida, R. F. M.; Viana, A. S.; Marcelo, F.; Ribeiro, R. T.; Macedo, M. P.; Airoidi, C.; Nicotra, F.; Martins, A.; Cabrita, E. J.; Jiménez-Barbero, J.; Rauter, A. P. Exploiting the therapeutic potential of 8- $\beta$ -D-glucopyranosylgenistein: Synthesis, antidiabetic activity, and molecular interaction with islet amyloid polypeptide and amyloid  $\beta$ -peptide (1–42). *J. Med. Chem.* **2014**, *57*, 9463–9472.
- (26) Rawat, P.; Kumar, M.; Rahuja, N.; Lal Srivastava, D. S.; Srivastava, A. K.; Murya, R. Synthesis and antihyperglycemic activity of phenolic C-glycosides. *Bioorg. Med. Chem. Lett.* **2011**, *21*, 228–233.
- (27) He, L.; Zhang, Y. Z.; Tanoh, M.; Chen, G.-R.; Praly, J.-P.; Chrysina, E. D.; Tiraidis, C.; Kosmopoulou, M.; Leonidas, D. D.; Oikonomakos, N. G. In the search of glycogen phosphorylase inhibitors: Synthesis of C-D-glucopyranosylbenzo(hydro)quinones – Inhibition of and binding to glycogen phosphorylase in the crystal. *Eur. J. Org. Chem.* **2007**, *2007*, 596–606.
- (28) Jaramillo, C.; Knapp, S. Synthesis of C-aryl glycosides. *Synthesis* **1994**, *1994*, 1–20.
- (29) Nomura, S.; Sakamaki, S.; Hongu, M.; Kawanishi, E.; Koga, Y.; Sakamoto, T.; Yamamoto, Y.; Ueta, K.; Kimata, H.; Nakayama, K.; Tsuda-Tsukimoto, M. Discovery of canagliflozin, a novel C-glucoside with thiophene ring, as sodium-dependent glucose cotransporter 2 inhibitor for the treatment of type 2 diabetes mellitus. *J. Med. Chem.* **2010**, *53*, 6355–6360.
- (30) Liao, H.; Leng, W.-L.; Hoang, K. L. M.; Yao, H.; He, J.; Voo, A. Y. H.; Liu, X.-W. Asymmetric syntheses of 8-oxabicyclo[3,2,1]octane and 11-oxabicyclo[5.3.1.0]undecane from glycals. *Chem. Sci.* **2017**, *8*, 6656–6661.
- (31) Jarreton, O.; Skrydstrup, T.; Espinosa, J.-F.; Jiménez-Barbero, J.; Beau, J.-M. Samarium diiodide promoted C-glycosylation: An application to the stereospecific synthesis of  $\alpha$ -1,2-C-mannobioside and its derivatives. *Chem. – Eur. J.* **1999**, *5*, 430–441.
- (32) Yuan, X.; Linhardt, R. Recent Advances in the synthesis of C-oligosaccharides. *Curr. Top. Med. Chem.* **2005**, *5*, 1393–1430.
- (33) dos Santos, R. G.; Jesus, A. R.; Caio, J. M.; Rauter, A. P. Fries-type reactions for the C-glycosylation of phenols. *Curr. Org. Chem.* **2011**, *15*, 128–148.
- (34) Matsumoto, T.; Katsuki, M.; Suzuki, K. New approach to C-aryl glycosides starting from phenol and glycosyl fluoride. Lewis acid-catalyzed rearrangement of O-glycoside to C-glycoside. *Tetrahedron Lett.* **1988**, *29*, 6935–6938.
- (35) Kometani, T.; Kondo, H.; Fujimori, Y. Boron trifluoride-catalyzed rearrangement of 2-aryloxytetrahydropyrans: a new entry to C-arylglycosidation. *Synthesis-Stuttgart.* **1988**, *12*, 1005–1007.
- (36) Furuta, T.; Kimura, T.; Kondo, S.; Mihara, H.; Wakimoto, T.; Nukaya, H.; Tsuji, K.; Tanaka, K. Concise total synthesis of flavone C-

- glycoside having potent anti-inflammatory activity. *Tetrahedron* **2004**, *60*, 9375–9379.
- (37) Kumazawa, T.; Kimura, T.; Matsuba, S.; Sato, S.; Onodera, J. Synthesis of 8-C-glucosylflavones. *Carbohydr. Res.* **2011**, *334*, 183–2271 193.
- (38) Mahling, J.-A.; Jung, K.-H.; Schmidt, R. R. Synthesis of flavone C-glycosides vitexin, isovitexin and isoemigenin. *Leibigs Ann. Chem.* **1995**, *1995*, 461–466.
- (39) Haverkamp, J.; van Dongen, J. P. C. M.; Vliegenthart, J. F. G. PMR and CMR spectroscopy of methyl 2,3,4,6-tetra-O-methyl- $\alpha$ - and  $\beta$ -D-glucopyranoside : An application to the identification of partially methylated glucoses. *Tetrahedron* **1973**, *29*, 3431–3439.
- (40) Wegmann, B.; Schmidt, R. R. The application of the trichloroacetimidate method to the synthesis of  $\alpha$ -D-gluco- and  $\alpha$ -D-galactopyranosides. *J. Carbohydr. Chem.* **1987**, *6*, 357–375. and references cited therein
- (41) Cai, X.; Ng, K.; Panesar, H.; Moon, S.-J.; Paredes, M.; Ishida, K.; Hertweck, C.; Minehan, T. G. Total synthesis of the antitumor natural product polycarcin V and evaluation of its DNA binding profile. *Org. Lett.* **2014**, *16*, 2962–2965.
- (42) Wei, X.; Liang, D.; Wang, Q.; Meng, X.; Li, Z. Total synthesis of mangiferin, homomangiferin, and neomangiferin. *Org. Biomol. Chem.* **2016**, *14*, 8821–8831.
- (43) Wu, Z.; Wei, G.; Lian, G.; Yu, B. Synthesis of mangiferin, isomangiferin, and homomangiferin. *J. Org. Chem.* **2010**, *75*, 5725–2292 5728.
- (44) Morris, G. P.; Clark, I. A.; Vissel, B. Inconsistencies and controversies surrounding the amyloid hypothesis of Alzheimer's disease. *Acta Neuropathol. Commun.* **2014**, *2*, 135.
- (45) Hardy, J.; Selkoe, D. J. The amyloid hypothesis of Alzheimer's disease: Progress and problems on the road to therapeutics. *Science* **2002**, *297*, 353–356.
- (46) Kittelberger, K. A.; Piazza, F.; Tesco, G.; Reijmers, L. G. Natural amyloid-beta oligomers acutely impair the formation of a contextual fear memory in mice. *PLoS One* **2012**, *7*, No. e29940.
- (47) Matrone, C.; Petrillo, F.; Nasso, R.; Ferretti, G. Fyn tyrosine kinase as harmonizing factor in neuronal functions and dysfunctions. *Int. J. Mol. Sci.* **2020**, *21*, 4444.
- (48) Sato, M.; Murakami, K.; Uno, M.; Nakagawa, Y.; Katayama, S.; Akagi, K.; Masuda, Y.; Takegoshi, K.; Irie, K. Site-specific inhibitory mechanism for amyloid  $\beta$ 42 aggregation by catechol-type flavonoids targeting the Lys residues. *J. Biol. Chem.* **2013**, *288*, 23212–23224.
- (49) Shoichet, B. K. Screening in a spirit haunted world. *Drug Discovery Today* **2006**, *11*, 607–615.
- (50) Seidler, J.; McGovern, S. L.; Doman, T. N.; Shoichet, B. K. Identification and prediction of promiscuous aggregating inhibitors among known drugs. *J. Med. Chem.* **2003**, *46*, 4477–4486.
- (51) Vallverdú-Queralt, A.; Biler, M.; Meudec, E.; Le Guernevé, C.; Vernhet, A.; Jean-Paul Mazauric, J.-P.; Legras, J. L.; Loonis, M.; Trouillas, P.; Cheynier, V.; Dangles, O. *p*-Hydroxyphenyl-pyranoanthocyanins: An experimental and theoretical investigation of their acid-base properties and molecular interactions. *Int. J. Mol. Sci.* **2016**, *17*, 1842.
- (52) McGovern, S. L.; Shoichet, B. K. Kinase inhibitors: not just for kinases anymore. *J. Med. Chem.* **2003**, *46*, 1478–1483.
- (53) Coan, K. E. D.; Shoichet, B. K. Stoichiometry and physical chemistry of promiscuous aggregate-based inhibitors. *J. Am. Chem. Soc.* **2008**, *130*, 9606–9612.
- (54) Bruno, F. F.; Trotta, A.; Fossey, S.; Nagarajan, S.; Nagarajan, R.; Samuelson, L. A.; Kumar, J. Enzymatic synthesis and characterization of polyQuercetin. *J. Macromol. Sci. A* **2010**, *47*, 1191–1196.
- (55) Momić, T.; Savić, J.; Černigoj, U.; Trebše, P.; Vasić, V. Protolytic equilibria and photodegradation of quercetin in aqueous solution. *Collect. Czech. Chem. Commun.* **2007**, *72*, 1447–1460.
- (56) Mezzetti, A.; Protti, S.; Lapouge, C.; Cornard, J.-P. Protic equilibria as the key factor of quercetin emission in solution. Relevance to biochemical and analytical studies. *Phys. Chem. Chem. Phys.* **2011**, *13*, 6858–6864.
- (57) de Granada-Flor, A.; Sousa, C.; Filipe, H. A. L.; Santos, M. S. C. S.; de Almeida, R. F. M. Quercetin dual interaction at the membrane level. *Chem. Commun.* **2019**, *55*, 1750–1753.
- (58) Zupancic, E.; Carreira, A. C.; de Almeida, R. F. M.; Silva, L. C. Biophysical implications of sphingosine accumulation in membrane properties at neutral and acidic pH. *J. Phys. Chem. B* **2014**, *118*, 4858–4866.
- (59) Zhou, Y.; Shi, J.; Chu, D.; Hu, W.; Guan, Z.; Gong, C.-X.; Iqbal, K.; Liu, F. Relevance of phosphorylation and truncation of Tau to the etiopathogenesis of Alzheimer's disease. *Front Aging Neurosci.* **2018**, *10*, 27.
- (60) Iqbal, K.; Liu, F.; Gong, C. X.; Grundke-Iqbal, I. Tau in Alzheimer disease and related tauopathies. *Curr. Alzheimer Res.* **2010**, *7*, 656–664.
- (61) Liu, F.; Shi, J.; Tanimukai, H.; Gu, J.; Gu, J.; Grundke-Iqbal, I.; Iqbal, K.; Gong, C. X. Reduced O-GlcNAcylation links lower brain glucose metabolism and tau pathology in Alzheimer's disease. *Brain* **2009**, *132*, 1820–1832.
- (62) Kópke, E.; Tung, Y. C.; Shaikh, S.; Alonso, A. C.; Iqbal, K.; Grundke-Iqbal, I. Microtubule-associated protein tau. Abnormal phosphorylation of a non-paired helical filament pool in Alzheimer disease. *J. Biol. Chem.* **1993**, *268*, 24374–22384.
- (63) Desmarais, J. A.; Unger, C.; Damjanov, I.; Meuth, M.; Andrews, P. Apoptosis and failure of checkpoint kinase 1 activation in human induced pluripotent stem cells under replication stress. *Stem Cell Res. Ther.* **2016**, *7*, 17.
- (64) Bischoff, H. The mechanism of alpha-glucosidase inhibition in the management of diabetes. *Clin. Invest. Med.* **1995**, *18*, 303–311.
- (65) de Melo, E. B.; da Silveira Gomes, A.; Carvalho, I.  $\alpha$ - and  $\beta$ -Glucosidase inhibitors: chemical structure and biological activity. *Tetrahedron* **2006**, *62*, 10277–10302.
- (66) Rauter, A. P.; Jesus, A.; Martins, A.; Dias, C.; Ribeiro, R.; Macedo, M. P.; Justino, J.; Mota-Filipe, H.; Pinto, R.; Sepodes, B.; Medeiros, M.; Jiménez Barbero, J.; Airoldi, C.; Nicotra, F. New C-Glycosylpolyphenol Antidiabetic Agents, Effect on Glucose Tolerance and Interaction with Beta-Amyloid. Therapeutic Applications of the Synthesized Agent(s) and of *Genista tenera* Ethyl Acetate Extracts Containing Some of Those Agents. US20,150,031,639A1, Oct 03, 2017.
- (67) Jean, L.; Thomas, B.; Tahiri-Alaoui, A.; Shaw, M.; Vaux, D. J. Heterologous amyloid seeding: Revisiting the role of acetylcholinesterase in Alzheimer's disease. *PLoS One* **2007**, *2*, No. e652.
- (68) Greig, N. H.; Utsuki, T.; Ingram, D. K.; Wang, Y.; Pepeu, G.; Scali, C.; Yu, Q.-S.; Mamczarz, J.; Holloway, H. W.; Giordano, T.; Chen, D.; Furukawa, K.; Sambamurti, K.; Brossi, A.; Lahiri, D. K. Selective butyrylcholinesterase inhibition elevates brain acetylcholine, augments learning and lowers Alzheimer  $\beta$ -amyloid peptide in rodent. *Proc. Natl. Acad. Sci. U. S. A.* **2005**, *102*, 17213–17218.
- (69) Diamant, S.; Podoly, E.; Friedler, A.; Ligumsky, H.; Livnah, O.; Soreq, H. Butyrylcholinesterase attenuates amyloid fibril formation *in vitro*. *Proc. Natl. Acad. Sci. U. S. A.* **2006**, *103*, 8628–8633.
- (70) Araujo, J. A.; Greig, N. H.; Ingram, D. K.; Sandin, J.; de Rivera, C.; Milgram, N. W. Cholinesterase inhibitors improve both memory and complex learning in aged beagle dogs. *J. Alzheimers Dis.* **2011**, *26*, 143–155.
- (71) Greig, N. H.; Lahiri, D. K.; Sambamurti, K. Butyrylcholinesterase: an important new target in Alzheimer's disease therapy. *Int. Psychogeriatr.* **2002**, *14*, 77–91.
- (72) Mushtaq, G.; Greig, N.; Khan, J.; Kamal, M. Status of acetylcholinesterase and butyrylcholinesterase in Alzheimer's disease and type 2 diabetes mellitus. *C.N.S. Neurol. Disord. Drug Targets* **2014**, *13*, 1432–1439.
- (73) Rao, A. A.; Sridhar, G. R.; Das, U. N. Elevated butyrylcholinesterase and acetylcholinesterase may predict the development of type 2 diabetes mellitus and Alzheimer's disease. *Med. Hypotheses* **2007**, *69*, 1272–1276.
- (74) Sato, K. K.; Hayashi, T.; Maeda, I.; Koh, H.; Harita, N.; Uehara, S.; Onishi, Y.; Oue, K.; Nakamura, Y.; Endo, G.; Kambe, H.; Fukuda, K. Serum butyrylcholinesterase and the risk of future type 2

- 2404 diabetes: the Kansai Healthcare Study. *Clin. Endocrinol. (Oxf)*. **2014**,  
2405 **80**, 362–367.
- 2406 (75) Iwasaki, T.; Yoneda, M.; Nakajima, A.; Terauchi, Y. Serum  
2407 butyrylcholinesterase is strongly associated with adiposity, the serum  
2408 lipid profile and insulin resistance. *Intern. Med.* **2007**, **46**, 1633–1639.
- 2409 (76) Zhang, Y.; Zhang, T.; Wang, F.; Xie, J. Brain tissue distribution  
2410 of spinosin in rats determined by a new high-performance liquid  
2411 chromatography-electrospray ionization-mass/mass spectrometry  
2412 method. *J. Chromatogr. Sci.* **2015**, **53**, 97–103.
- 2413 (77) Di, L.; Kerns, E. H. Profiling drug-like properties in discovery  
2414 research. *Curr. Opin. Chem. Biol.* **2003**, **7**, 402–408.
- 2415 (78) Yang, J. J.; Ursu, O.; Lipinski, C. A.; Sklar, L. A.; Oprea, T. L.;  
2416 Bologa, C. G. Badapple: promiscuity patterns from noisy evidence.  
2417 *Aust. J. Chem.* **2016**, **8**, 29.
- 2418 (79) Ingólfsson, H. I.; Thakur, P.; Herold, K. F.; Hobart, E. A.;  
2419 Ramsey, N. B.; Periole, X.; de Jong, D. H.; Zwama, M.; Yilmaz, D.;  
2420 Hall, K.; Maretzky, T.; Hemmings, H. C., Jr.; Blobel, C.; Marrink, S.  
2421 J.; Koçer, A.; Sack, J. T.; Andersen, O. S. Phytochemicals perturb  
2422 membranes and promiscuously alter protein function. *ACS Chem. Biol.*  
2423 **2014**, **9**, 1788–1798.
- 2424 (80) Bols, M.; Hazell, R. G.; Thomsen, I. B. 1-Azafagomine: A  
2425 hydroxyhexahydropyridazine that potently inhibits enzymatic glyco-  
2426 side cleavage. *Chem. – Eur. J.* **1997**, **3**, 940–947.
- 2427 (81) Cornish-Bowden, A. A simple graphical method for  
2428 determining the inhibition constants of mixed, uncompetitive and  
2429 non-competitive inhibitors. *Biochem. J.* **1974**, **137**, 143–144.
- 2430 (82) Ellman, G. L.; Courtney, K. D.; Andres, V., Jr.; Featherstone, R.  
2431 M. A new and rapid colorimetric determination of acetylcholinester-  
2432 ase activity. *Biochem. Pharmacol.* **1961**, **7**, 88–95.
- 2433 (83) Walsh, D. M.; Klyubin, I.; Fadeeva, J. V.; Cullen, W. K.; Anwyl,  
2434 R.; Wolfe, M. S.; Rowan, M. J.; Selkoe, D. J. Naturally secreted  
2435 oligomers of amyloid beta protein potently inhibit hippocampal long-  
2436 term potentiation in vivo. *Nature* **2002**, **416**, 535–539.
- 2437 (84) Shankar, G. M.; Welzel, A. T.; McDonald, J. M.; Selkoe, D. J.;  
2438 Walsh, D. M. Isolation of low-n amyloid  $\beta$ -protein oligomers from  
2439 cultured cells, CSF, and brain. *Methods Mol. Biol.* **2011**, **670**, 33–44.
- 2440 (85) Shi, Y.; Kirwan, P.; Livesey, F. J. Directed differentiation of  
2441 human pluripotent stem cells to cerebral cortex neurons and neural  
2442 networks. *Nat. Protoc.* **2012**, **7**, 1836–1846.
- 2443 (86) VCCLAB. *Virtual Computational Chemistry Laboratory*; [http://](http://www.vcclab.org)  
2444 [www.vcclab.org](http://www.vcclab.org), accessed April 23, 2019.
- 2445 (87) Kansy, M.; Senner, F.; Gubernator, K. Physicochemical high  
2446 throughput screening: parallel artificial membrane permeation assay in  
2447 the description of passive absorption processes. *J. Med. Chem.* **1998**,  
2448 **41**, 1007–1010.